



UNIVERSITÀ
DI SIENA
1240

DIPARTIMENTO DI BIOTECNOLOGIE, CHIMICA E FARMACIA

**DOTTORATO DI RICERCA IN SCIENZE CHIMICHE E
FARMACEUTICHE**

CICLO XXXIII

COORDINATORE: PROFESSOR MAURIZIO TADDEI

**Development of novel pyrazolo[3,4-*d*]pyrimidines as
anticancer agents: synthesis of potent c-Src/Abl
inhibitors**

SETTORE SCIENTIFICO DISCIPLINARE: CHIM/08

TUTOR:

PROF. FEDERICO CORELLI

DOTTORANDO:

SALVATORE DI MARIA

ANNO ACCADEMICO: 2019/2020

*This thesis is dedicated to
professor Maurizio Botta*

Summary

The interest in protein tyrosine kinases has increased in recent years, particularly since their oncogenicity in human cells has been recognized. Tyrosine kinases promote phosphorylation of many proteins involved in cellular signaling pathways and the deregulation of their normal activity leads to diseases, such as cancer. In this context, several pyrazolo[3,4-d]pyrimidines have been developed as Tyrosine Kinase Inhibitor (TKI) and some of them have revealed promising in vitro and in vivo antitumor activity.

In this thesis I describe the work done during my three years of PhD, which concerns the design and synthesis of novel pyrazolo[3,4-d]pyrimidines able to inhibit the protein tyrosine kinase c-Src and Abl, involved in cancer processes.

The first chapter provides a general introduction on Protein Kinases, focusing on the major non-receptor tyrosine kinases c-Src and Abl. Here, the protein activation mechanisms and some structural aspects have been described.

The second chapter is dedicated to the development of potent c-Src/Abl inhibitors for the treatment of Chronic Myeloid Leukemia (CML). Optimization of molecules, through the design and synthesis of novel derivatives, has been successfully performed and new promising anticancer agents have been obtained.

The third chapter describes the elaboration of five novel families of pyrazolo[3,4-d]pyrimidines designed through merge-hybridization with TKIs approved in cancer therapy. Thereby, a small library of c-Src inhibitors against Hepatocellular Carcinoma (HCC) has been developed.

Finally, the last chapter illustrates the optimization process of two pyrazolo[3,4-d]pyrimidine compounds, Si306 and Si409, with the aim of improving some pharmacological properties for the treatment of Glioblastoma Multiforme (GBM) through the design and synthesis of a small set of derivatives.

Index:

Chapter I:	7
1. Protein kinases.....	7
1.1 Tyrosine Kinases (TK).....	8
1.2 Protein kinase c-Src.....	10
1.3 Protein kinase c-Abl.....	12
1.4 Role of c-Src and c-Abl in cancers.....	14
2. References	15
Chapter II:	19
Novel pyrazolo[3,4- <i>d</i>]pyrimidine as c-Src/Abl kinases inhibitors: synthesis and biological evaluation for CML treatment.	
1. Introduction	19
1.1 Chronic Myeloid Leukemia (CML).....	19
1.2 Treatment options.....	21
2. State of the art.....	23
3. Aim of the project.....	25
4. Results	26
4.1 Synthesis.....	26
4.2 Biological assays and SAR considerations	30
5. Conclusion.....	35
6. Materials and method	36
7. References	47
Chapter III:	52
Design by means of a merge-hybridization approach and synthesis of new pyrazolo[3,4- <i>d</i>]pyrimidine inhibitors active against the hepatocellular carcinoma (HCC)	
1. Introduction	52
1.1 Hepatocellular Carcinoma (HCC).....	52
1.2 Treatment options and novel targets	53
2. State of the art.....	56
3. Aim of the project.....	58
4. Results	59
4.1 Part I.....	59
4.1.1 Design of new pyrazolo[3,4- <i>d</i>]pyrimidine derivatives	59

4.1.2	Synthesis	62
4.1.3	Biological data	76
4.2	Part II.....	79
4.2.1	C4 optimization of 41c: design, synthesis and biological evaluation.....	79
4.2.2	C6 and N1 optimization of 41c: design, synthesis and biological evaluation	81
5.	Conclusion.....	85
6.	Materials and methods.....	86
7.	References	103
Chapter IV:		107
Optimization of Si306 and Si409: design, synthesis and biological evaluation of novel pyrazolo[3,4- <i>d</i>]pyrimidines active against Glioblastoma Multiforme (GBM)		
1.	Introduction	107
1.1	Glioblastoma Multiforme (GBM).....	107
1.2	Treatment options.....	108
2.	State of the art.....	109
3.	Aim of the project.....	111
4.	Results	111
4.1	Development of Si306 derivatives: design, synthesis and enzymatic assay	111
4.2	Development of Si409 derivatives: design, synthesis and enzymatic assay	115
4.3	Cells viability assay.....	118
5.	Conclusion.....	119
6.	Materials and methods.....	119
7.	References	124

List of figures:

Figure 1.1	Illustration of catalysed phosphorylation of protein substrate.	7
Figure 1.2	Three examples of proteins of the Receptor Tyrosine Kinases (RTKs).	8
Figure 1.3	Structural organization of NRTKs. SH2/SH3: Src-homology 2/3; PH: Pleckstrinhomology; TH: Tec-homology; F-BAR: Bin-Amphiphysin-Rvs; SAM: Sterile- α -motif; CRIB: Cdc42/Rac-interactive-binding-motif; FERM: 4.1 protein-ezrin-radixin-moesin; FAT: focaladhesion-targeting.....	10
Figure 1.4	Representation of the structural domain of human c-Src and viral v-Src.	11
Figure 1.5	Illustration of primary structure of Src Family Kinases (SFKs) members.	12
Figure 1.6	Structural organization of c-Abl. FABD: F-actin binding domain.	13

Figure 1.7 Illustration of c-Abl protein structure.....	13
Figure 2.1 Gene translocation in Philadelphia chromosome.....	20
Figure 2.2 Bcr-Abl signaling pathways in CML.	21
Figure 2.3 Structures of CML approved compounds imatinib 1 , dasatinib 2 and ponatinib 3	22
Figure 2.4 General structure of in-house pyrazolo[3,4- <i>d</i>]pyrimidines and compound S29 (4).	23
Figure 2.5 Structure and Ki values of Si223 (5).....	24
Figure 2.6 Optimization process of in-house pyrazolo[3,4- <i>d</i>]pyrimidines 6 , 7 , and 8	25
Figure 3.1 Stages and clinical practice for management of hepatocellular carcinoma.	53
Figure 3.2 Structure of Sorafenib 1 , Regorafenib 2 and Dasatinib 3	54
Figure 3.3 mTOR and RAS pathways involved in HCC.....	55
Figure 3.4 Structures of main TKIs: Imatinib 4 , Nilotinib 5 , and PP2 6	56
Figure 3.5 Pyrazolo[3,4- <i>d</i>]pyrimidine scaffold with substituted N1, C6 and C4 positions. The structures of Si192 7 and other potent Src/Abl pyrazolo[3,4- <i>d</i>]pyrimidine inhibitors 8 , 9 have been reported in Chapter II.	57
Figure 3.6 X-Ray crystal structure of c-Src with ligand Si192.	59
Figure 3.7 Design of amino-benzamide, amino-benzylether and ureidic derivatives as c-Abl inhibitors.....	60
Figure 3.8 Design of aminothiazole and imidazole derivatives as c-Src inhibitors.	61
Figure 3.9 Phenol-Glu310 interaction on c-Src kinase pocket.	79
Figure 3.10 Optimization of 41c by hydrogen replacement with bromine or methyl group...	80
Figure 3.11 C6 and N1 diversifications of hit compound 41c	82
Figure 4.1 Structure of TKIs Regorafenib 1 , Dasatinib 2 , and PP2 3	108
Figure 4.2 Pyrazolo[3,4- <i>d</i>]pyrimidines scaffold and structure of Si306 (4a), and Si409 (5a).	109
Figure 4.3 Optimization of 4a	112
Figure 4.4 Design of Si409 derivatives.	115
Figure 4.5 Possible transformation of 5b into 5a	118

Chapter I

1. Protein kinases

Protein kinases (PTKs) regulate the biological activity of various human proteins through the phosphorylation of specific amino acids, thereby inducing their conformational change [1,2]. Specifically, PTKs catalyze the reaction of phosphorylation using ATP as the source of phosphate to transfer it on specific serine, threonine, or tyrosine residues in substrate proteins (Figure 1.1).

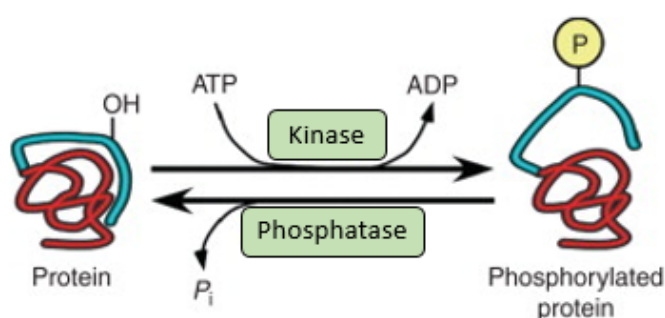


Figure 1.1 Illustration of catalyzed phosphorylation of protein substrate.

The importance of protein phosphorylation in cell signaling is due to the fact that protein kinase domains are found in 2% of eukaryotic genes [3]. Identification and classification of these proteins is based on the human kinome analysis from which 518 protein kinases have been identified, of which 478 belong to a single superfamily of proteins, characterized by sequence similarity and biochemical function. Moreover, these kinases can be divided into several families and sub-families, such as tyrosine kinases (TK), tyrosine kinase-like (TKL), Ca²⁺/calmodulin-dependent protein kinase (CAMK), casein kinase I gamma (CSNK1), serine/threonine-protein kinase (STE and AGC), receptor guanylate cyclases (RGC) and others. The additional 40 kinases form the ‘atypical’ kinase group, because they have no sequence similarity with the typical superfamily kinases [4,5]. Kinases are particularly prominent in signal transduction and, in this context, a diversity on specific kinase functions has been observed. However, protein kinases serve to orchestrate the activity of several physiological processes, like cell cycle progression [6], cell motility [7,8], and apoptosis [9]. For these reasons, subtle changes in their kinase activity can lead to various cellular alterations, such as architecture remodeling and abnormal functionality, which in turn can degenerate into a wide

variety of pathologies including cancer, inflammatory diseases, diabetes, and neurodegenerative diseases.

1.1 Tyrosine Kinases (TK)

Tyrosine kinases are a family of approximately 90 human proteins capable of phosphorylating the amino acid tyrosine of another protein, leading to conformational changes and activation of the latter [10]. These proteins are one of the most important PK groups involved in cancer biology and are divided into two main families namely 58 receptor and 32 non-receptor tyrosine kinases.

▪ *Receptor Tyrosine Kinases (RTKs)*

Receptor Tyrosine Kinases (RTKs) are a large family of cell surface receptors which display intrinsic protein tyrosine kinase activity [11]. RTKs are characterized by an extracellular portion that usually binds polypeptide ligands, a transmembrane helix, and a cytoplasmic moiety which possesses kinase catalytic activity (Figure 1.2).

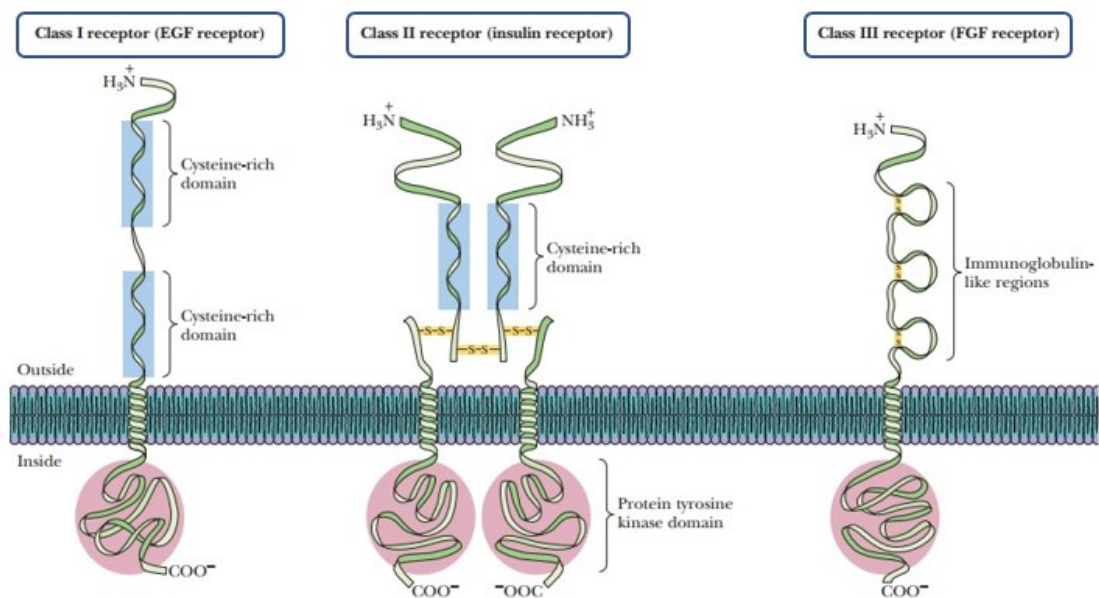


Figure 1.2 Three examples of proteins of the Receptor Tyrosine Kinases (RTKs).

Based on the type of extracellular portion, RTKs have been subdivided into several receptor groups (Figure 1.2). Epidermal growth factor (EGF) is a monomeric class I receptor and contains a pair of Cys-rich repeat sequences, while the insulin receptor is a glycoprotein composed of two globular subunits arranged in a $\alpha_2\beta_2$ tetramer [12]. Class III of kinase receptors is represented by fibroblast growth factors (FGF) which exhibits multiple immunoglobulin-like domains. Cytoplasmic domain of these proteins contains the juxtamembrane region, followed by the conserved kinase core and the carboxy-terminal region. After ligand binding, these receptors undergo dimerization with subsequent auto-phosphorylation of tyrosine residue [13,14]. As a result, the protein kinase is activated and produces new binding sites for the intracellular signal transduction molecules present in the vicinity. However, it has been observed that different physiological ligands employ different strategies for inducing the active dimeric state [15,16].

▪ ***Non-Receptor Tyrosine Kinases (NRTKs)***

Non-Receptor Tyrosine Kinases (NRTKs) are a family of cytosolic enzymes that act on specific protein involved in cellular pathways through the phosphorylation of tyrosine residues, thus allowing their activation and signal transduction [17]. Unlike receptor tyrosine kinases, NRTKs lack the extra-cellular domain, which allows the ligand binding, and the transmembrane region, but possess other domains that mediate protein-protein, protein-lipid, and protein-DNA interactions. However, the most relevant portion is the catalytic kinase domain [18], which is about 275 residues in length and is found to be extremely important in the classification of NRTKs. These enzymes are organized into nine sub-families based on sequence similarities, primarily within the kinase domains [19], including Abl, FES, JAK, ACK, SYK, TEC, FAK, Src, and CSK (Figure 1.3).

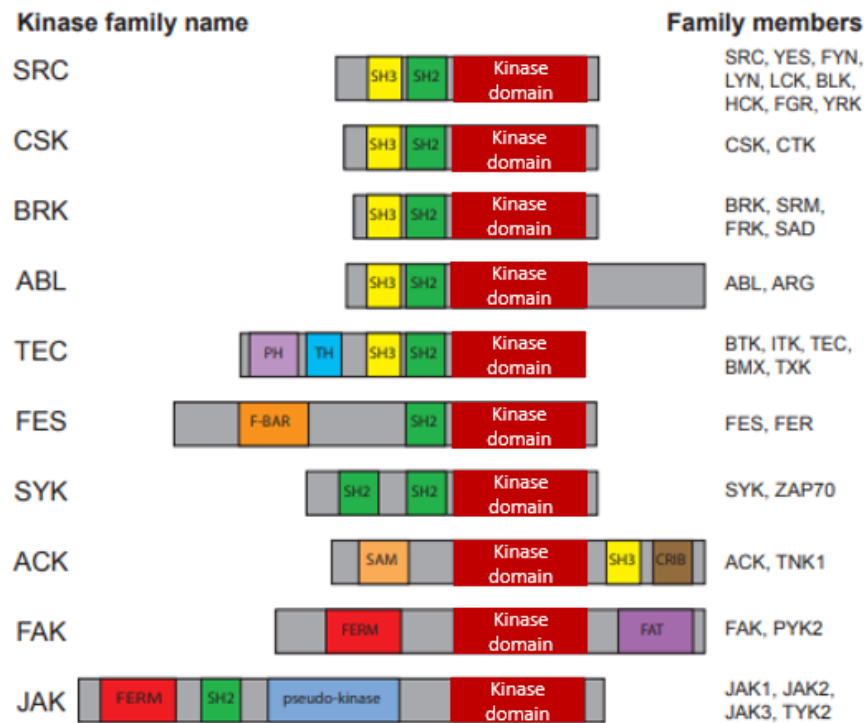


Figure 1.3 Structural organization of NRTKs. SH2/SH3: Src-homology 2/3; PH: Pleckstrinhomology; TH: Tec-homology; F-BAR: Bin-Amphiphysin-Rvs; SAM: Sterile- α -motif; CRIB: Cdc42/Rac-interactive-binding-motif; FERM: 4.1 protein-ezrin-radixin-moesin; FAT: focaladhesion-targeting.

NRTKs play a broad role in cell signaling and regulate a huge array of cellular functions such as cell survival, division, adhesion, gene expression and immune response. Recent studies have shown that NRTKs are mutated in several cancers, including leukemia, lymphomas, gliomas, and other solid tumors, leading to aberrant activation [20]. Mutations that alter the constitutive kinase activity result in the generation of oncogenes, such as c-Src and Abl.

1.2 Protein kinase c-Src

After the discovery that tumor development in chickens originated from the v-Src retrovirus gene, encoded by the Raus Sarcoma virus [21], interest in the human homologous c-Src protein has increased because it plays an interesting role in a wide variety of cancer processes [22,23]. c-Src is a NRTK expressed in all human cells and specializes in transduction messages that control cell proliferation, migration and apoptosis.

In particular, c-Src is a 60-kilodalton phosphoprotein (pp60^{c-src}) consisting of 563 amino acids and subdivided into four main domains involved in the enzymatic functionality [24].

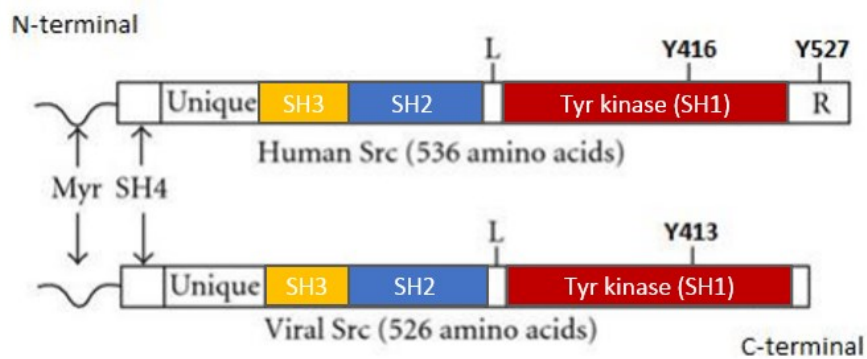


Figure 1.4 Representation of the structural domain of human c-Src and viral v-Src.

The SH4 domain (Src Homology 4) is responsible for interaction with cell membranes through the binding between myristic acid and the N-terminal segment (Figure 1.4), while the SH3 domain generates conformational changes which regulate the interactions with substrates [25]. The latter domain possesses a small split that binds the chains of other proteins, bringing them closer to the kinase domain and allowing the addition of phosphate. The SH2 domain also modulates substrate recognition and is connected to the kinase domain by a linker. However, the highest relevance in the structure of c-Src was observed in the SH1 domain which shows the catalytic function and contains the Tyr416 residue. This domain consists of two lobes where the catalytic site is located, and their movement varies the opening angle of core, thus allowing the entry of ATP and the release of ADP. In the catalytic core a key role is played by several amino acids, such as Lys295, which generates ionic interactions with the α and β phosphates of ATP, or Asp 386, which facilitates the nucleophilic attack on phosphorus γ . Finally, c-Src shows a small tail in the C-terminal region. This final sequence contains Tyr527 which participates in protein inactivation mechanism as a regulatory site through phosphorylation by other tyrosine kinases, including Csk and Chk [26]. Under basal conditions *in vivo*, Src is phosphorylated at Tyr527, and phosphotyrosine 527 binds intramolecularly Arg175 on Src SH2 domain [27]. This movement forces to stabilize closed conformation where the SH3 domain is blocked, thus avoiding interaction with other proteins and maintaining the catalytic domain in inactive conformation. Tyr416 phosphorylation stabilizes the active protein conformation and promotes kinase activity in c-Src. However, the activation mechanism requires the preliminary dephosphorylation of Tyr527 to give the free open protein.

From the study of cell signaling pathways it emerged that specific proteins with similar structural characteristics to c-Src are involved in several mechanisms [28]. c-Src protein is the progenitor of the Src Family kinases (SFKs), a group of proteins who share a highly conserved

structure in kinase domains and in other protein segments, such as myristoylated or palmitoylated SH4 domain and carboxy terminal tail (Figure 1.5).

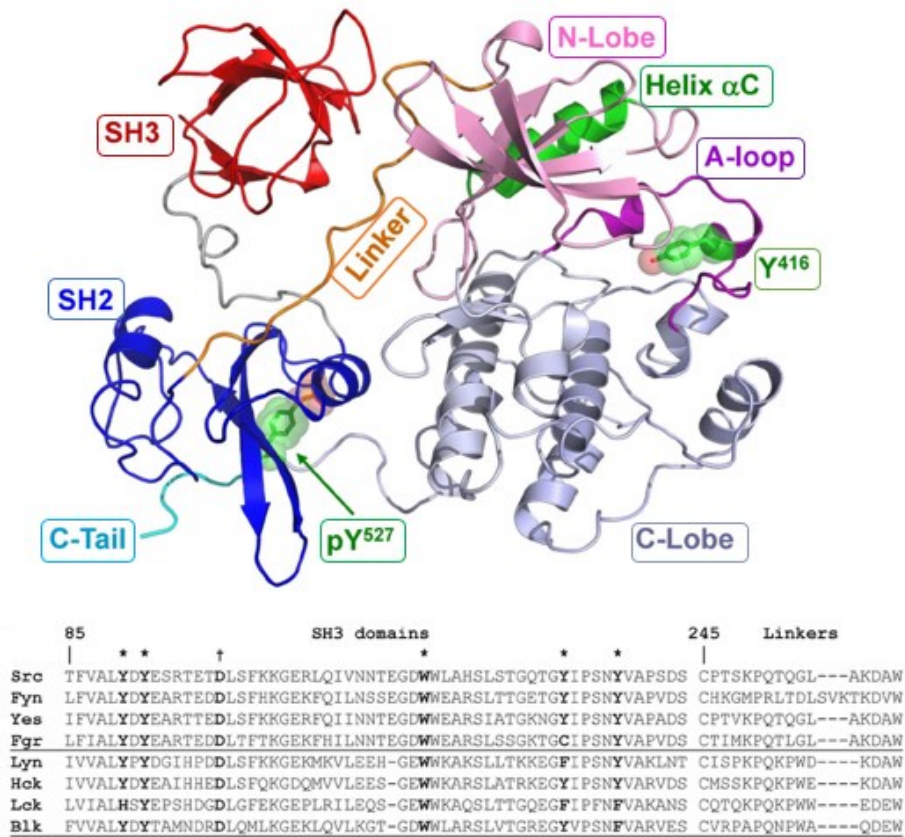


Figure 1.5 Illustration of primary structure of Src Family Kinases (SFKs) members.

SFK has 11 members: c-Src, Fyn, Yes, Blk, Yrk, Frk (also known as Rak), Fgr, Hck, Lck, Srm, and Lyn. Src, Yes, Yrk, and Fyn are ubiquitously expressed in a variety of tissues with high levels in platelets, neurons and some epithelial tissues, whereas Blk, Fgr, Hck, Lck, and Lyn are found primarily in hematopoietic cells [29].

1.3 Protein kinase c-Abl

c-Abl is a NRTK first identified following studies of the Abelson murine lymphosarcoma virus (*A-MuLV*) [30]. The product of the virally transduced oncogene, v-Abl, showed tyrosine kinase activity and represents an altered form of human Abl1, which was later found as part of activated fusion oncoprotein, Bcr-Abl [31]. Over the years, this protein has proved to be

particularly interesting and has been extensively studied for its involvement in various diseases, such as cancer, inflammatory processes and neurodegenerative diseases [32]. c-Abl is ubiquitously expressed in human cells and is encoded by the ABL1 gene, located on chromosome 9. Sequencing studies identified ABL2 (also known as Arg) as a paralog of ABL1, which conserved domain structure. Moreover, the human ABL1 gene can give rise to two alternative splicing transcripts, Abl1a and Abl1b [33], both regulators of different cellular processes during normal homeostasis. The 1b splicing variant is myristoylated at the N-terminus whereas the 1a variant is shorter and not myristoylated (Figure 1.6).



Figure 1.6 Structural organization of c-Abl. FABD: F-actin binding domain.

The N-terminal Cap is critical for the c-Abl 1b self-inhibition mechanism and this region is followed by SH3 and SH2 domains which, like SFK, play a role in substrate interaction and regulation. The bi-lobed kinase domain also reveals homology with the amino acid sequence shown in the SFKs, while the C-terminal tail regions of c-Abl is distinct. A carboxy-terminal extension contains last exon region which shows nuclear localization signals (NLS) and Nuclear Export Signal (NES) that allow c-Abl to shuttle between nucleus and cytoplasm [34,35].

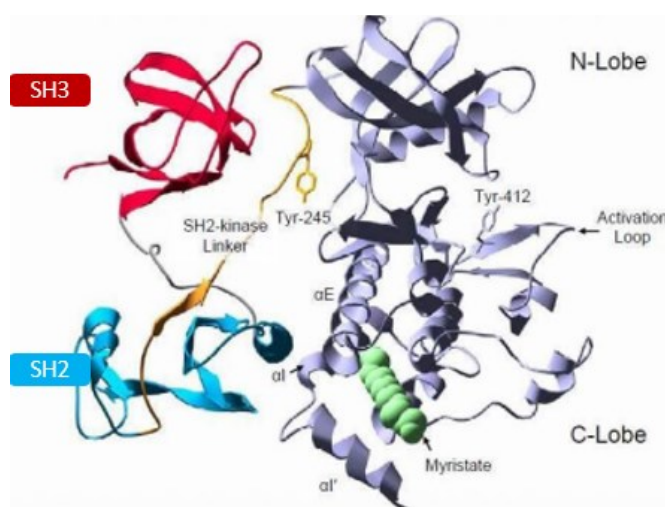


Figure 1.7 Illustration of c-Abl protein structure.

However, c-Abl regulates F-actin in the cytoskeleton via an F-actin-binding domain (FABD) at the C-terminus and induces cell migration [36]. c-Abl is negatively regulated through intramolecular interactions that generate the inactive protein conformation. This is stabilized by interactions between the SH3 domain and a proline-rich SH2-kinase linker that promotes self-inhibition. Furthermore, a fundamental role in this mechanism is played by the myristate, which can bind the hydrophobic pocket of the kinase C lobe, thus forcing the SH2 and SH3 domains to maintain a closed conformation [37]. In this way, the SH2 domain forms a tight protein-protein interface with the kinase domain whose interaction is stabilized by a network of hydrogen bonds. Conversion of inactive c-Abl to its active form requires the disruption of these intramolecular interactions [38] and the full activation of this kinase is achieved by the phosphorylation of several tyrosine residues. Phosphorylation of Tyr245 in the SH2- kinase domain linker (Figure 1.7) could inhibit the intramolecular interaction with SH3 domain. In addition, this phosphorylation is coupled by a concomitant phosphorylation of Tyr412 in the kinase activation loop, thus stabilizing the kinase active conformation [39]. However, c-Abl can be phosphorylated by SFKs and tyrosine kinase receptors (PDGFr). Its kinase activity is increased by multiple stimuli leading to cytoskeletal reorganization and by other cellular signals such as oxidative stress or DNA damage [40]. Abl kinases regulate signaling pathways implicated in cell architecture remodeling that are important for cellular protrusions, cell migration and adhesion [41], also being able to modulate cell survival and proliferation [42].

1.4 Role of c-Src and c-Abl in cancers

Several studies have identified the protein tyrosine kinases (TKs) as promising targets for cancer treatment since it was recognized that the enhancement of TK activity is linked with cancer development and other proliferative diseases [10-11]. The relationship between c-Src activation and cancer progression is highlighted by the fact that numerous c-Src substrates are phosphorylated in tumor cells, and many of these have been correlated to processes inducing invasiveness and metastasis [25]. Indeed, c-Src proto-oncogenes result strongly implicated in the initiation and progression of numerous human cancers, including breast, pancreas, liver, and brain cancer. The c-Abl protein has also proved particularly interesting in cancer research after the discovery of the chimeric protein Bcr-Abl, responsible for the development of Chronic Myeloid Leukemia (CML). For these reasons, many Tyrosine Kinases Inhibitors (TKIs) have been tested for their *in vitro* and *in vivo* antitumoral activity, and some of them have been

approved by the Food and Drug Administration (FDA) for current use in anticancer chemotherapy. A subclass of TKIs with remarkable antiproliferative activity is represented by SFK and Abl inhibitors. These competitive ATP inhibitors have shown particularly positive results in the treatment of cancers in which these targets are involved. The rapid onset of resistance to common anticancer drugs in advanced patients has promoted the development and approval of several TKIs. However, many of these have failed in clinical trials leading to orphan drug designation and for these reasons it is essential to find new anticancer agents for the treatment of particular cancers, where therapy is not available.

2. References

- [1] Hunter, T.; Cooper, J.A.; Protein-tyrosine kinases. *Annu. Rev. Biochem.* **1985**, *54*, 897-930.
- [2] Cohen, P. The origins of protein phosphorylation. *Nat. Cell Biol.* **2002**, *4*, E127-E130.
- [3] Rubin, G.M.; Yandell, M.D.; Wortman, J.R.; Gabor Miklos, G.L.; Nelson, C.R.; Hariharan, I.K.; Fortini, M.E.; Li, P.W.; Apweiler, R.; Fleischmann, W.; Cherry, J.M.; Henikoff, S.; Skupski, M.P.; Misra, S.; Ashburner, M.; Birney, E.; Boguski, M.S.; Brody, T.; Brokstein, P.; Celniker, S.E.; Chervitz, S.A.; Coates, D.; Cravchik, A.; Gabrielian, A.; Galle, R.F.; Gelbart, W.M.; George, R.A.; Goldstein, L.S.; Gong, F.; Guan, P.; Harris, N.L.; Hay, B.A.; Hoskins, R.A.; Li, J.; Li, Z.; Hynes, R.O.; Jones, S.J.; Kuehl, P.M.; Lemaitre, B.; Littleton, J.T.; Morrison, D.K.; Mungall, C.; O'Farrell, P.H.; Pickeral, O.K.; Shue, C.; Vossball, L.B.; Zhang, J.; Zhao, Q.; Zheng, X.H.; Lewis S. Comparative genomics of the eukaryotes. *Science* **2000**, *287* (5461), 2204–2215.
- [4] Vieth, M.; Higgs, R.E.; Robertson, D.H.; Shapiro, M.; Gragg, E.A.; Hemmerle, H. Kinomics-structural biology and chemogenomics of kinase inhibitors and targets. *Biochim. Biophys. Acta.* **2004**, *1697* (1-2), 243-257.
- [5] Manning, G.; Whyte, D.B.; Martinez, R.; Hunter, T.; Sudarsanam, S. The protein kinase complement of the human genome. *Science* **2002**, *298* (5600), 1912-1934.
- [6] Morgan, D.O. Principles of CDK regulation. *Nature* **1995**, *374*, 131-134.
- [7] Hauck, C.R.; Sieg, D.J.; Hsia, D.A.; Loftus, J.C.; Gaarde, W.A.; Monia B.P.; Schlaepfer, D.D. Inhibition of focal adhesion kinase expression or activity disrupts epidermal growth

factor-stimulated signaling promoting the migration of invasive human carcinoma cells. *Cancer Res.* **2001**, *61* (19), 7079-7090.

[8] Schlaepfer, D.; Hauck, C.; Sieg, D.J. Signaling through focal adhesion kinase. *Prog. Biophys. Mol. Biol.* **1999**, *71* (3-4), 435-478.

[9] Wada, T.; Penninger, J.M. Mitogen-activated protein kinases in apoptosis regulation. *Oncogene* **2004**, *23* (16), 2838-2849.

[10] Robinson, D.R.; Wu, Y.; Lin, S. The protein tyrosine kinase family of the human genome. *Oncogene* **2000**, *19* (49), 5548–5557.

[11] Du, Z.; Lovely C.M. Mechanisms of receptor tyrosine kinase activation in cancer. *Mol. Cancer* **2018**, *17* (1), 58.

[12] A. Lemmon, M.A.; Schlessinger, J. Cell signaling by receptor-tyrosine kinases. *Cell* **2010**, *141* (7), 1117–1134.

[13] Li, E.; Hristova, K. Receptor tyrosine kinase transmembrane domains. *Cell Adh. Migr.* **2010**, *4* (2), 249-254.

[14] Ferguson, K.M.; Berger, M.B.; Mendrola, J.M.; Cho, H.; Leahy, D.J.; Lemmon, M.A. EGF activates its receptor by removing interactions that autoinhibit ectodomain dimerization. *Mol. Cell* **2003**, *11* (2), 507–517.

[15] Levitzki, A.; Gazit, A. Tyrosine kinase inhibition: an approach to drug development. *Science* **1995**, *267* (5205), 1782-1788.

[16] Schlessinger, J. Cell Signaling by Receptor Tyrosine Kinases. *Cell* **2000**, *103* (2), 211–225.

[17] Neet, K.; Hunter, T. Vertebrate non-receptor protein–tyrosine kinase families. *Gen. Cells* **1996**, *1* (2), 147-169.

[18] Songyang, Z.; Carraway III, K.L.; Eck, M.J.; Harrison, S.C.; Feldman, R.A.; Mohammadi, M.; Schlessinger, J.; Hubbard, S.R.; Smith, D.P.; Eng, C.; Lorenzo, M.J.; Ponder, B.A.J.; Mayer, B.J.; Cantley, L.C. Catalytic specificity of protein-tyrosine kinases is critical for selective signaling. *Nature* **1995**, *373* (6514), 536–539.

[19] Siveen, K.S., Prabhu, K.S., Achkar, I.W., Kuttikrishnan, S., Shyam, S., Khan, A.Q., Merhi, M., Dermime, S., Uddin, S. Role of non receptor tyrosine kinases in hematological malignances and its targeting by natural products. *Mol. Cancer* **2018**, *17* (1), 31.

- [20] Scheijen, B.; Griffin, J.D. Tyrosine kinase oncogenes in normal hematopoiesis and hematological disease. *Oncogene* **2002**, *21* (21), 3314–3333.
- [21] Roskoski, R. Src protein–tyrosine kinase structure and regulation. *Biochem. Biophys. Res. Com.* **2004**, *324* (4), 1155–1164.
- [22] Wheeler, D.L.; Iida, M.; Dunn, E.F. The Role of Src in Solid Tumors. *The Oncologist* **2009**, *14* (7), 667–678.
- [23] Guarino, M. Src signaling in cancer invasion. *J. Cell. Physiol.* **2010**, *223* (1), 14–26.
- [24] Cayer, M.P.; Proulx, M.; Ma, X.Z.; Sakac, D.; Giguère, J.F.; Drouin, M.; Néron, S.; Branch, D.R.; Jung, D. 2009. c-Src tyrosine kinase co-associates with and phosphorylates signal transducer and activator of transcription 5b which mediates the proliferation of normal human B lymphocytes. *Clin. Exp. Immun.* **2009**, *156* (3), 419–427.
- [25] Brown, M.T.; Cooper, J.A. Regulation, substrates and functions of src. *Biochim. Biophys. Acta* **1996**, *1287* (2-3), 121–149.
- [26] Zrihan, S.; Lim, J.; Keydar, I.; Sliwkowski, M.X.; Groopman, J.E.; Avraham, H. Association of csk-homologous kinase (CHK) (formerly MATK) with HER-2/ErbB-2 in breast cancer cells. *Bio. Chem.* **1997**, *272* (3), 1856–1863.
- [27] Cooper, J.A.; Gould, K.L.; Cartwright, C.A.; Hunter, T. Tyr527 is phosphorylated in pp60c-src: implications for regulation. *Science* **1986**, *231* (4744), 1431–1434.
- [28] Sirvent, A.; Benistant, C.; Roche, S. Oncogenic signaling by tyrosine kinases of the SRC family in advanced colorectal cancer. *Am. J. Cancer. Res.* **2012**, *2* (4), 357–371.
- [29] Parsons, S.; Parsons, T. Src family kinases, key regulators of signal transduction. *Oncogene* **2004**, *23* (48), 7906–7909.
- [30] Abelson, H.T.; Rabstein, L.S. Lymphosarcoma: virus-induced thymic-independent disease in mice. *Cancer Res.* **1970**, *30* (8), 2213–2222.
- [31] Aleem, S.U.; Craddock, B.P.; Miller, W.T. Constitutive activity in an ancestral form of Abl tyrosine kinase. *PLoS ONE* **2015**, *10* (6), e0131062.
- [32] Schlatterer, S.D.; Acker, C.M.; Davies, P. c-Abl in Neurodegenerative Disease. *J. Mol. Neurosci.* **2011**, *45* (3), 445–452.
- [33] Sawyers, C.L.; McLaughlin, J.; Goga, A.; Havlik, M.; Witte, O. The nuclear tyrosine kinase c-Abl negatively regulates cell growth. *Cell* **1994**, *77* (1), 121–131.

- [34] Wang, J.Y.J. Regulation of cell death by the Abl tyrosine kinase. *Oncogene* **2000**, *19* (49), 5643-5650.
- [35] Wen, S.T.; Jackson, P.K.; Van Etten, R.A. The cytostatic function of c-Abl is controlled by multiple nuclear localization signals and requires the p53 and Rb tumor suppressor gene products. *EMBO J.* **1996**, *15* (7), 1583-1595.
- [36] Woodring, P.J.; Hunter, T.; Wang J.Y.J. Regulation of F-actin-dependent processes by the Abl family of tyrosine kinases. *J. Cell Sci.* **2003**, *116* (Pt 13), 2613-2626.
- [37] Nagar, B.; Hantschel, O.; Young, M.A.; Scheffzek, K.; Veach, D.; Bornmann, W.; Clarksonet, B.; Superti-Furga, G.; Kuriyan, J. Structural Basis for the Autoinhibition of c-Abl Tyrosine Kinase. *Cell* **2003**, *112*, 859–871.
- [38] Hantschel, O.; Nagar, B.; Guettler, S.; Kretschmar, J.; Dorey, K.; Kuriyan, J.; Superti-Furga, G. A myristoyl/phosphotyrosine switch regulates c-Abl. *Cell* **2003**, *112* (6), 845-857.
- [39] Brasher, B.B.; Van Etten, R.A. c-Abl has high intrinsic tyrosine kinase activity that is stimulated by mutation of the Src homology 3 domain and by autophosphorylation at two distinct regulatory tyrosines. *J. Biol. Chem.* **2000**, *275* (45), 35631-35637.
- [40] Colicelli, J. ABL tyrosine kinases: evolution of function, regulation, and specificity. *Sci. Signal.* **2010**, *3* (139), re6.
- [41] Bradley, W.D.; Koleske, A.J. Regulation of cell migration and morphogenesis by Abl-family kinases: emerging mechanisms and physiological contexts. *J. Cell Sci.* **2009**, *122* (Pt 19), 3441-3454.
- [42] Greuber, E.K.; Smith-Pearson, P.; Wang, J.; Pendergast, A.M. Role of ABL family kinases in cancer: from leukaemia to solid tumours. *Nat. Rev. Cancer.* **2013**, *13* (8), 559-571.

Chapter II

Novel pyrazolo[3,4-d]pyrimidine as c-Src/Abl kinases inhibitors: synthesis and biological evaluation for CML treatment.

1. Introduction

1.1 Chronic Myeloid Leukemia (CML)

Chronic Myeloid Leukemia (CML) is a blood cancer belonging to myeloproliferative disorders [1], identified in 1845 by Craige and Bennett [2,3]. At diagnosis, CML is characterized by marked overproduction of granulocytes resulting from neoplastic transformation of the pluripotent stem cell of the bone marrow during the hematopoietic process. The incidence in CML increases by age, with the average age of patients being 67 years. Moreover, statistics show that it occurs more frequently in men than in women. In 2012, 5430 cases were diagnosed in the United States and 610 patients died [4]. Three distinctive phases characterize CML progression [5]:

1. Chronic phase: during this initial phase there is an expansion of myeloid compartment but the cells retain their physiological capacity to differentiate. This phase has a duration of 4-6 years and responds to treatments. The typical symptoms are fatigue, anorexia, and weight loss, but 40% of patients are also asymptomatic, and in these patients, the diagnosis is based solely on an abnormality on physical examination, known as splenomegaly, which is found in no more than 50% of patients.

2. Accelerated phase: it has an average duration of 6-18 months. During this phase, the first immature cells begin to appear in the blood and the patients show progressive splenomegaly and myelofibrosis with a reduced response to treatment.

3. Blast phase: this is the final stage of disease where occurs the transformation into acute leukemia. The immature cells (blasts) dominate and survival is measured in weeks or months. Complete loss of drug response and bleeding complications may occur at this stage [6].

Approximately 95% of CML patients report a genetic alteration which generates the Philadelphia chromosome, typical hallmark of this tumor [7]. This chromosome, which was first described in 1960 by Nowell and Hungerford [8], derives from a genetic translocation between chromosome 9 and 22 (Figure 2.1) and encodes the Bcr-Abl chimeric protein kinase which plays a key role in the early development of CML [9].

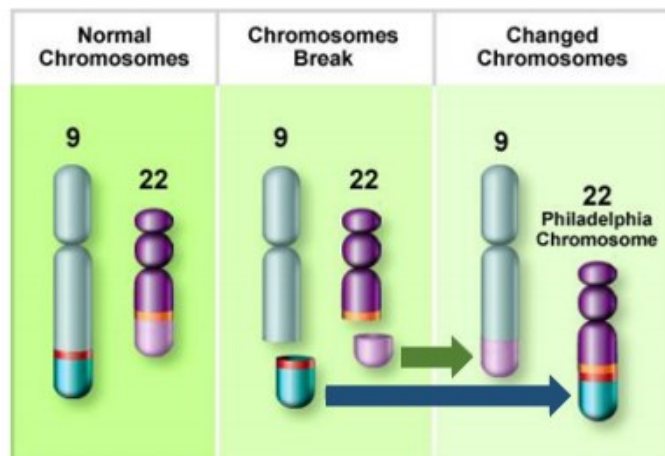


Figure 2.1 Gene translocation in Philadelphia chromosome.

Specific breakpoints in chromosomal translocation lead to distinct forms of Bcr-Abl (p185 Bcr-Abl, p210 Bcr-Abl, and p230 Bcr-Abl), all with constitutive kinase activity [10]. Aberrant activation of Bcr-Abl in CML triggers signaling pathways involved in altered processes of cell proliferation, transcription and survival [11]. PI3K activation triggers the signaling pathway that generates the non-phosphorylated form of Bad that binds members of the antiapoptotic Bcl family, thus intervening in cell survival processes (Figure 2.2). On the other hand, Ras and Jack-Stat activation were observed to induce mitogenic signals revealing a role in the cellular response to growth factors.

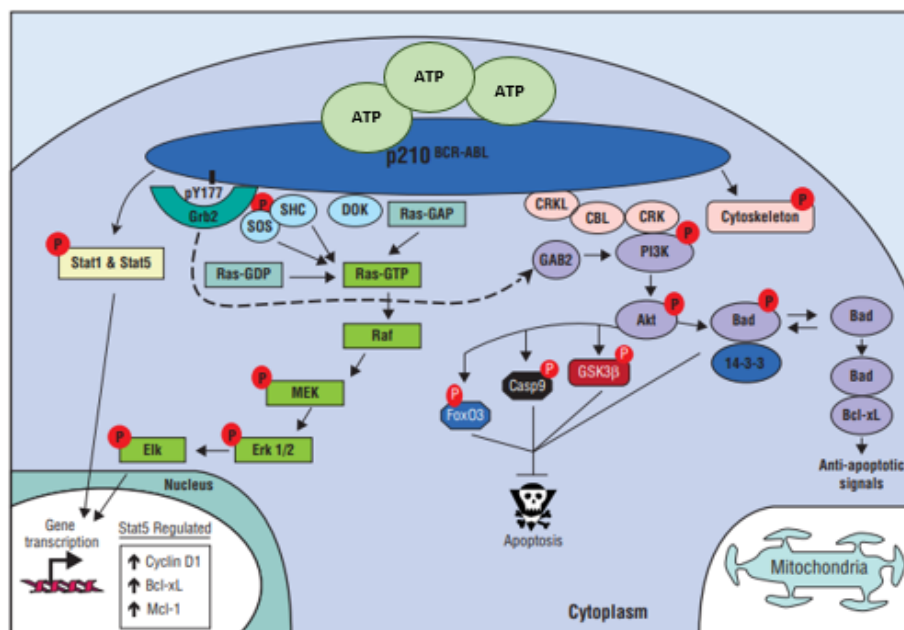


Figure 2.2 Bcr-Abl signaling pathways in CML.

1.2 Treatment options

Historically, the first treatment of CML was carried out in 1865 using Fowler's solution (1% Arsenic trioxide) [12,13]. Later, with the discovery of X-rays, radiation therapy was mainly used to alleviate symptoms caused by splenomegaly. In 1950, with the advancement of chemotherapy, busulfan and hydroxyurea were used in the treatment of CML, which for some years were the first choices treatment but did not eradicate the malignant clone of the disease. Lastly, in 1980, using Interferon alpha (IFN- α) this problem was overcome since it acts on the Philadelphia Chromosome, obtaining a favorable pharmacological effects such as an increase in patient survival. Nevertheless, it was poorly tolerated due to frequent and serious side effects. One currently valid remedy is the transplantation of stem cells into the bone marrow, which works in parallel with chemotherapy. Only with the arrival of the new millennium, following the targeted therapy approach, tyrosine kinase inhibitors (TKIs), which block the Bcr-Abl fusion protein involved in the development of the disease, have been used in the treatment of CML. Pharmacological inhibition by TKIs is the main strategy for the treatment of CML. In 2001, Imatinib **1** (Figure 2.3) was the first FDA and EMA approved targeted therapy for CML patients [14,15]. Imatinib has demonstrated significant clinical efficacy in the treatment of CML, producing durable responses and prolonged patient survival and has long been the drug

of choice for CML therapy [16]. Unfortunately, clinical complications due to the generation of Bcr-Abl fusion protein-dependent or independent resistance mechanisms may occur during treatment with Imatinib. Independent resistance mechanisms include metabolism of imatinib by CYP3A4, its uptake by efflux pumps, and overexpression of Src family kinase (SFK) proteins. [17,18]. On the other hand, among the mechanisms related to Bcr-Abl we find the amplification of the BCR-ABL gene with consequent marked expression of the fusion protein, and point mutations in the kinase domain of Bcr-Abl. The search for compounds able to overcome these resistances culminated with the approval of dual Src/Bcr-Abl inhibitor Dasatinib **2** (Figure 2.3) in 2006 [19]. Several studies have shown that Src is activated by Bcr-Abl and is implicated in imatinib resistance being responsible for the progression of the disease [20,21]. Dasatinib was active against all the imatinib resistant Bcr-Abl point mutations except T315I (substitution of the amino acid threonine 315 with an isoleucine) [22]. This gatekeeper mutation is the most difficult to overcome and confers additional oncogenic activities to Philadelphia chromosome positive leukemia. Ponatinib **3** (Figure 2.3), is the only approved drug active on the Abl(T315I) mutation [23]. However, shortly after its release on the market in 2012, Ponatinib was temporarily suspended due to dangerous cardiovascular toxicity and was subsequently re-authorized under further monitoring [24].

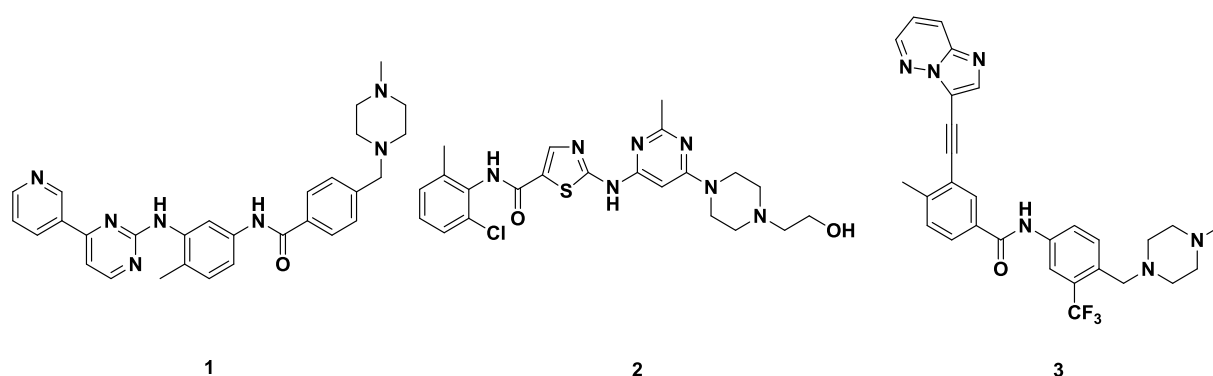


Figure 2.3 Structures of CML approved compounds Imatinib **1**, Dasatinib **2** and Ponatinib **3**.

2. State of the art

The identification of compounds capable of fighting CML and having good pharmacokinetic and toxicological properties appears as an important goal in medicinal chemistry. In this context, our research group produced a large library of small TKI molecules endowed with a pyrazolo[3,4-*d*]pyrimidine nucleus (Figure 2.4). These compounds act as ATP mimetics and are nanomolar/micromolar inhibitors of Src and/or Bcr-Abl [25,26]. Furthermore, pyrazolo[3,4-*d*]pyrimidines exhibit potent antiproliferative activity on cell lines expressing this tyrosine kinases.

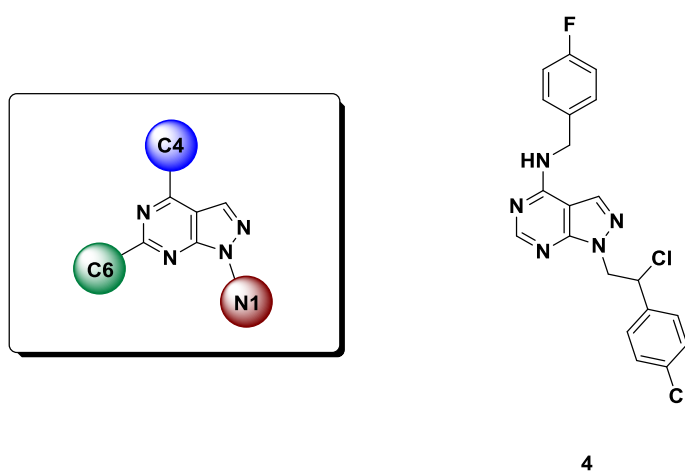
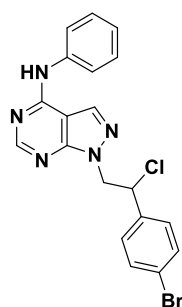


Figure 2.4 General structure of in-house pyrazolo[3,4-*d*]pyrimidines and compound S29 (4).

Over the years, several pyrazolo[3,4-*d*]pyrimidines have been investigated as anticancer agents against CML. S29 (4), the structure of which is reported in Figure 2.4, was one of the first molecules studied in this disease. S29 shows potent inhibition of target Abl(*wt*) with K_i value of 80 nM together with favorable antiproliferative activity in the cell line transducing wild type Bcr-Abl (IC_{50} range = 0.7-4.3 μ M) and three of the most common mutations associated to resistance to imatinib *in vivo* (T315I, Y253F and E255K) [27,28]. Another relevant member of this library of compounds is Si223 (Figure 2.5) which is of interest as it inhibits the mutated form Abl (T315I) with significant selectivity and high potency. Moreover, this pyrazolo[3,4-*d*]pyrimidine showed a 50% reduction in tumor volume in a *in vivo* mouse model expressing 32D-T315I CML cells [29].



5

Abl(T315I) K_i = 0.090 μ M
Abl(wt) K_i = 0.610 μ M

Figure 2.5 Structure and K_i values of Si223 (**5**).

Despite these intriguing biological activities, the pyrazolo[3,4-*d*]pyrimidines produced in-house by our research group generally suffer from substandard pharmacokinetic properties. Accordingly, different formulation studies have been performed [30,31] and several families of pyrazolo[3,4-*d*]pyrimidines have been designed and synthesized with the aim of identifying anticancer agents with optimized pharmacokinetic profiles [32]. In particular, the combination of molecular modeling studies with organic synthesis has facilitated the development of multiple generations of pyrazolo[3,4-*d*]pyrimidines with a good balance of efficacy and water solubility. Recently, an X-ray crystallography study of Src in complex with compound **6** (Figure 2.6) coupled with a Monte Carlo/Free energy perturbation (MC/FEP) analysis suggested that the introduction of a hydroxyl group in the *meta* position on the aniline ring in C4 could lead to favorable ΔG values [33]. These predicted values are expected to greatly increase the enzymatic inhibitory potency of the corresponding compounds. Based on this structure-based hypothesis, a set of pyrazolo[3,4-*d*]pyrimidines bearing a hydroxyphenyl substituent on the nitrogen at C4 position of the core scaffold was synthesized. Derivative **7** (Figure 2.6) was found to be more potent than **6** (70 nM vs 240 nM against Src) in agreement with the computational prediction and both R,S enantiomers showed the same inhibitory potency on the target [33]. The MC/FEP analysis also suggested the introduction of a chlorine atom in the *ortho* position on the aniline ring [34]. Thus, during my first year of PhD I worked on the synthesis of a small set of compounds (**8a-I**) characterized by this substitution, thus obtaining new potent c-Src inhibitors, which exhibited K_i values in the low nanomolar range. The results of this research have been the subject of a scientific publication [34].

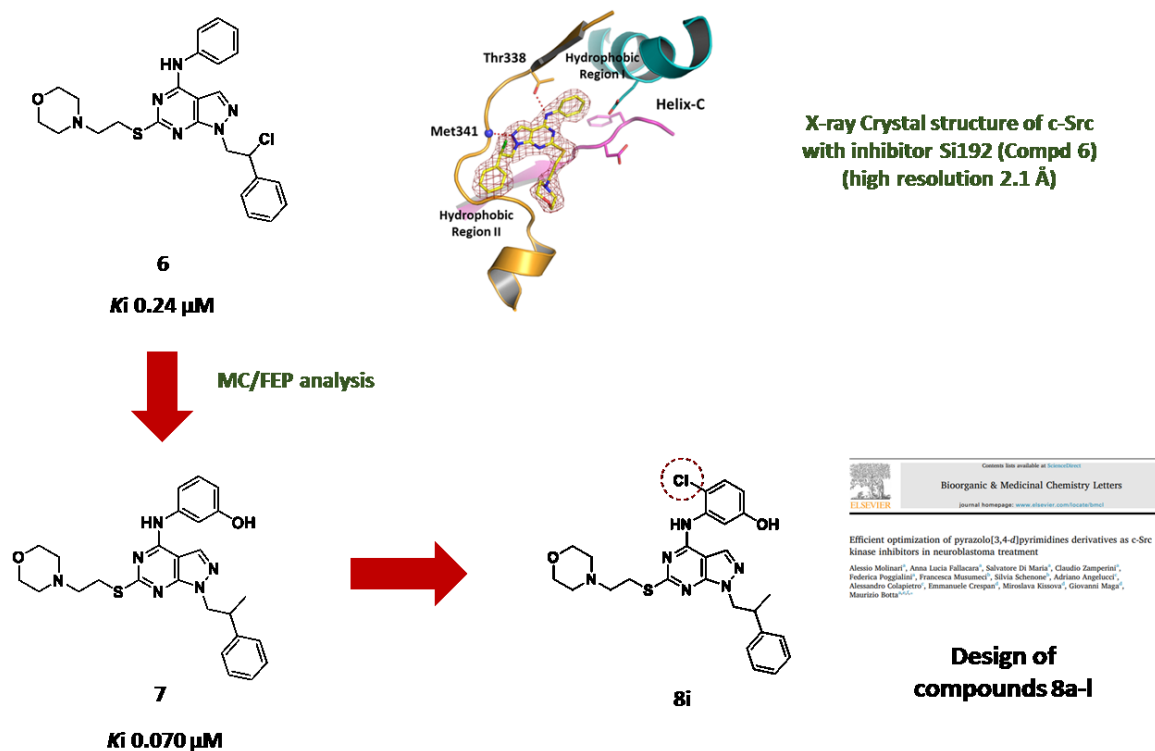


Figure 2.6 Optimization process of in-house pyrazolo[3,4-*d*]pyrimidines **6**, **7**, and **8**.

Hence, the validity of the *in silico* prediction was confirmed with these data, thus revealing a promising model to follow for the future design of new potent tyrosine kinases inhibitors as anticancer agents.

3. Aim of the project

In this project I worked on the synthesis of novel pyrazolo[3,4-*d*]pyrimidine derivatives with the objective of discover effective agents for the CML treatment. Considering that many pyrazolo[3,4-*d*]pyrimidines acting as c-Src inhibitors often also showed activity toward Bcr-Abl and based on the high homology between their kinase domains, the set of compounds 8a-l (described by *Molinari et al.* [34]) was screened in order to investigate the pharmacological anti-leukemia properties. In this section, with the aim of generating other potent c-Src/Abl inhibitors and expanding the SAR, a set of second generation compounds was synthesized and analyzed by enzymatic assay. Based on this preliminary result, compounds were selected and tested on the mutated isoform of Abl(T315I) and on the immortalised K562 cell lines, isolated from a patient with CML in blast crisis. Subsequently, for selected compounds the *in vitro* PK properties, such as water solubility, membrane permeability and metabolic stability on liver microsomes, were studied.

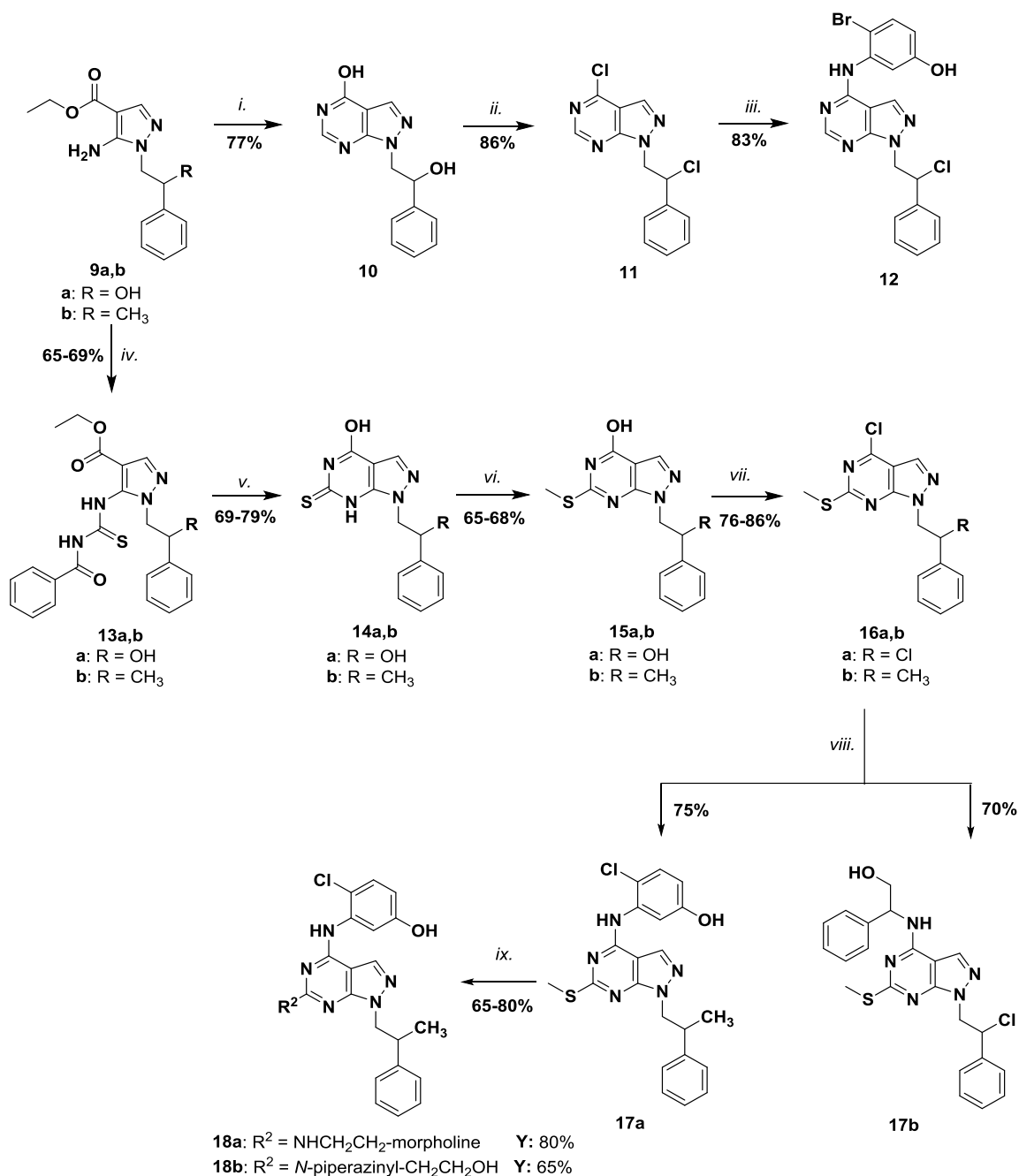
Results

4.1 Synthesis

The synthetic pathway toward new generation compounds follows the classical approach used by our research group for the preparation of pyrazolo[3,4-*d*]pyrimidine derivatives [35]. The intermediates **9a,b** were the starting points for obtaining the C6-substituted and C6-unsubstituted derivatives **12**, **17b** and **18a,b** (Scheme I). In detail, the synthesis of C6-unsubstituted pyrazolo[3,4-*d*]pyrimidine **12** started with the cyclization of compound **9a** with formamide at 190 °C for 8 h to obtain compound **10**, which is reacted with the Vilsmeier complex (POCl₃/DMF 1:1) to yield the dihalogenated derivative **11**. Aromatic nucleophilic substitution reaction of **11** with an excess of 3-amino-4-bromophenol in absolute ethanol gave the final compound **12**.

Preparation of C6-substituted compounds employed a different synthetic approach. Compounds **9a,b** reacted with benzoyl isothiocyanate in anhydrous THF at reflux for 6 hours giving the key intermediates **13a,b** which were subsequently cyclized in 2N NaOH at reflux to obtain the pyrazolo[3,4-*d*]pyrimidin-4-ones **14a,b**. Alkylation of the nucleophilic thiocarbonyl group with iodomethane in dry THF generated compounds **15a,b** as white solids. The following treatment of **15a,b** with the Vilsmeier complex in dry CHCl₃ at reflux allowed to obtain **16a,b**, which on reaction with appropriate amines afforded the compounds **17a** and **17b**. Compound **17a** was oxidized by using *m*-chloroperbenzoic acid in anhydrous dichloromethane at rt and then the sulfone group was displaced by 4-(2-aminoethyl)morpholine or 1-(2-hydroxyethyl)piperazine in butanol/DMSO (2:1) at 120 °C in order to obtain compounds **18a,b**.

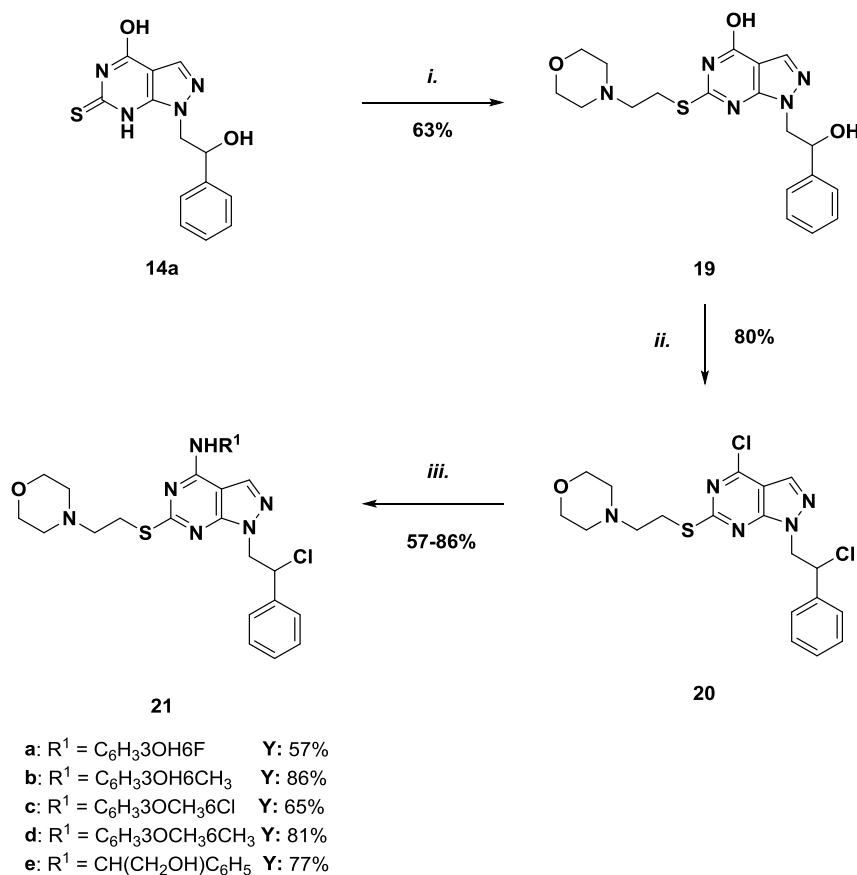
Scheme I. Synthesis of compounds 12, 17b and 18a,b.



Reagents and conditions: *i.*) NH₂CHO, 190 °C, 8 h; *ii.*) POCl₃, dry DMF, dry CHCl₃, reflux, 3.5 h; *iii.*) 3-amino-4-bromophenol, EtOH, 80 °C, 4 h; *iv.*) benzoylthiocyanate, dry THF, reflux, 6 h; *v.*) 2 N NaOH, reflux, 5 h; *vi.*) CH₃I, dry THF, reflux, 10 h; *vii.*) POCl₃, dry DMF, dry CHCl₃, reflux, 4 h; *viii.*) appropriate amine, EtOH, 80 °C, 4-10 h; *ix.*) a. *m*CPBA, dry DCM, rt, 2.5 h; b. 4-(2-aminoethyl)morpholine or 1-(2-hydroxyethyl)piperazine, butanol/ DMSO 2:1, 120 °C, 12 h.

The synthesis of 6-(2-morpholin-4-ylethyl)thio derivatives **21a-e** started from the key intermediate **14a** (Scheme II). Alkylation of the latter with 4-(2-chloroethyl)morpholine hydrochloride on thiocarbonyl group gave the intermediate **19**. Then Vilsmeier reaction followed by nucleophilic aromatic substitution with appropriate aminophenol in EtOH at reflux provided compounds **21a-e**.

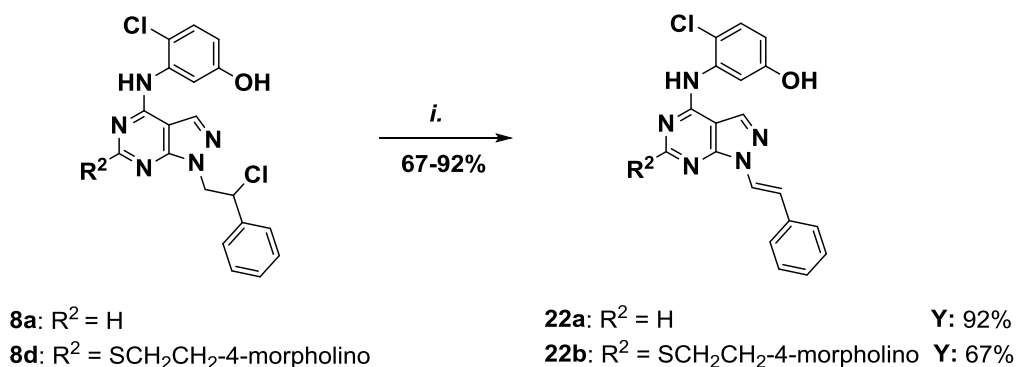
Scheme II. Synthesis of compounds **21a-e**.



Reagents and conditions: *i.*) 4-(2-chloroethyl)morpholine hydrochloride, NaOH, EtOH, DMF, reflux, 3h; *ii.*) POCl₃, dry DMF, dry CHCl₃, reflux, 3.5 h; *iii.*) appropriate aminophenol, EtOH, 80° C, 12-24 h.

Compounds **22a,b** were obtained from the first generation compounds **8a,d** via elimination reaction in the presence of 2 N NaOH as reported in Scheme III. Both **22a,b** showed *trans* geometry for the double bond in N1-styryl chain, as demonstrated by the coupling constant values $J=14.6$ and $J=15.0$ Hz (**22a** and **22b**, respectively) between the two hydrogen atoms.

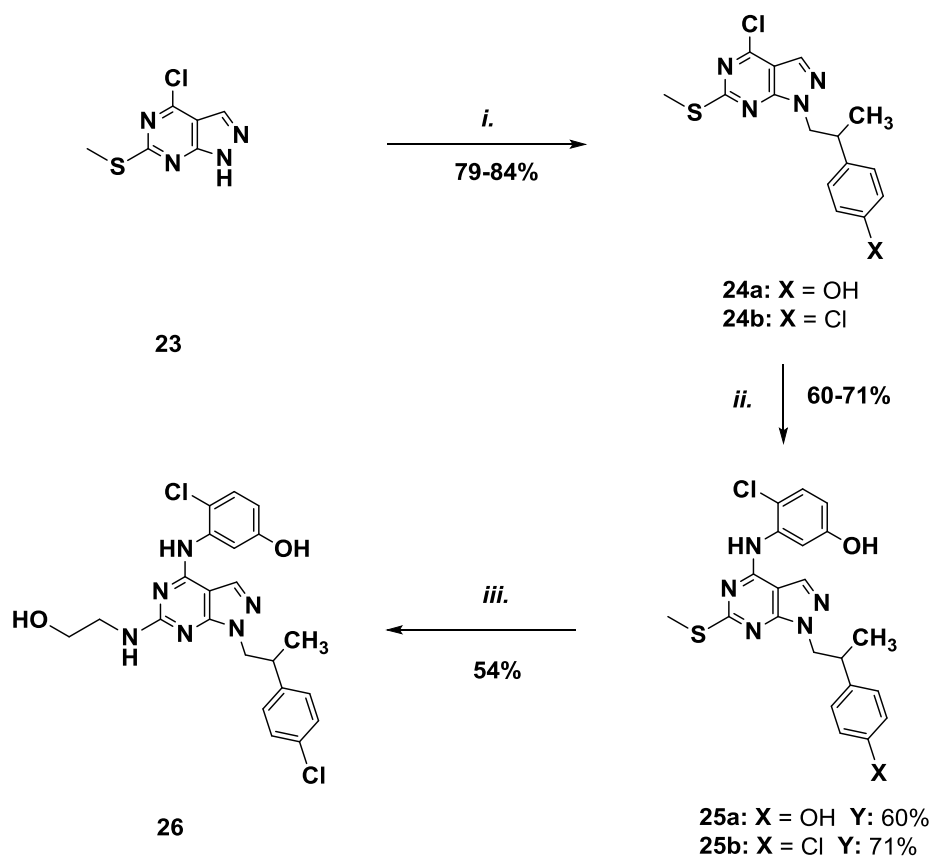
Scheme III. Synthesis of compounds 22a,b.



Reagents and conditions: *i.*) 3.5 N NaOH, absolute EtOH, reflux, 10 h.

A different synthetic approach was used in the preparation of compounds **25a,b** and **26** (Scheme IV). The starting compound **23**, previously described in the literature [26], was reacted in the N1 position with arylethanols using a microwave-irradiated Mitsunobu reaction.

Scheme IV. Synthesis of compounds 25a,b and 26.

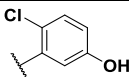
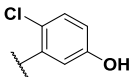
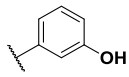
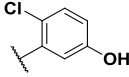
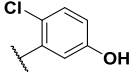
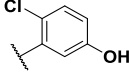
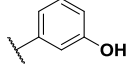
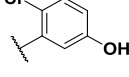


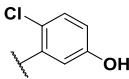
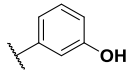
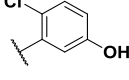
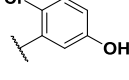
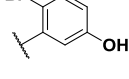
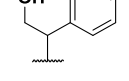
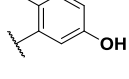
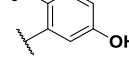
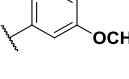
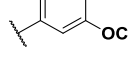
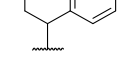
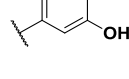
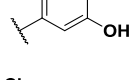
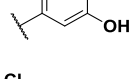
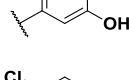
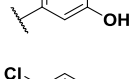
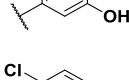
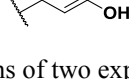
Reagents and conditions: *i.*) appropriate alcohol, Ph₃P, DIAD, dry THF, μ W: 100 °C, 3 min, 250 psi; *ii.*) 3-amino-4-chlorophenol, EtOH, reflux, 12; *iii.*) 1. *m*CPBA, dry DCM, rt, 2 h; 2. DMSO/butanol (1:2), ethanolamine, reflux, 8 h.

The aromatic nucleophilic substitution of **24a** or **24b** with 3-amino-4-chlorophenol, under reflux conditions in absolute ethanol, allowed us to obtain compounds **25a** and **25b**. The insertion at C-6 of a polar chain (compound **26**) was achieved by oxidation of the methylthio group of compound **25b** with *m*-chloroperbenzoic acid followed by replacement of the sulfone or sulfoxide group by the nucleophilic attack of ethanolamine in butanol/DMSO mixture (2:1).

3.2 Biological assays and SAR considerations

Table 1. Biological evaluation of first and second generation compounds. Enzyme inhibition and cell viability data.

Compd	A	X	R ¹	R ²	Biological Data ^a		
					Abl(<i>wt</i>) Ki (nM)	c-Src Ki (nM)	K562 cells IC ₅₀ (μM)
8a	CH ₂ CH(Cl)	H		H	2.7	17.0	0.0906 ± 1.4
8b	CH ₂ CH(Cl)	H		SCH ₃	14.0	3.5	-
8c	CH ₂ CH(Cl)	H		SCH ₂ CH ₂ -4-morpholino	n.d.	190.0	-
8d	CH ₂ CH(Cl)	H		SCH ₂ CH ₂ -4-morpholino	2.0	3.5	>10
8e	CH ₂ CH(Cl)	H		NHCH ₂ CH ₂ OH	3.7	74.0	>10
8f	CH ₂ CH(CH ₃)	H		H	16.5	120.0	5.75 ± 0.61
8g	CH ₂ CH(CH ₃)	H		SCH ₃	540.0	840.0	-
8h	CH ₂ CH(CH ₃)	H		SCH ₃	16.6	50.0	0.60 ± 0.07

8i	CH ₂ CH(CH ₃)	H		SCH ₂ CH ₂ -4-morpholino	35.0	60.0	>10
8j	CH ₂ CH(CH ₃)	H		NHCH ₂ CH ₂ OH	161.0	300.0	0.0612 ± 1.5
8k	CH ₂ CH(CH ₃)	H		NHCH ₂ CH ₂ OH	5.2	23.0	0.0508 ± 1.2
8l	CH ₂ CH(CH ₃)	H		NHCH ₂ CH ₂ NH ₂	28.2	33.0	-
12	CH ₂ CH(Cl)	H		H	91.0	58.5	>10
17b	CH ₂ CH(Cl)	H		SCH ₃	n.d.	n.d.	-
21a	CH ₂ CH(Cl)	H		SCH ₂ CH ₂ -4-morpholino	175.8	147.6	-
21b	CH ₂ CH(Cl)	H		SCH ₂ CH ₂ -4-morpholino	14.6	9.1	>10
21c	CH ₂ CH(Cl)	H		SCH ₂ CH ₂ -4-morpholino	n.d.	n.d.	-
21d	CH ₂ CH(Cl)	H		SCH ₂ CH ₂ -4-morpholino	n.d.	n.d.	-
21e	CH ₂ CH(Cl)	H		SCH ₂ CH ₂ -4-morpholino	n.d.	n.d.	-
18a	CH ₂ CH(CH ₃)	H		NHCH ₂ CH ₂ -4-morpholino	11.3	85.2	>10
18b	CH ₂ CH(CH ₃)	H		<i>N</i> -piperazinyl-CH ₂ CH ₂ OH	400.5	159.5	-
22a	CH=CH	H		H	0.05	3.7	0.48 ± 0.05
22b	CH=CH	H		SCH ₂ CH ₂ -4-morpholino	20.0	3.0	>10
25a	CH ₂ CH(CH ₃)	OH		SCH ₃	22.5	77.0	7.76 ± 1.2
25b	CH ₂ CH(CH ₃)	Cl		SCH ₃	19.2	158.5	6.46 ± 0.5
26	CH ₂ CH(CH ₃)	Cl		NHCH ₂ CH ₂ OH	15.1	19.8	0.59 ± 0.7

^a Values are the means of two experiments; n.d. not determined; - not tested.

All compounds reported in Table 1 are characterized by a pyrazolo[3,4-*d*]pyrimidine core decorated with different chains in N1, C4 and C6 positions (Figure 2.4). The X-ray crystallographic study of c-Src complexed with the inhibitor **6**, as reported in Tintori *et al* [33], highlighted the N1 and the NH on C4 position of the pyrazolo-pyrimidine ring as key features for the protein-ligand interaction. Furthermore, the crystal structure of the complex pointed out the presence of the I and II hydrophobic regions in the kinase site which can accommodate different substituents. Starting from these data and taking into account the high homology between protein kinases c-Src and Abl in the catalytic site, we decided to explore the chemical space around the two hydrophobic pockets through the synthesis and the biological evaluation of new sets of pyrazolopyrimidine derivatives. In order to define SARs that adequately correlate the substituents on the scaffold to the enzymatic inhibitory activity toward the protein kinase c-Src or Abl, compounds have been designed which bear point changes on the aminophenol ring located in C4-position of the pyrazolo[3,4-*d*]pyrimidine nucleus combined with different chains on N1 and C6. The presence of the chlorine atom on the *ortho* position of the aminophenol ring is essential for having a favorable inhibitory activity towards targeted tyrosine kinases. In particular, members of the first generation compounds **8a**, **8b**, **8d** and **8e** possess high inhibitory activity against Abl and c-Src kinases. Compound **8d** indeed, bearing the thioethylmorpholino chain in C6, resulted the most active derivative among compounds **8a-l** with a K_i value of 2 and 3.5 nM towards Abl and Src, respectively. For this reason, most of the second generation compounds maintain the same substituents at N1 and C6 positions, while the effect of point modification at C4 has been explored. The replacement of the chlorine atom (**8d**) with a methyl group afforded the slightly less active compound **21b** ($K_i = 14.6$ nM for Abl, $K_i = 9.1$ nM for c-Src) which on the other hand showed significantly increased water solubility (0.029 $\mu\text{g/mL}$ for compound **8d** vs 0.125 $\mu\text{g/mL}$ for compound **21b**, Table 3). On the other hand, the replacement of the chlorine atom with the smaller and more electronegative fluorine atom (compound **21a**) causes a decrease in the inhibitory activity on kinases. The enzymatic inhibitory activity was completely lost through the alkylation of phenol hydroxyl group in the compounds **21c** and **21d**. This reveals the crucial importance of this OH group in the enzymatic inhibition mechanism as a possible hydrogen bond donor towards amino acids of the kinases site. As can be noticed in Table 1, it was observed that compounds bearing a 2-chloro-2-phenylethyl chain in N1 (**8a-e**) are generally more active than the corresponding 2-phenylpropyl derivatives (**8f-l**), although they exhibit a lower metabolic stability evaluated on human liver microsomes (Table 3). Among the last generation compounds, derivative **22b**, bearing the same decoration pattern of **8d** in C4 and C6, but a styryl chain in N1, showed a favorable inhibitory activity, with K_i values of 20 and 3 nM towards Abl and Src, respectively, thereby suggesting

this chain as a promising substituent to design future inhibitors. In particular, the compound **22b** revealed a considerable ability to inhibit the mutated isoform of Abl, T315I, if compared with other compounds reported in Table 2. This effect could be due to the presence of N1-styryl chain, as a similar effect has been observed for the analogue C4-unsubstituted compound **22a**.

Table 2. Screening of selected compounds against Abl(T315I)

Compd	Abl(T315I) inhibition %	
	10 μ M	100 μ M
8a	0	0
8d	18	34
8e	0	11
8f	0	26
8h	9.8	64.7
8j	0	0
8k	0	0
12	0	0
21b	0	5
18a	0	24.8
22a	17	37
22b	69.2	94.7
25a	0	7
25b	0	0
26	0	0

However, despite the favorable results in terms of enzymatic inhibition and membrane permeability, all compounds with a thioethyl morpholinyl chain that were tested on K562 cell culture (i.e. **8d**, **8i**, **21b**, **22b**) showed low antiproliferative activity and water solubility, which prevented their further development. With the aim of improving solubility in water, compound **18a** was obtained by replacing the sulfur atom in the thioethylmorpholine chain of **8i** with a hydrogen bond donor NH group. Consequently, **18a** exhibits significantly greater water solubility (0.550 μ g/mL) than its analog **8i** (Table 3). The unsubstituted C6 derivatives (**8a**, **8f**, **12** and **22a**) provide on average good K_i values on c-Src/Abl (Table 1), though a noticeable inhibition of K562 cell viability was observed only for compound **8a** only (IC₅₀ value: 90 nM). Even if this category of derivatives shows an appreciable permeability of biological membranes, unfortunately it has an unsatisfactory water solubility and metabolic stability.

A notable increase in water solubility was observed for **8j** (134.2 $\mu\text{g/mL}$), obtained through the introduction of the ethanolamine side chain at C6 of the pyrazolo[3,4-*d*]pyrimidine scaffold.

Table 3. *In vitro* ADME of selected compounds.

Compd	<i>In vitro</i> ADME			
	Water solubility ($\mu\text{g/mL}$) ^a	Pampa Papp. 10^{-6} cm/sec	Metabolic stability (%) ^b	Metabolite formation ^c
8a	0.053	4.39	86.3	M2= 7.6 ^e M3= 6.1 ^f
8b	0.038	3.23	96.4	M1=0.90 ^d M1=1.35 ^d M2=1.08 ^e M3=0.16 ^f
8c	0.197	4.44	98.7	
8d	0.029	9.74	96.9	M1= 0.7 ^d M2= 1.5 ^e M3= 0.9 ^f
8e	0.042	2.7	97.2	M1=2.8 ^d
8f	0.062	2.51	86.1	M1= 13.9 ^d
8g	0.100	6.81	99.0	
8h	0.044	8.33	92.7	M1=6.1 ^d M1=1.2 ^d
8i	0.031	11.2	97.9	M3=1.05 ^f M3=1.14 ^f
8j	134.2	0.2	99.4	M3=0.62 ^f
8k	0.103	0.1	97.9	M3=2.13 ^f
12	0.052	5.97	96.7	M1= 2.2 ^d M2= 1.1 ^e
21b	0.125	4.24	98.6	M1=1.4 ^d
18a	0.550	4.08	95.3	M1=4.7 ^d
22a	0.048	6.02	98.8	M3=1.2 ^f
22b	0.036	5.50	97.6	M1=1.98 ^d M1=0.40 ^d
25b	0.039	6.14	96.9	M3=0.7 ^f M3=2.4 ^f
26	0.061	4.14	96.9	M3=3.1 ^f

^a Determined by UV/LC-MS; ^b Metabolic stability was assessed using human liver microsomes; ^c Protocol applied; ^d M1 = M-HCl+O (-36 + 16); ^e M2 = M-Cl+OH (-35 + 17); ^f M3 = M+OH (+16).

This polar chain influences some pharmacokinetic properties but preserves the favorable enzymatic inhibition typical of novel aminophenol derivatives. In addition, derivatives **8j** and **8k** reveal K562 antiproliferative activity of 60 nM and 50 nM, respectively, resulting the most potent molecules among cell screening candidates.

In order to explore other hydrophobic kinase regions, an additional decoration on **8k** structure was realized through the *para* chlorine atom substitution on the phenylpropyl chain. As a result, compound **26** showed a potent kinase inhibition, as reported in Table 1, while it reveals an unsatisfactory inhibition of K562 cell viability (IC₅₀ value: 590 nM). However, the lipophilic contribute of the chlorine atom decreases its water solubility while improving its membrane permeability as reported in Table 3. Finally, C6 thiomethyl derivatives **25a** and **25b** exhibited significant inhibitory activity against the target kinases but are characterized by unfavorable in vitro ADME profile and antiproliferative activity on K562 cell cultures.

4. Conclusion

Thanks to the possibility of using an easy and versatile synthetic approach, a significant number of pyrazolo[3,4-*d*]pyrimidine derivatives were synthesized which allowed to identify significant SARs. Some members of this new family of compounds gave favorable results in the CML study, in particular compounds **8a**, **8j** and **8k** which showed high inhibition of c-Src/Abl(wt) kinase activity as well as of K562 cell viability. Molecular modeling studies, using docking and molecular dynamics approaches, have shed light on the behavior of these three inhibitors in the Abl enzymatic pocket. On the other hand, inhibitory activity towards mutated Abl (T315I) was displayed only by compounds **22a** and **22b**, both characterized by a styryl chain in the N1 position of the pyrazolo[3,4-*d*]pyrimidine scaffold. However, this preliminary study allowed us to evaluate a new family of derivatives and to select the most promising compounds for the future in vivo preclinical development as possible anti-leukemic agents.

5. Materials and method

All commercially available chemicals were used as purchased. DCM was dried over calcium hydride. Anhydrous reactions were run under a positive pressure of dry N₂ or argon. TLC was carried out using Merck TLC plates silica gel 60 F254. Chromatographic purifications were performed on columns packed with Merk 60 silica gel, 23-400 mesh, for flash technique. ¹H NMR and ¹³C NMR spectra were recorded on a Bruker Avance DPX400 (at 400 MHz for ¹H and 101 MHz for ¹³C). Chemical shifts are reported relative to tetramethylsilane at 0.00 ppm. Mass spectra (MS) data were obtained using an Agilent 1100 LC/MSD VL system (G1946C) with a 0.4 mL min⁻¹ flow rate using a binary solvent system of 95:5 = CH₃OH:H₂O. UV detection was monitored at 254 nm. MS were acquired in positive and negative mode scanning over the mass range m/z 50-1500. The following ion source parameters were used: drying gas flow, 9 mL min⁻¹; nebulizer pressure, 40 psi; drying gas temperature, 350 °C. The accurate masses were measured by the LTQ-Orbitrap XL (Thermo Scientific, Bremen, Germany) mass spectrometer interfaced with an electrospray ionization (ESI) source characterized by spray voltage 4.5 kV, nitrogen as sheat gas (10 a.u). The resolution of accurate masses is 30000. MS/MS spectra were recorded with an isolation windows of 2 mass units, collision energy of 15, 16 or 17 V and Helium as collision gas.

Microwave Irradiation Experiments.

Microwave irradiation experiments were realized using a CEM Discover Synthesis Unit (CEM Corp., Matthews, NC). The machine consists of a continuous focused microwave power delivery system with operator selectable power output from 0 to 300 W. The temperature of the contents of the vessels was monitored using a calibrate infrared temperature control mounted under the reaction vessel. All the experiments were performed using a stirring option whereby the contents of the vessel are stirred by means of a rotating magnetic plate located below the floor of the microwave cavity and a Teflon-coated magnetic stir bar in the vessel.

Procedures

The synthesis of the final compounds **8a-l** and intermediates **9a,b** and **23** have been already reported by us [26,34,35].

1-(2-Hydroxy-2-phenylethyl)-1,5-dihydro-4H-pyrazolo[3,4-d]pyrimidin-4-one (10)

Ethyl 5-amino-1-(2-hydroxy-2-phenylethyl)-1H-pyrazole-4-carboxylate **9a** (5 mmol, 1.50 g) was suspended in formamide (180 mmol, 7.2 mL) and the mixture was heated at 190 °C for 8 hours. After cooling at room temperature, water was added (40 mL) and the product was filtered by suction. Recrystallization from absolute ethanol afforded the intermediate **10** as a white solid. Yield: (77%). M.p.: 270-271 °C (dec.). ¹H NMR (400 MHz, DMSO-d₆): δ 12.06 (s, 1H), 8.04 (s, 1H), 8.00 (s, 1H), 7.30-7.27 (m, 4H), 7.23 (dd, *J* = 9, 4.4 Hz, 1H), 5.59 (bs, 1H), 5.24-4.89 (m, 1H), 4.47-4.41 (m, 1H), 4.32-4.27 (m, 1H). MS: 255.5 m/z [M-1]⁻.

4-Chloro-1-(2-chloro-2-phenylethyl)-1H-pyrazolo[3,4-d]pyrimidine (11)

The Vilsmeier complex, previously prepared from fresh distilled POCl₃ (35 mmol, 3.26 mL) and dry DMF (35 mmol, 2.71 mL) at 0 °C, was added to a suspension of 1-(2-hydroxy-2-phenylethyl)-1,5-dihydro-pyrazolo[3,4-*d*]pyrimidin-4-one **10** (3.50 mmol, 900 mg) in anhydrous CHCl₃ (25 mL). The mixture was stirred at reflux for 3.5 hours, then saturated solution of NaHCO₃ was added until pH 7. The organic layer was washed with 5% LiCl aqueous solution (3 x 80 mL), dried (Na₂SO₄) and concentrated under reduced pressure obtaining a crude oil. The latter was purified by flash chromatography using petroleum ether (PE) (b.p. 40-60 °C)/EtOAc (96:4) as the eluent to afford the desired compound **11** as a white solid. Yield: (86%). M.p.: 105-106 °C. ¹H NMR (400 MHz, CDCl₃): δ ppm 8.75 (s, 1H), 8.18 (s, 1H), 7.43 (d, *J* = 7.2 Hz, 2H), 7.37-7.19 (m, 3H), 5.55-5.53 (m, 1H), 5.11-5.06 (m, 1H), 4.89-4.84 (m, 1H). MS: 292.1 m/z [M-1]⁻.

General procedure for the synthesis of compounds 13a,b

Benzoyl isothiocyanate (24 mmol, 4.02 g) was added dropwise to a solution of the suitable intermediate **9a,b** (22 mmol) in dry THF (70 mL) precooled at 0 °C. Then the mixture was refluxed for 6 hours and THF was removed under reduced pressure affording a pale yellow oil.

The crude was purified by flash chromatography using PE (b.p. 40-60 °C)/EtOAc (95:5) as the eluent to obtain the desired compound **13a** or **13b** as a white solid.

Ethyl 5-[[(benzoylamino)carbonothioyl]amino]-1-(2-hydroxy-2-phenylethyl)-1H-pyrazole-4-carboxylate (13a)

Yield: (65%). M.p.: 171-172 °C. ¹H NMR (400 MHz, CDCl₃): δ ppm 12.05 (s, 1H), 8.70 (s, 1H), 8.02 (s, 1H), 7.98-7.05 (m, 10H), 4.68-4.58 (m, 1H), 3.97-4.20 (m, 5H), 1.29 (t, *J* = 7.0, 3H). MS: 437.4 m/z [M-1]⁻.

Ethyl-5-[[(benzoylamino)carbonothioyl]amino]-1-(2-phenylpropyl)-1H-pyrazole-4-carboxylate (13b)

Yield: (69%). M.p.: 112-113 °C (dec.). ¹H NMR (400 MHz, CDCl₃): δ ppm 11.71 (bs, 1H), 9.58 (s, 1H), 7.94 (s, 1H), 7.89 (d, *J* = 7.2 Hz, 2H), 7.63 (t, *J* = 7.2 Hz, 1H), 7.50 (t, *J* = 7.6, 2H), 7.25-7.19 (m, 3H), 7.09 (d, *J* = 7.6, 2H), 4.20-4.04 (m, 4H), 3.50-3.42 (m, 1H), 1.28 (m, 3H), 1.21 (d, *J* = 6.8, 3H). MS: 436.3 m/z [M-1]⁻.

General procedure for the synthesis of compounds 14a,b

A suspension of the compound **13a,b** (12 mmol) in 2 N NaOH (75 mL) was refluxed for 5 hours. The clear solution was cooled at 0 °C, diluted with water (35 mL) and then acidified with glacial acetic acid to obtain a white precipitate. The crude was filtered by suction and recrystallized from absolute ethanol affording a white solid.

1-(2-Hydroxy-2-phenylethyl)-6-thioxo-1,5,6,7-tetrahydro-4H-pyrazolo[3,4-d]pyrimidin-4-one (14a)

Yield: (69%). M.p.: 264-267 °C. ¹H NMR (400 MHz, DMSO-d₆): δ ppm 13.32 (bs, 1H), 12.14 (s, 1H), 7.99-7.95 (m, 1H), 7.46-7.28 (m, 5H), 5.64 (bs, 1H), 4.94-4.90 (m, 1H), 4.66-4.58 (m, 1H), 4.26-4.19 (m, 1H). MS: m/z 287.6 [M-1]⁻.

1-(2-Phenylpropyl)-6-thioxo-1,5,6,7-tetrahydro-4H-pyrazolo[3,4-d]pyrimidin-4-one (14b)

Yield: (79%). M.p.: 192-193 °C. ¹H NMR (400 MHz, DMSO-d₆): δ ppm 13.24 (bs, 1H), 12.05 (s, 1H), 7.89 (s, 1H), 7.28-7.17 (m, 5H), 4.49-4.43 (m, 1H), 4.36-4.31 (m, 1H), 3.32-3.26 (m, 1H), 1.14-1.12 (m, 3H). MS: 285.4 m/z [M+1]⁺.

General procedure for the synthesis of compounds 15a,b

Iodomethane (17 mmol, 2.47 g) was added dropwise to a solution of the intermediate **14a,b** (3 mmol) in dry THF (15 mL) precooled at 0 °C. The reaction mixture was refluxed for 10 hours and, after cooling, the solvent was evaporated. The crude oil was purified by flash chromatography eluting with DCM/MeOH (97:3) to give the desired compound **15a** or **15b** as a white solid.

1-(2-Hydroxy-2-phenylethyl)-6-(methylthio)-1,5-dihydro-4H-pyrazolo[3,4-d]pyrimidin-4-one (15a)

Yield: (68%). M.p.: 208-210 °C (dec.). ¹H NMR (400 MHz, DMSO-d₆): δ ppm 12.30 (bs, 1H), 7.94 (s, 1H), 7.26-7.23 (m, 5H), 5.62 (bs, 1H), 5.09-5.06 (m, 1H), 4.45-4.38 (m, 1H), 4.35-4.30 (m, 1H), 2.49 (s, 3H) MS: m/z 299.8 [M-1]⁻.

6-(Methylthio)-1-(2-phenylpropyl)-1,5-dihydro-4H-pyrazolo[3,4-d]pyrimidin-4-one (15b)

Yield: (65%). M.p.: 162-163 °C. ¹H NMR (400 MHz, DMSO-d₆): δ ppm 10.72 (bs, 1H), 7.99 (s, 1H), 7.22-7.10 (m, 5H), 4.45-4.35 (m, 2H), 3.47-3.44 (m, 1H), 2.55 (s, 3H), 1.28-1.25 (m, 3H). MS: m/z 298.9 [M-1]⁻.

General procedure for the synthesis of compounds 16a,b

The Vilsmeier complex, previously prepared from fresh distilled POCl₃ (23.5 mmol, 2.2 mL) and anhydrous DMF (23.5 mmol, 1.8 mL) at 0 °C, was added to a suspension of the suitable intermediate **15a,b** (2.35 mmol) in anhydrous CHCl₃ (17 mL). The mixture was refluxed for 4 h, then saturated solution of NaHCO₃ was added until pH 7. The organic phase was washed with 5% LiCl aqueous solution (4 x 50 mL), dried (Na₂SO₄) and concentrated under reduced pressure. The crudes were purified by flash chromatography using a mixture of PE (b.p. 40-60 °C)/EtOAc (98:2) as the eluent to afford the desired compounds **16a,b**.

4-Chloro-1-(2-chloro-2-phenylethyl)-6-(methylthio)-1H-pyrazolo[3,4-d]pyrimidine (16a)

White solid. Yield: (76 %). M.p.: 95-96 °C. ¹H NMR (400 MHz, CDCl₃): δ ppm 8.00 (s, 1H), 7.38-7.24 (m, 5H), 5.53-5.45 (m, 1H), 4.97-4.92 (m, 1H), 4.84-4.78 (m, 1H), 2.60 (s, 3H). MS: 337.6 m/z [M-1]⁻.

4-Chloro-6-(methylthio)-1-(2-phenylpropyl)-1H-pyrazolo[3,4-d]pyrimidine (16b)

Yellow oil. Yield: (86 %). ¹H NMR (400 MHz, CDCl₃): δ ppm 7.97 (s, 1H), 7.25-7.15 (m, 5H), 4.57 (dd, *J* = 12.5, 7.9 Hz, 1H), 4.49 (dd, *J* = 12.5, 7.9 Hz, 1H), 3.55-3.50 (m, 1H), 2.58 (s, 3H), 1.29-1.23 (m, 3H). MS: m/z 319.2 [M+1]⁺.

1-(2-Hydroxy-2-phenylethyl)-6-[(2-morpholin-4-ylethyl)thio]-1,5-dihydro-4H-pyrazolo[3,4-d]pyrimidin-4-one (19)

A solution of NaOH (5.20 mmol, 208 mg) in absolute ethanol (5 mL) and 4-(2-chloroethyl)morpholine hydrochloride (3.46 mmol, 644 mg) were added to a solution of 1-(2-hydroxy-2-phenylethyl)-6-thioxo-1,5,6,7-tetrahydro-4H-pyrazolo[3,4-d]pyrimidin-4-one **14a** (3 mmol, 1.00 g) in DMF (5 mL). The reaction mixture was refluxed for 3 hours, cooled and concentrated under reduced pressure. Cold water (60 mL) was added and the white solid was filtered, washed with water, and recrystallized from absolute ethanol. Yield: (63%). M.p.: 201-203 °C. ¹H NMR (400 MHz, DMSO-*d*₆): δ ppm 10.28 (bs, 1H), 7.93 (s, 1H), 7.35-7.19 (m, 5H), 5.57 (bs, 1H), 5.08-5.02 (m, 1H), 4.39-4.34 (m, 1H), 4.26-4.22 (m, 1H), 3.54-3.52 (m, 4H), 3.30-3.18 (m, 2H), 2.67-2.57 (m, 2H), 2.47-2.39 (m, 4H). MS: 401.4 m/z [M+1]⁺.

4-Chloro-1-(2-chloro-2-phenylethyl)-6-[(2-morpholin-4-ylethyl)thio]-1H-pyrazolo[3,4-d]pyrimidine (20)

The Vilsmeier complex, previously prepared from fresh distilled POCl₃ (21.2 mmol, 1.98 mL) and anhydrous DMF (21.2 mmol, 1.66 mL) at 0 °C, was added to a suspension of 1-(2-hydroxy-2-phenylethyl)-6-[(2-morpholin-4-ylethyl)-thio]-1,5-dihydro-4H-pyrazolo[3,4-d]pyrimidin-4-one **19** (2.12 mmol, 850 mg) in anhydrous CHCl₃ (15 mL). The mixture was refluxed for 3.5 h, then cooled at room temperature and treated with saturated solution of NaHCO₃ until pH 7. The organic layer was washed with 5% LiCl aqueous solution (4 x 80 mL), dried (Na₂SO₄) and concentrated under reduced pressure obtaining a crude oil. The latter was purified by flash chromatography eluting with PE (b.p. 40-60 °C)/EtOAc (96:4) to afford the desired compound

20 as a white solid. Yield: (80%). M.p.: 106-107 °C. ¹H NMR (400 MHz, CDCl₃): δ ppm 7.99 (s, 1H), 7.39-7.37 (m, 2H), 7.33-7.28 (m, 3H), 5.49-5.45 (m, 1H), 4.98-4.92 (m, 1H), 4.75-4.70 (m, 1H), 3.75-3.70 (m, 4H), 3.41-3.24 (m, 2H), 2.82-2.70 (m, 2H), 2.60-2.55 (m, 4H). MS: m/z 438.1 [M+1]⁺.

General procedure for the synthesis of compounds 24a,b

The suitable 2-phenyl-propan-1-ol derivative (0.90 mmol) was added to an ice-cooled solution of 4-chloro-6-(methylthio)-1*H*-pyrazolo[3,4-*d*]pyrimidine **23** (0.60 mmol, 120 mg) and triphenylphosphine (0.90 mmol, 235 mg) in anhydrous THF (9 mL). Then, diisopropyl azodicarboxylate (DIAD) (0.90 mmol, 181 mg) was added dropwise. After stirring at 4 °C for 20 minutes, the reaction was allowed to warm to room temperature. The solution was heated under μW irradiation at 100 °C for 3 minutes (λ = 300 Wmax, P = 250 psi). THF was removed under reduced pressure and the crude was purified by flash chromatography using PE (40-60 °C)/AcOEt 9:1 as the eluent to obtain the desired compound **24a** or **24b**.

*4-{2-[4-Chloro-6-(methylthio)-1*H*-pyrazolo[3,4-*d*]pyrimidin-1-yl]-1-methylethyl}phenol (24a)*

Yellow oil. Yield: 79%. ¹H NMR (400 MHz, CDCl₃): δ ppm 7.99 (s, 1H), 6.85-6.79 (m, 4H), 5.29 (s, 1H), 3.68-3.60 (m, 2H), 3.59-3.47 (m, 1H), 2.55 (s, 3H), 1.22-1.20 (m, 3H). MS: 334.2 m/z [M-1]⁻.

*4-Chloro-1-[2-(4-chlorophenyl)propyl]-6-(methylthio)-1*H*-pyrazolo[3,4-*d*]pyrimidine (24b)*

Yellow oil. Yield: 84%. ¹H NMR (400 MHz, CDCl₃): δ ppm 7.97 (s, 1H), 7.18-7.10 (m, 4H), 4.53-4.48 (m, 2H), 3.58-3.47 (m, 1H), 2.59 (s, 3H), 1.29-1.27 (m, 3H). MS: 352.4 m/z [M-1]⁻.

*4-Bromo-3-{{1-(2-chloro-2-phenylethyl)-1*H*-pyrazolo[3,4-*d*]pyrimidin-4-yl}amino}phenol (12)*

3-Amino-4-bromophenol (0.32 mmol, 60 mg) was added to a suspension of 4-chloro-1-(2-chloro-2-phenylethyl)-1*H*-pyrazolo[3,4-*d*]pyrimidine **11** (0.171 mmol, 50 mg) in absolute ethanol (3 mL), and the reaction mixture was stirred at reflux for 4 hours. After cooling, ethanol was removed under reduced pressure and the crude was purified by flash chromatography using

DCM/MeOH (98:2 to 97:3) as the eluent and recrystallized in DCM to obtain the final compound **12** (white solid). Yield: 83%. M.p.: 225-227 °C. ¹H NMR (400 MHz, Acetone-d₆): δ ppm 9.06 (bs, 1H), 8.43 (s, 1H), 8.11 (s, 1H), 7.84 (d, *J* = 2.1 Hz, 1H), 7.53 (d, *J* = 7.6 Hz, 2H), 7.45 (d, *J* = 8.6 Hz, 1H), 7.40-7.29 (m, 3H), 7.23 (dd, *J* = 8.6, 2.1 Hz, 1H), 5.68-5.65 (m, 1H), 5.06-4.99 (m, 1H), 4.88-4.82 (m, 1H). ¹³C NMR (100 MHz, Acetone-d₆) δ 155.21, 154.52, 154.10, 153.98, 139.97, 138.39, 132.66, 131.63, 128.89, 128.67, 127.52, 113.75, 109.16, 103.33, 101.24, 60.40, 53.17. MS: 444.9 m/z [M-1]⁻.

General procedure for the synthesis of compounds 17b, 21a-e, and 25a-b

The suitable amino alcohol (0.69 mmol) was added to a suspension of the intermediate **16a**, **20** or **23a,b** (0.23 mmol) in absolute ethanol (4 mL), and the reaction mixture was stirred at reflux for 4-10 hours, monitoring the reaction by TLC. After cooling, ethanol was removed under reduced pressure and the crude was purified by flash chromatography using a mixture of DCM/MeOH (98:2 to obtain compounds **17b** and **21a-e**, 97:3, to obtain compounds **25a,b**) as the eluent to afford the desired compounds as white solids.

2-([1-(2-Chloro-2-phenylethyl)-6-(methylthio)-1H-pyrazolo[3,4-d]pyrimidin-4-yl]amino)-2-phenylethanol (17b)

White solid. Yield: 70%. M.p.: 169-171 °C (dec.). ¹H NMR (400 MHz, Acetone-d₆): δ ppm 8.14-8.11 (m, 1H), 7.50-7.43 (m, 4H), 7.34-7.18 (m, 6H), 5.80-5.54 (m, 1H), 5.52-5.45 (m, 1H), , 4.87-4.81 (m, 1H), 4.77-4-70 (m, 1H), 4.48 (bs, 1H), 3.86-3.83 (m, 2H), 2.44 (s, 3H). ¹³C NMR (100 MHz, Acetone-d₆) δ 169.19, 155.59, 154.59, 141.22, 138.48, 132.53, 128.88, 128.66, 128.22, 127.61, 127.16, 127.01, 123.37, 65.23, 60.31, 57.00, 53.02, 13.34. MS: m/z 438.5 [M-1]⁻.

3-([1-(2-Chloro-2-phenylethyl)-6-[(2-morpholin-4-ylethyl)thio]-1H-pyrazolo[3,4-d]pyrimidin-4-yl]amino)-4-fluorophenol (21a)

Yield: 57%. M.p.: 118-119 °C. ¹H NMR (400 MHz, CDCl₃): δ ppm 10.5 (bs, 1H) 8.35 (s, 1H), 7.93 (s, 1H), 7.44-7.42 (m, 2H), 7.34-7.22 (m, 4H), 7.10-6.91 (m, 1H), 6.63-6.42 (m, 1H), 5.54-5.50 (m, 1H), 4.95-4.90 (m, 1H), 4.73-4.67 (m, 1H), 3.84-3.82 (m, 4H), 3.46-3.25 (m, 2H), 2.90-2.85 (m, 2H), 2.67-2.62 (m, 4H). ¹³C NMR (100 MHz, CDCl₃): δ ppm 168.14, 155.11, 152.99, 152.83, 137.88, 130.44, 128.99, 128.71, 127.46, 126.44, 118.98, 115.47, 109.93, 108.85, 99.47, 65.43, 60.12, 60.06, 53.87, 53.80, 27.24. MS: 528.2 m/z [M-1]⁻.

3-({1-(2-Chloro-2-phenylethyl)-6-[(2-morpholin-4-ylethyl)thio]-1H-pyrazolo[3,4-d]pyrimidin-4-yl}amino)-4-methylphenol (21b)

Yield: 86%. M.p.: 203-206 °C. ¹H NMR (400 MHz, CDCl₃): δ ppm 9.22 (bs, 1H), 7.43-7.24 (m, 8H), 7.05 (d, *J* = 8.2 Hz, 1H), 6.67 (d, *J* = 7.8 Hz, 1H), 5.68-5.26 (m, 1H), 4.84 (dd, *J* = 14.0, 8.9 Hz, 1H), 4.63 (dd, *J* = 14.0, 5.8 Hz, 1H), 3.78-3.72 (m, 4H), 3.40-3.17 (m, 2H), 2.92-2.67 (m, 2H), 2.60-2.52 (m, 4H), 2.16 (s, 3H). ¹³C NMR (100 MHz, CDCl₃): δ ppm 167.86, 155.69, 155.13, 153.93, 150.73, 143.49, 137.99, 136.09, 132.18, 131.52, 128.91, 128.71, 127.32, 114.37, 99.17, 66.14, 60.21, 59.25, 53.66, 32.09, 27.32, 16.69. MS: 524.5 m/z [M-1]⁻.

N-(2-Chloro-5-methoxyphenyl)-1-(2-chloro-2-phenylethyl)-6-[(2-morpholin-4-ylethyl)thio]-1H-pyrazolo[3,4-d]pyrimidin-4-amine (21c)

Yield: 65%. M.p.: 97-99 °C (dec.). ¹H NMR (400 MHz, CDCl₃): δ ppm 11.2 (bs, 1H), 7.91 (s, 1H), 7.58-7.54 (m, 1H), 7.45-7.24 (m, 6H), 6.74-6.68 (m, 1H), 5.53-5.49 (m, 1H), 4.94-4.89 (m, 1H), 4.73-4.67 (m, 1H), 3.81 (s, 3H), 3.79-3.73 (m, 4H), 3.52-3.13 (m, 2H), 2.97-2.69 (m, 2H), 2.65-2.57 (m, 4H). ¹³C NMR (100 MHz, CDCl₃): δ ppm 177.95, 168.86, 162.61, 158.91, 153.84, 137.93, 135.27, 131.39, 129.83, 129.01, 128.79, 127.31, 111.96, 109.73, 98.93, 66.88, 60.22, 58.16, 55.69, 53.90, 53.53, 27.60. MS: 560.1 m/z [M+1]⁺.

1-(2-Chloro-2-phenylethyl)-N-(5-methoxy-2-methylphenyl)-6-[(2-morpholin-4-ylethyl)thio]-1H-pyrazolo[3,4-d]pyrimidin-4-amine (21d)

Yield: 81%. M.p.: 96-98 °C (dec.). ¹H NMR (400 MHz, CDCl₃): δ ppm 11.1 (bs, 1H), 7.40-7.37 (m, 3H), 7.32-7.20 (m, 3H), 6.92-6.86 (m, 2H), 6.60 (s, 1H), 5.48-5.44 (m, 1H), 4.88-4.82 (m, 1H), 4.66-4.60 (m, 1H), 3.75 (s, 3H), 3.74-3.70 (m, 4H), 3.42-3.18 (m, 2H), 2.89-2.67 (m, 2H), 2.59-2.56 (m, 4H), 2.13 (s, 3H). ¹³C NMR (100 MHz, CDCl₃): δ ppm 168.52, 158.69, 156.58, 155.34, 138.04, 136.34, 132.99, 131.84, 128.92, 128.73, 127.53, 127.25, 114.25, 113.46, 97.76, 66.94, 60.21, 58.36, 55.46, 53.69, 53.57, 27.55, 16.98. MS: 540.1 m/z [M+1]⁺.

2-({1-(2-Chloro-2-phenylethyl)-6-[(2-morpholin-4-ylethyl)thio]-1H-pyrazolo[3,4-d]pyrimidin-4-yl}amino)-2-phenylethanol (21e)

Yield: 77%. M.p.: 94-98 °C (dec.). ¹H NMR (400 MHz, CDCl₃): δ ppm 10.53 (bs, 1H), 7.72 (s, 1H), 7.37-7.29 (m, 10H), 6.12 (bs, 1H), 5.50-5.42 (m, 1H), 5.35-5.25 (m, 1H), , 4.88-4.83 (m, 1H), 4.65-4.60 (m, 1H), 4.02-3.98 (m, 2H), 3.75-3.68 (m, 4H), 3.30-3.21 (m, 2H), 2.78-2.70 (m, 2H), 2.57-2.0 (m, 4H). ¹³C NMR (100 MHz, CDCl₃): δ ppm 168.51, 156.03, 154.74, 143.71, 138.93, 138.00, 129.04, 128.98, 128.77, 128.11, 127.33, 126.79, 114.96, 108.35, 66.61, 66.27, 60.27, 58.37, 57.78, 53.80, 53.47, 44.78. MS: 538.8 m/z [M+1]⁺.

4-Chloro-3-{{1-[2-(4-hydroxyphenyl)propyl]-6-(methylthio)-1H-pyrazolo[3,4-d]pyrimidin-4-yl}amino}phenol (25a)

Yield: 60%. M.p.: 100-102 °C (dec.). ¹H NMR (400 MHz, Acetone-d₆): δ ppm 8.79 (bs, 1H), 8.60 (s, 1H), 8.02 (s, 1H), 7.68 (s, 1H), 7.50 (s, 1H), 7.34 (d, *J* = 8.7 Hz, 1H), 6.89 (d, *J* = 8.3 Hz, 2H), 6.79 (d, *J* = 8.7 Hz, 1H), 6.61 (d, *J* = 8.3 Hz, 2H), 5.13-5.04 (m, 1H), 3.18 (dd, *J* = 13.6, 8.8 Hz, 1H), 3.01 (dd, *J* = 13.6, 6.7 Hz, 1H), 2.47 (s, 3H), 1.52 (d, *J* = 6.7 Hz, 3H). ¹³C NMR (100 MHz, Acetone-d₆): δ ppm 168.44, 156.72, 155.83, 154.50, 154.25, 136.46, 135.92, 130.93, 130.04, 129.91, 129.25, 118.72, 114.91, 114.24, 98.64, 54.60, 52.20, 41.17, 18.95. MS: 441.7 m/z [M-1]⁻.

4-Chloro-3-{{1-[2-(4-chlorophenyl)propyl]-6-(methylthio)-1H-pyrazolo[3,4-d]pyrimidin-4-yl}amino}phenol (25b)

White solid. Yield: 71%. M.p.: 173-175 °C. ¹H NMR (400 MHz, Acetone-d₆): δ ppm 8.66 (bs, 1H), 7.64 (s, 1H), 7.49 (s, 1H), 7.34 (d, *J* = 8.7 Hz, 1H), 7.28-7.23 (m, 4H), 6.81 (dd, *J* = 8.7, 2.8 Hz, 1H), 4.51 (dd, *J* = 13.6, 7.7 Hz, 1H), 4.41 (dd, *J* = 13.6, 7.7 Hz, 1H), 3.59-3.50 (m, 1H), 2.51 (s, 3H), 1.26 (d, *J* = 7.7 Hz, 3H). ¹³C NMR (100 MHz, Acetone-d₆): δ ppm 168.95, 156.76, 154.74, 154.63, 142.63, 135.84, 131.72, 131.30, 130.07, 129.01, 128.30, 128.26, 118.85, 114.40, 98.39, 52.90, 39.39, 18.37, 13.20. MS: 459.3 m/z [M-1]⁻.

General procedure for the synthesis of compounds 18a,b

3-Chloroperbenzoic acid (*m*-CPBA) (2.25 mmol, 388 mg) was added to a solution of 4-chloro-3-{{6-(methylthio)-1-(2-phenylpropyl)-1H-pyrazolo[3,4-*d*]pyrimidin-4-yl}amino}phenol **8h**

(1.07 mmol, 380 mg) in anhydrous DCM (20 mL) at 0 °C and the reaction mixture was stirred at room temperature for 2.5 h. After removal of solvent under vacuum, the residue was dissolved in EtOAc (180 mL) and saturated solution of NaHCO₃ was added dropwise until pH 7. Organic phase was washed with brine, dried (Na₂SO₄), filtered and concentrated under reduced pressure, affording a mixture of sulfone and sulfoxide derivatives, which was employed in the next step without additional purification. The crude was dissolved in DMSO/butan-1-ol (1:2) (6 mL), 4-(2-aminoethyl)morpholine or 1-(2-hydroxyethyl)piperazine (5.35 mmol) was added and the reaction mixture was stirred at 120 °C for 12 h. Water was added and the product was extracted with EtOAc (5 x 60 mL), washed with brine (40 mL), dried (Na₂SO₄), and concentrated under reduced pressure. The residual 1-butanol and DMSO were removed under nitrogen flow affording a brown solid. The crudes were purified by flash chromatography, using PE (b.p. 40-60 °C)/EtOAc (8:2 to 6:4) as the eluent, followed by crystallization from DCM to obtain final compounds **18a** and **18b** as white solid.

4-Chloro-3-{[6-[(2-morpholin-4-ylethyl)amino]-1-(2-phenylpropyl)-1H-pyrazolo[3,4-d]pyrimidin-4-yl]amino}phenol (18a)

White solid. Yield: 80% over two steps. M.p.: 102-104 °C. ¹H NMR (400 MHz, Acetone-d₆): δ ppm 10.11 (bs, 1H), 8.27 (bs, 1H), 7.81 (bs, 1H), 7.71 (s, 1H), 7.27-7.24 (m, 5H), 7.16-7.13 (m, 1H), 6.68-6.64 (m, 1H), 6.10-6.05 (m, 1H), 4.43-4.17 (m, 2H), 3.71-3.43 (m, 7H), 2.59-2.55 (m, 2H), 2.48-2.43 (m, 4H), 1.18 (d, *J* = 6.9 Hz, 3H). ¹³C NMR (100 MHz, Acetone-d₆): δ ppm 161.19, 156.61, 155.19, 144.14, 136.46, 130.93, 129.68, 128.36, 127.22, 127.18, 126.42, 117.45, 113.21, 112.80, 96.11, 66.36, 57.82, 53.71, 52.61, 40.25, 39.70, 18.53. MS: *m/z* 507.1 [M-1].

4-Chloro-3-{[6-[4-(2-hydroxyethyl)piperazin-1-yl]-1-(2-phenylpropyl)-1H-pyrazolo[3,4-d]pyrimidin-4-yl]amino}phenol (18b)

White solid. Yield: 65% over two steps. M.p.: 99-103 °C (dec.). ¹H NMR (400 MHz, Acetone-d₆): δ ppm 8.21 (bs, 1H), 7.66 (s, 1H), 7.59 (s, 1H), 7.29-7.22 (m, 5H), 7.16-7.12 (m, 1H), 6.72-6.68 (m, 1H), 4.38 (dd, *J* = 13.5, 7.0 Hz, 1H), 4.28 (dd, *J* = 13.5, 8.4 Hz, 1H), 3.84-3.77 (m, 4H), 3.64-3.61 (m, 3H), 3.55-3.48 (m, 1H), 2.53-2.50 (m, 6H), 1.21 (d, *J* = 7.0 Hz, 3H). ¹³C NMR (100 MHz, Acetone-d₆): δ ppm 166.36, 149.39, 148.73, 147.82, 144.08, 136.39, 130.89,

129.78, 128.32, 127.20, 126.34, 125.72, 113.14, 108.99, 103.53, 60.32, 58.62, 53.20, 52.64, 44.30, 39.81, 18.55. MS: m/z 506.7 [M-1]⁻

General procedure for the synthesis of compounds 22a,b

A solution of 3.5 N NaOH (4 mL) was added to derivative **8a** or **8d** (0.12 mmol) dissolved in ethanol (3 mL) and the reaction mixture was refluxed for 10 hours. Ethanol was removed under reduced pressure and the residual basic solution was neutralized by adding dropwise 0.1 N HCl until pH 7. The aqueous solution was extracted with EtOAc (3 x 60 mL), then the organic phase was dried (Na₂SO₄) and evaporated under reduced pressure. The crudes were recrystallized from ethanol affording the desired compounds **22a,b** as white solids.

(E)-4-Chloro-3-{[1-(2-phenylvinyl)-1H-pyrazolo[3,4-d]pyrimidin-4-yl]amino}phenol (22a)

Yield: 92%. M.p.: 278-280 °C. ¹H NMR (400 MHz, Acetone-d₆): δ ppm 8.93 (bs, 1H), 8.46 (s, 1H), 8.09 (d, *J* = 14.6 Hz, 1H), 7.95 (s, 1H), 7.62 (d, *J* = 7.5 Hz, 2H), 7.52 (d, *J* = 2.6 Hz, 1H), 7.45 (d, *J* = 14.6 Hz, 1H), 7.41-7.35 (m, 4H), 7.28 (t, *J* = 7.5 Hz, 1H), 6.85 (dd, *J* = 8.6, 2.6 Hz, 1H). ¹³C NMR (100 MHz, Acetone-d₆): δ ppm 156.92, 156.04, 155.88, 153.46, 135.83, 135.62, 133.49, 130.22, 128.82, 127.42, 126.22, 121.86, 119.12, 116.73, 114.72, 114.66, 101.75. MS: 362.7 m/z [M+1]⁺

(E)-4-Chloro-3-({6-[(2-morpholin-4-ylethyl)thio]-1-(2-phenylvinyl)-1H-pyrazolo[3,4-d]pyrimidin-4-yl}amino)phenol (22b)

Yield: 67%. M.p.: 189-191 °C. ¹H NMR (400 MHz, CDCl₃): δ ppm 8.42 (bs, 1H), 8.03 (s, 1H), 7.94 (d, *J* = 15.0 Hz, 1H), 7.65 (s, 1H), 7.54-7.48 (m, 3H), 7.35 (d, *J* = 15.0 Hz, 1H), 7.31-7.26 (m, 4H), 6.65-6.60 (m, 1H), 3.90-3.86 (m, 4H), 3.44-3.40 (m, 2H), 3.96-3.92 (m, 2H), 2.70-2.67 (m, 4H). ¹³C NMR (100 MHz, CDCl₃): δ ppm 172.01, 158.42, 157.64, 154.02, 138.71, 134.89, 132.23, 133.56, 129.31, 128.62, 128.59, 128.50, 127.91, 121.82, 107.3, 102.45, 100.56, 67.81, 57.45, 56.81, 29.90. MS: 508.7 m/z [M-1]⁻

4-Chloro-3-({1-[2-(4-chlorophenyl)propyl]-6-[(2-hydroxyethyl)amino]-1H-pyrazolo[3,4-d]pyrimidin-4-yl}amino)phenol (26)

m-CPBA (0.47 mmol, 80 mg) was added to a solution of 4-chloro-3-(1-(2-(4-chlorophenyl)propyl)-6-(methylthio)-1*H*-pyrazolo[3,4-*d*]pyrimidin-4-ylamino)phenol **25b** (0.22 mmol, 102 mg) in anhydrous DCM (10 mL) at 0 °C. The reaction mixture was stirred at room temperature for 2 hours. The solvent was removed by rotary evaporation and the residue was dissolved in EtOAc (170 mL), then it was treated with saturated solution of NaHCO₃ until pH 7. The organic layer was washed with brine, dried (Na₂SO₄) and concentrated under reduced pressure, affording a mixture of sulfone and sulfoxide derivatives. The mixture was dissolved in DMSO/*n*-butanol (1:2) (3 mL), ethanolamine (0.67 mmol, 40 μL) was added, and the reaction mixture was refluxed for 8 hours. The solvents were removed by air flow and the product was purified by flash chromatography using DCM/MeOH (99:1) as the eluent to obtain the compound **26** as a white solid. Yield: 54% over two steps. M.p.: 97-99 °C (dec.). ¹H NMR (400 MHz, Acetone-*d*₆): δ ppm 10.18 (bs, 1H), 8.27 (bs, 1H), 7.84 (s, 1H), 7.69 (s, 1H), 7.30-7.25 (m, 5H), 6.70-6.68 (m, 1H), 6.20-6.17 (m, 1H), 4.40-4.24 (m, 2H), 3.78-3.75 (m, 2H), 3.58-3.55(m, 3H), 3.09 (bs, 1H), 1.23-1.22 (m, 3H). ¹³C NMR (100 MHz, Acetone-*d*₆): δ ppm 161.54, 156.58, 155.21, 142.94, 136.39, 131.60, 130.93, 129.77, 129.60, 129.04, 128.27, 116.83, 113.08, 112.84, 96.10, 52.44, 44.18, 39.20, 18.44, 18.37. MS: 472.5 m/z [M+1]⁺.

6. References

- [1] Lee, S.J. Chronic myelogenous leukaemia. *Brit. J. Haematol.* **2000**, *111* (4), 993-1009.
- [2] Craigie, D. Case of disease of the spleen in which death took place in consequence of the presence of purulent matter in the blood. *Edinb. Med. Surg. J.* **1854**, *64* (165), 400-423.
- [3] Bennett, J.H.; Case of hypertrophy of the spleen and liver, in which death took place from suppuration of the blood. *Edinb. Med. Surg. J.* **1845**, *64*, 413-423.
- [4] Höglund, M.; Sandin, F.; Simonsson, B. Epidemiology of chronic myeloid leukaemia: an update. *Ann. Hematol.* **2015**, *94* (Suppl. 2), S241-S247.
- [5] Bonifacio, M.; Stagno, F.; Scaffidi, L.; Krampera, M.; Di Raimondo, F.; Management of chronic myeloid leukemia in advanced phase. *Front. Oncol.* **2019**, *9*, 1132.

- [6] Hehlmann, R.; How I treat CML blast crisis. *Blood* **2012**, *120* (4), 737–747.
- [7] Kang, Z.-J.; Liu, Y.-F.; Xu, L.-Z.; Long, Z.-J.; Huang, D.; Yang, Y.; Liu, B.; Feng, J.-X.; Pan, Y.-J.; Yan, J.-S.; Liu, Q. The Philadelphia chromosome in leukemogenesis. *Chin. J. Cancer* **2016**, *35* (1), 48.
- [8] Nowell, P.C.; Hungerford, D.A. A minute chromosome in human chronic granulocytic leukemia. *Science* **1960**, *132* (8), 1497.
- [9] Nowell, P.C. Discovery of the Philadelphia chromosome: a personal perspective. *J. Clin. Invest.* **2007**, *117* (8), 2033-2035.
- [10] Ross, T.S.; Mgbemena, V.E.; Re-evaluating the role of BCR/ABL in chronic myelogenous leukemia. *Mol. Cell. Oncol.* **2014**, *1* (3), e963450.
- [11] O'Hare, T.; Deininger, M.W.N.; Eide, C.A.; Clackson, T.; Druker, B.J. Targeting the BCR-ABL Signaling Pathway in Therapy-Resistant Philadelphia Chromosome-Positive Leukemia. *Clin. Cancer Res.* **2011**, *17* (2), 212-221.
- [12] Goldman J.M. Chronic myeloid leukemia: a historical perspective. *Sem. Hematol.* **2010**, *47* (4), 302–311.
- [13] Santos, F.; Kantarjian, H.; Quintás-Cardama, A.; Cortes, J. Evolution of Therapies for Chronic Myelogenous Leukemia. *Cancer J.* **2011**, *17* (6), 465–476.
- [14] Iqbal, N.; Iqbal, N. Imatinib: a breakthrough of targeted therapy in cancer. *Chemother. Res. Pract.* **2014**, *2014* (2), 357027.
- [15] Wei, G.; Rafiyath, S.; Liu, D.; First-line treatment for chronic myeloid leukemia: dasatinib, nilotinib, or imatinib. *J. Hematol. Oncol.* **2010**, *3* (1), 47.
- [16] Larson, R.A.; Druker, B.J.; Guilhot, F.; O'Brien, S.G.; Riviere, G.J.; Krahnke, T.; Gathmann, I.; Wang, Y.; IRIS (International Randomized Interferon vs STI571) Study Group. Imatinib pharmacokinetics and its correlation with response and safety in chronic-phase chronic myeloid leukemia: a subanalysis of the IRIS study. *Blood* **2008**, *111* (8), 4022-4028.
- [17] Van Erp, N.P.; Gelderblom, H.; O. Karlsson, M.; Li, J.; Zhao, M.; Ouwerkerk, J.; Nortier, J.W.; Guchelaar, H.-J.; Baker, S.D.; Sparreboom, A. Influence of CYP3A4 Inhibition on the Steady-State Pharmacokinetics of Imatinib. *Clin. Cancer Res.* **2007**, *13* (24), 7394-7400.
- [18] Quintás-Cardama, A.; Kantarjian, H.; Cortes, J. Targeting ABL and SRC kinases in chronic myeloid leukemia: experience with dasatinib. *Future Oncol.* **2006**; *2* (6), 655-665.

- [19] Keskin, D.; Sadri, S.; Eskazan, A.E. Dasatinib for the treatment of chronic myeloid leukemia: patient selection and special considerations. *Drug Des. Devel. Ther.* **2016**, *10*, 3355–3361.
- [20] Pene-Dumitrescu, T.; Smithgall, T.E. Expression of a Src family kinase in chronic myelogenous leukemia cells induces resistance to imatinib in a kinase-dependent manner. *J. Biol. Chem.* **2010**, *285* (28), 21446-21457
- [21] Bixby, D.; Talpaz, M. Mechanisms of resistance to tyrosine kinase inhibitors in chronic myeloid leukemia and recent therapeutic strategies to overcome resistance. *Hematology Am. Soc. Hematol. Educ. Program.* **2009**, *2009* (1), 461–476.
- [22] O'Hare, T.; Walters, D.K.; Stoffregen, E.P.; Jia, T.; Manley, P.W.; Mestan, J.; Cowan-Jacob, S.W.; Lee, F.Y.; Heinrich, M.C.; Deininger, M.W.N.; Druker, B.J. In vitro activity of Bcr-Abl inhibitors AMN107 and BMS-354825 against clinically relevant imatinib-resistant Abl kinase domain mutants. *Cancer Res.* **2005**, *65* (11), 4500-4505.
- [23] Huang, W.S.; Metcalf, C.A.; Sundaramoorthi, R.; Wang, Y.; Zou, D.; Thomas, R.M.; Zhu, X.; Cai, L.; Wen, D.; Liu, S.; Romero, J.; Qi, J.; Chen, I.; Banda, G.; Lentini, S.P.; Das, S.; Xu, Q.; Keats, J.; Wang, F.; Wardwell, S.; Ning, Y.; Snodgrass, J.T.; Broudy, M.I.; Russian, K.; Zhou, T.; Commodore, L.; Narasimhan, N.I.; Moheemad, Q.K.; Iuliucci, J.; Rivera, V.M.; Dalgarno, D.C.; Sawyer, T.K.; Clackson, T.; Shakespeare, W.C. Discovery of 3-[2-(imidazo[1,2-b]pyridazin-3-yl)ethynyl]-4-methyl-N-{4-[(4-methylpiperazin-1-yl)methyl]-3-(trifluoromethyl)phenyl}benzamide (AP24534), a potent, orally active pan-inhibitor of breakpoint cluster region-abelson (BCR-ABL) kinase including the T315I gatekeeper mutant. *J. Med. Chem.* **2010**, *53* (12), 4701-4719.
- [24] Gainor, J.F.; Chabner, B.A. Ponatinib: Accelerated Disapproval. *Oncologist* **2015**, *20* (8), 847-848.
- [25] Schenone, S.; Radi, M.; Musumeci, F.; Brullo, C.; Botta, M. Biologically driven synthesis of pyrazolo[3,4-*d*]pyrimidines as protein kinase inhibitors: an old scaffold as a new tool for medicinal chemistry and chemical biology studies. *Chem. Rev.* **2014**, *114* (14), 7189–7238.
- [26] Vignaroli, G.; Mencarelli, M.; Sementa, D.; Crespan, E.; Kissova, M.; Maga, G.; Schenone, S.; Radi, M.; Botta, M. Exploring the Chemical Space around the Privileged Pyrazolo[3,4-*d*]pyrimidine Scaffold: Toward Novel Allosteric Inhibitors of T315I-Mutated Abl. *ACS Comb. Sci.* **2014**, *16* (4), 168–175.

- [27] Santucci, M.A.; Corradi, V.; Mancini, M.; Manetti, F.; Radi, M.; Schenone, S.; Botta, M. C6-unsubstituted pyrazolo[3,4-*d*]pyrimidines are dual Src/Abl inhibitors effective against imatinib mesylate resistant chronic myeloid leukemia cell lines. *Chem. Med. Chem.* **2009**, *4* (1), 118-126.
- [28] Manetti, F.; Brullo, C.; Magnani, M.; Mosci, F.; Chelli, B.; Crespan, E.; Schenone, S.; Naldini, A.; Bruno, O.; Trincavelli, M.L.; Maga, G.; Carraro, F.; Martini, C.; Bondavalli, F.; Botta, M. Structure-based optimization of pyrazolo[3,4-*d*]pyrimidines as Abl inhibitors and antiproliferative agents toward human leukemia cell lines. *J. Med. Chem.* **2008**, *51* (5), 1252-1259.
- [29] Radi, M.; Tintori, C.; Musumeci, F.; Brullo, C.; Zamperini, C.; Dreassi, E.; Fallacara, A.L.; Vignaroli, G.; Crespan, E.; Zanolli, S.; Laurenzana, I.; Filippi, I.; Maga, G.; Schenone, S.; Angelucci, A.; Botta, M. Design, Synthesis, and Biological Evaluation of Pyrazolo[3,4-*d*]pyrimidines Active in Vivo on the Bcr-Abl T315I Mutant. *J. Med. Chem.* **2013**, *56* (13), 5382–5394.
- [30] Vignaroli, G.; Calandro, P.; Zamperini, C.; Coniglio, F.; Iovenitti, G.; Tavanti, M.; Colecchia, D.; Dreassi, E.; Valoti, M.; Schenone, S.; Chiariello, M.; Botta, M. Improvement of pyrazolo[3,4-*d*]pyrimidines pharmacokinetic properties: nanosystem approaches for drug delivery. *Sci. Rep.* **2016**, *6*, 21509.
- [31] Vignaroli, G.; Zamperini, C.; Dreassi, E.; Radi, M.; Angelucci, A.; Sanità, P.; Crespan, E.; Kissova, M.; Maga, G.; Schenone, S.; Musumeci, F.; Botta, M. Pyrazolo[3,4-*d*]pyrimidine Prodrugs: Strategic Optimization of the Aqueous Solubility of Dual Src/Abl Inhibitors. *ACS Med. Chem. Lett.* **2013**, *4* (7), 622–626.
- [32] Radi, M.; Dreassi, E.; Brullo, C.; Crespan, E.; Tintori, C.; Bernardo, V.; Valoti, M.; Zamperini, C.; Daigl, H.; Musumeci, F.; Carraro, F.; Naldini, A.; Filippi, I.; Maga, G.; Schenone, S.; Botta, M. Design, Synthesis, Biological Activity, and ADME Properties of Pyrazolo[3,4-*d*]pyrimidines Active in Hypoxic Human Leukemia Cells: A Lead Optimization Study. *J. Med. Chem.* **2011**, *54* (8), 2610–2626.
- [33] Tintori, C.; Fallacara, A.L.; Radi, M.; Zamperini, C.; Dreassi, E.; Crespan, E.; Maga, G.; Schenone, S.; Musumeci, F.; Brullo, C.; Richters, A.; Gasparrini, F.; Angelucci, A.; Festuccia, C.; Delle Monache, S.; Rauh, D.; Botta, M. Combining X-ray Crystallography and Molecular Modeling toward the Optimization of Pyrazolo[3,4-*d*]pyrimidines as Potent c-Src Inhibitors Active in Vivo against Neuroblastoma. *J. Med. Chem.* **2015**, *58* (1), 347–361.

[34] Molinari, A.; Fallacara, A.L., Di Maria, S.; Zamperini, C.; Poggialini, F.; Musumeci, F.; Schenone, S.; Angelucci, A.; Colapietro, A.; Crespan, E.; Kissova, M.; Maga, G.; Botta, M. Efficient optimization of pyrazolo[3,4-*d*]pyrimidines derivatives as c-Src kinase inhibitors in neuroblastoma treatment. *Bioorg. Med. Chem. Lett.* **2018**, *28* (21), 3454–3457.

[35] Radi, M.; Brullo, C.; Crespan, E.; Tintori, C.; Musumeci, F.; Biava, M.; Schenone, S.; Dreassi, E.; Zamperini, C.; Maga, G.; Pagano, D.; Angelucci, A.; Bologna, M.; Botta, M. Identification of potent c-Src inhibitors strongly affecting the proliferation of human neuroblastoma cells. *Bioorg. Med. Chem. Lett.* **2011**, *21* (19), 5928–5933.

Chapter III

Design by means of a merge-hybridization approach and synthesis of new pyrazolo[3,4-d]pyrimidine inhibitors active against the hepatocellular carcinoma (HCC)

1. Introduction

1.1 Hepatocellular Carcinoma (HCC)

Hepatocellular carcinoma (HCC) is the most common type of liver solid cancer and is the second leading cause of cancer related deaths worldwide. HCC has heterogeneous incidence, as it develops at all ages, and depends on some risk factors [1]. However, an epidemiological study found that the burden of HCC is higher in Africa and East Asia, despite its incidence and mortality are rapidly increasing in Europe and the United States. The genesis of HCC is a multistep process initiated by external stimuli that lead to genetic alterations in hepatocytes, resulting in proliferation, apoptosis, dysplasia and neoplasia [2]. Nevertheless, knowledge of the neoplastic transformation of hepatocytes in HCC is limited. Histologically, malignant hepatocytes exhibit all the characteristics of benign hepatocytes, with the exception of the iron granules accumulation. Cytoplasmic aggregates may include steatosis, fibrinogen (pale bodies), glycogen (clear cells) or glycoprotein inclusions and Mallory-Denk bodies [3]. Several factors associated with the aetiology of HCC have a direct influence on disease progression and include chronic liver damage caused by inflammation and fibrosis, infection by hepatitis B or hepatitis C virus, metabolic syndrome, alcohol abuse, and ingestion of the fungal metabolite aflatoxin B1. Liver cirrhosis progresses to HCC in 80-90% of the cases. Despite regular surveillance to detect incipient HCC in these patients, this cancer is often diagnosed at an advanced stage [4].

1.2 Treatment options and novel targets

The treatment options are represented mainly by surgical resection, liver transplantation, or ablation available for 30% of very early and early stage HCC patients (Figure 3.1), whereas palliative treatment is given in patients who cannot benefit from this type of care. Among palliative treatments, only chemoembolization has been proven to be effective, while other remedies are under investigation. Transcatheter arterial chemoembolization (TACE) is performed by cannulating the tumor feeding artery and releasing chemotherapeutic agents [5]. The impact of TACE is not clear, but an improvement in survival has been observed for patients diagnosed with intermediate stage of HCC and functional liver (Figure 3.1).

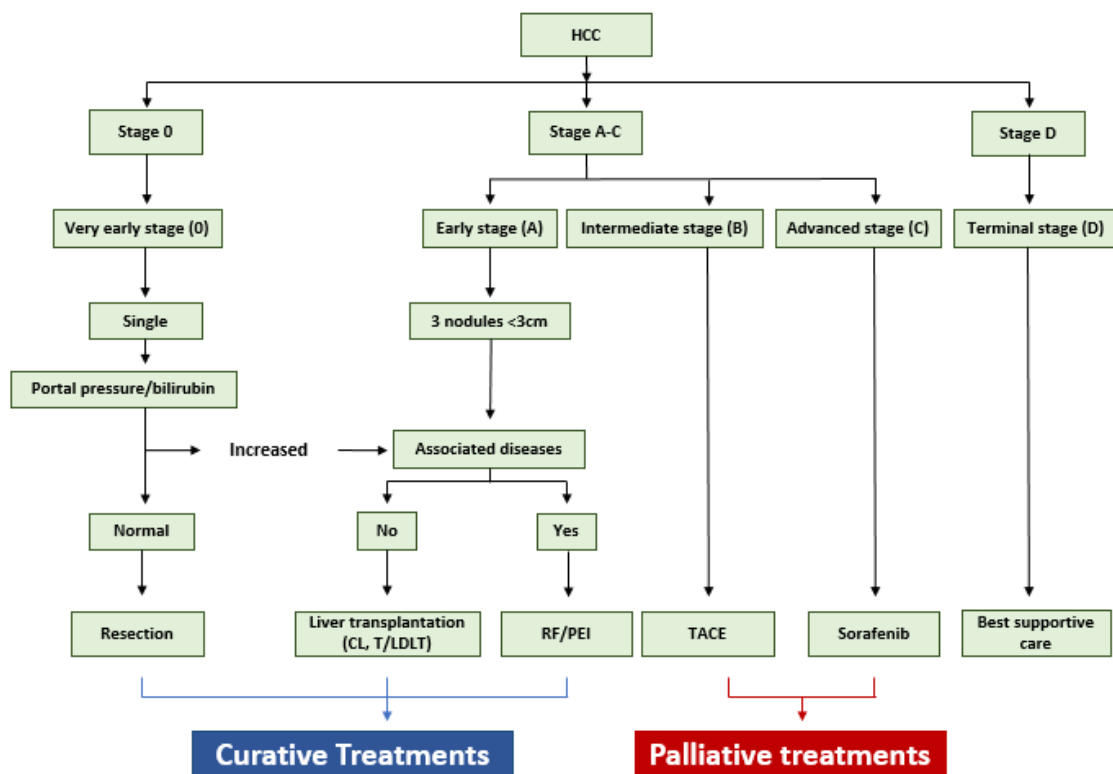


Figure 3.1 Stages and clinical practice for management of hepatocellular carcinoma.

However, this technique cannot be used in patients with advanced cirrhosis and hepatic decompensation since complications due to ischemic damage associated with embolization are generated, which decrease liver function [6]. Systemic chemotherapy remains the main treatment for patients with advanced HCC who are not candidates for surgical resection or liver transplantation. Nevertheless, this disease is not very responsive to chemotherapy owing to drug resistance mechanisms, since malignant cells show multiple efflux pumps on their surface.

Over the years various drugs have been used for the treatment of HCC, such as Doxorubicin, Cisplatin and Fluorouracil, which recorded a 10% response showing a low pharmacological impact [7]. For these reasons, several multi-kinase inhibitors were approved later using the targeted therapy approach. Sorafenib **1** (Figure 3.2) was the first TKI approved in 2007 by the US Food and Drug Administration (FDA) for systemic treatment of HCC and remains the first-line therapy in patients with unresectable diseases (Figure 3.1). Sorafenib is an oral agent which inhibits Raf-kinases and other receptors with kinase activity, such as VEGFR and PDGFR, thus displaying antiangiogenic and proapoptotic properties [8]. However, second choice multi-kinases inhibitors such as Regorafenib, Lenvatinib or Carbozatinib are used in patients who show a decrease in response to sorafenib in HCC. Regorafenib **2**, approved by FDA in 2017, possesses anti-angiogenetic activity, due to inhibition of VEGFR-TIE2 tyrosine kinases, and improves patients survival [9,10].

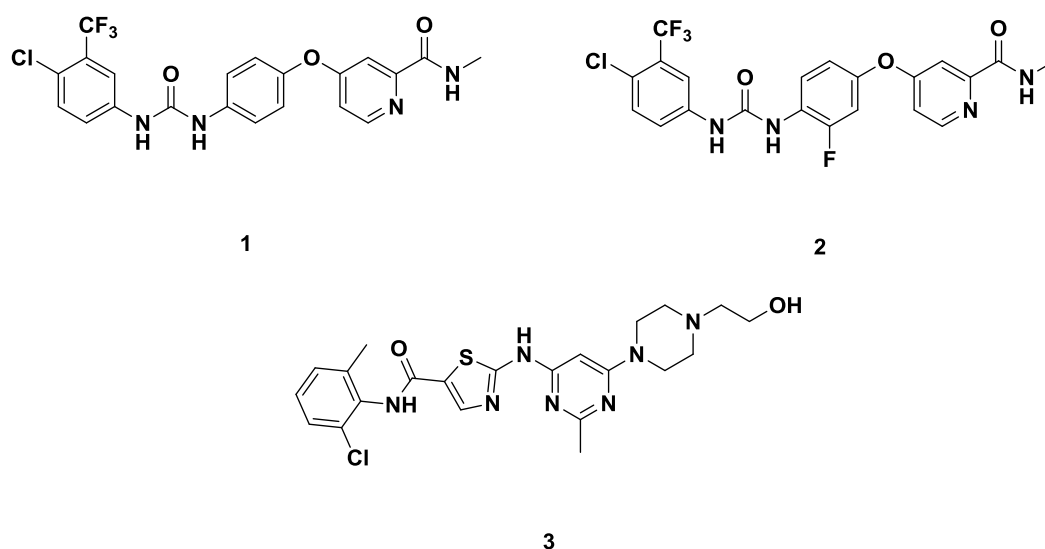


Figure 3.2 Structure of Sorafenib **1**, Regorafenib **2** and Dasatinib **3**.

Among the signaling pathways involved in the HCC progression, the mTOR cascade has been identified, where some NRTKs play a key role [11]. mTOR activity is regulated by a number of oncoproteins and tumor suppressors (Figure 3.3, including the tyrosine kinase c-Src [12,13]. The level of c-Src expression has been correlated with cancer progression and the protein results often activated in the early stage of HCC. It is involved in the development of diseases promoting the processes of cell proliferation and angiogenesis and activating the focal adhesion kinase (FAK). FAK is a non-receptor tyrosine kinase involved in the control of cell-extracellular matrix interactions that regulate migration, motility, and survival. Therefore, in

response to adhesion signals, active c-Src can bind and phosphorylate FAK, which plays an important role in integrin signaling resulting in cytoskeleton reorganization required for cell movement [14]. However, the Ras-Raf-1-ERK1/2 signaling pathway is also relevant for the progression of HCC, particularly promoting processes of cell proliferation and survival [15]. In this case, another non-receptor tyrosine kinase, c-Abl, is involved in this cellular cascade: as it has been shown in some studies, its activation is required for CLDN1-induced invasiveness in HCC. Downstream of c-Abl are a number of interacting proteins to include Stats, Erk, CrkL, paxillin and Fak [16].

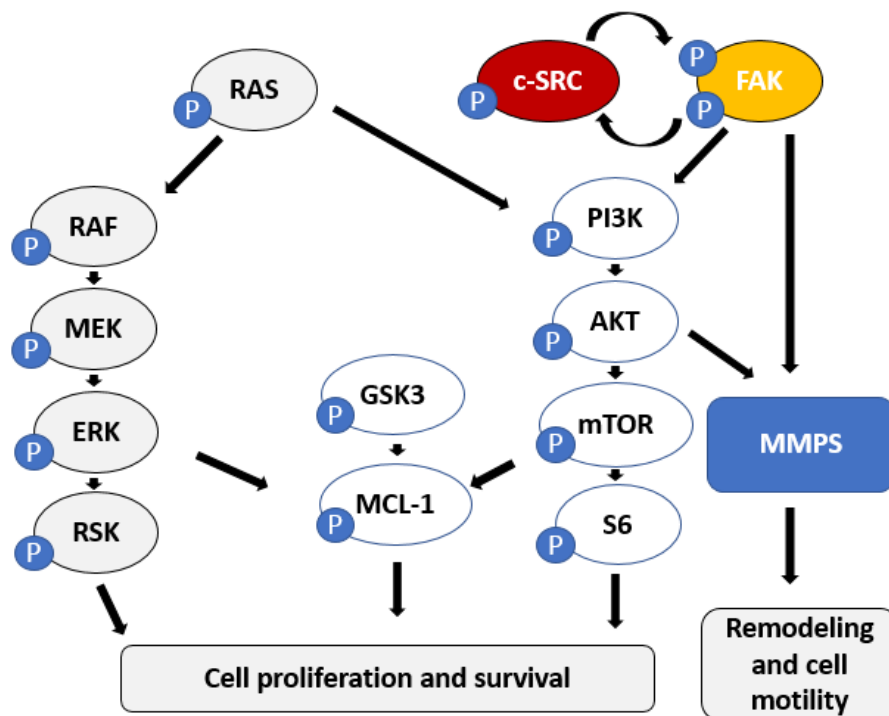


Figure 3.3 mTOR and RAS pathways involved in HCC.

Therefore, the blocking of this target through treatment with tyrosine kinase inhibitors (TKIs) could prove to be a starting point for bringing novel agents into HCC therapy. Dasatinib **3** (Figure 3.2), a potent oral SFK/Abl inhibitor, has demonstrated multiple effects on solid tumors significantly reducing adhesion of various Extracellular Matrix (ECM) proteins and cells migration, as reported in *Chang et al* [17]. Furthermore, the combination with another specific inhibitor, involved in the same enzyme cascade, can be used to observe a synergistic effect or to overcome the drug resistance of the tumor cell lines [18].

2. State of the art

The over regulation of NRTKs is involved in development of various cancers and their blocking represents a possible pharmacological strategy for the treatment of solid and blood tumors [19]. Commercial tyrosine kinases inhibitors (TKIs) block the kinase activity in some members of NRTK, resulting effective in chemotherapy if utilized in specific phases of disease [20]. Among the known TKIs that act on c-Abl we find Imatinib **4** and Nilotinib **5** (Figure 3.4) which inhibit the inactive form of the protein and are widely used in the therapy of chronic myeloid leukemia (CML). However, it has been observed that Sorafenib **1** (Figure 3.2), which blocks the Raf-kinases involved in HCC, also inhibits the c-Abl protein [21].

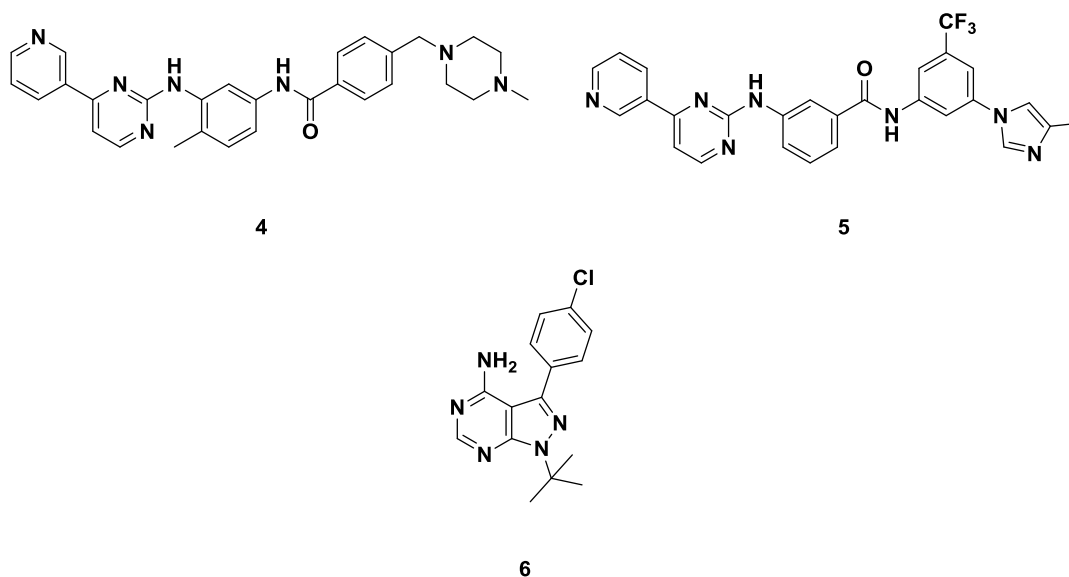


Figure 3.4 Structures of main TKIs: Imatinib **4**, Nilotinib **5**, and PP2 **6**.

On the other hand, among the most studied c-Src inhibitors we find Dasatinib **3** and PP2 **6**. Dasatinib is a potent SFK/Abl inhibitor and was widely analyzed as a chemotherapeutic agent in various cancers. The multikinase inhibitor Dasatinib **3** blocks c-Src activity at 0.4 nM concentrations (IC_{50} value) [22] revealing a potent antiproliferative activity on tumor cell cultures where this protein is hyperexpressed or hyperactivated, therefore it is used in the therapy of various tumor pathologies. A novel therapeutic application of Dasatinib could concern hepatocellular carcinoma (HCC) because it reveals the c-Src involvement in signaling pathways that lead to tumor development. In fact, in recent study, Dasatinib was analyzed on

some HCC cell cultures resulting effective to inhibits viability with a favorable median IC_{50} value [17]. HCC has an inefficient standard therapy and for this reason is of notable importance the pharmacological research of novel inhibitors to be applied in chemotherapy. In addition, the development of tumor resistance mechanisms and the low tolerability of patients lead to the continuous demand for novel therapeutic agents.

In recent years, several pyrazolo[3,4-*d*]pyrimidines have been developed in our research group as a possible alternative to TKIs available in cancer therapies [23]. A large library of compounds has been generated by decorating the pyrazolo[3,4-*d*]pyrimidine scaffold (Figure 3.5) with specific substituents into N1, C6 and C4 positions in order to inhibit with high potency c-Src and/or c-Abl kinase activity. Furthermore, a second pharmacological mechanism revealed the possible inhibition of P-Gp proteins involved in cancer resistances [24].

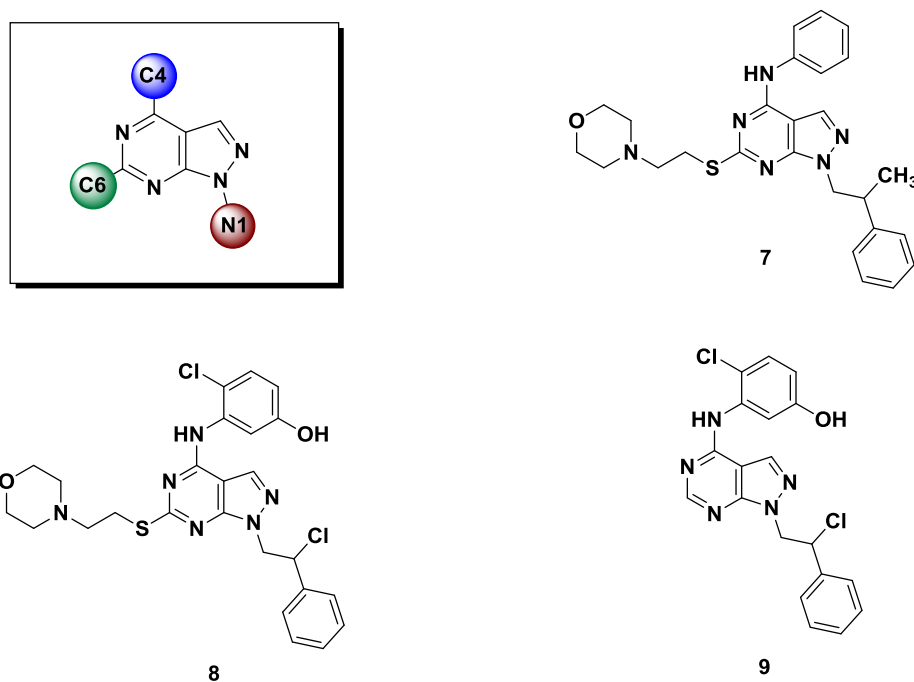


Figure 3.5 Pyrazolo[3,4-*d*]pyrimidine scaffold with substituted N1, C6 and C4 positions. The structures of Si192 7 and other potent Src/Abl pyrazolo[3,4-*d*]pyrimidine inhibitors 8, 9 have been reported in Chapter II.

Several pyrazolo[3,4-*d*]pyrimidine derivatives have been analyzed in tumors involving Src family kinase (SFK) proteins, such as neuroblastoma [25], prostate cancer [26], lymphoma [27], and others. The c-Src progenitor, showing the conserved sequence in the ATPase site with other SFK members and the c-Abl protein, has been extensively studied through X-ray

crystallographic analysis of the protein in complex with the Si192 inhibitor (Figure 3.5). From MC/FEP analysis on c-Src [28] a small group of potent competitive inhibitors was identified and synthesized [29]. These new compounds showed a good balance between water solubility and inhibitory potency, while also revealing good antiproliferative activity on several cell lines expressing these targets.

3. Aim of the project

An interesting medicinal chemistry strategy recently developed entails the structural hybridization of clinically used drugs to generate new bioactive entities with higher probability rate, improve PK-related properties and circumvent drug resistance. The primary objective of this project was the synthesis of pyrazolo[3,4-*d*]pyrimidine of new generation hybridized with commercial TKIs, in order to engender in the first part of the work a small library of compounds with high inhibitory activity on non-receptors tyrosine kinases involved in cancers process, namely Abl and c-Src. After the preliminary screening on these proteins, in the part second of the project the most promising derivatives were selected and optimized to improve their inhibitory activity on the target, PK properties, and to analyze their tumor application, in particular in HCC. In this project I worked on the design, the chemical synthesis and the organization of subsequent pharmacological studies.

4. Results

4.1 Part I

4.1.1 Design of new pyrazolo[3,4-*d*]pyrimidine derivatives

Considering the c-Src X-Ray crystal structure complexed with ligand Si192 in ATP site [28] it is possible to observe an accessible hydrophobic pocket where sterically hindered chains could enter and generate favorable ligand-protein interactions (Figure 3.6). Moreover, this domain is rich in amino acid sequences that play a key role in the execution of the kinase activity and in conformational changes control.

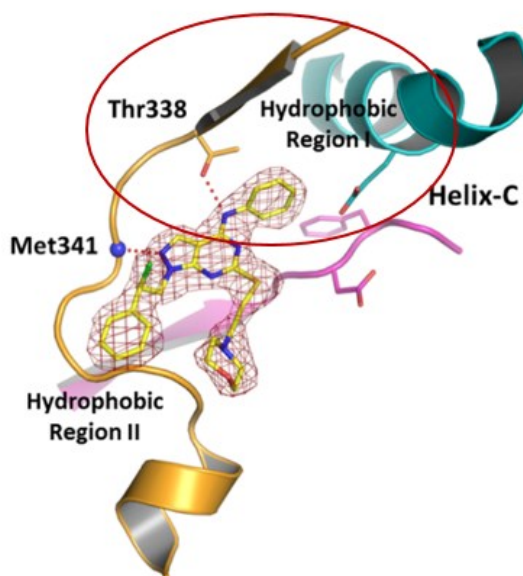


Figure 3.6 X-Ray crystal structure of c-Src with ligand Si192.

The merge-hybridization process [30] between the TKIs used in therapy and some potent pyrazolo[3,4-*d*]pyrimidine compounds, has generated five class of derivatives with a specific protein target. However, the TKIs chain was chosen because it results to be the active moiety which interacts through key-lock model with protein pocket. [31]

■ Design of *c*-Abl inhibitors

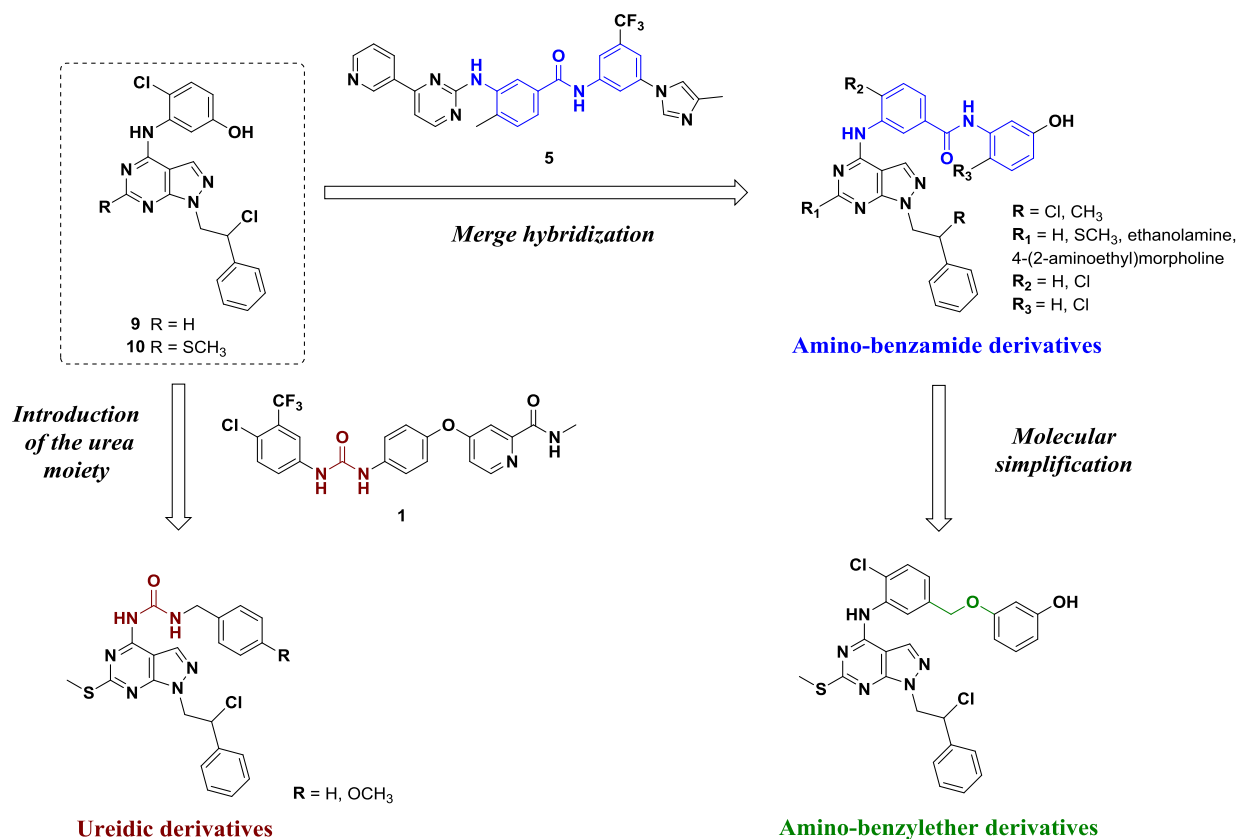


Figure 3.7 Design of amino-benzamide, amino-benzylether and ureidic derivatives as *c*-Abl inhibitors.

The family of amino-benzamide derivatives arises by the hybridization process between pyrazolo[3,4-*d*]pyrimidine **9**, which shows a potent Abl inhibition (compound **8a** in **chapter II**) and Nilotinib **5**, Abl selective inhibitor used in CML therapy (Figure 3.7) [32]. The aminobenzamide chain of Nilotinib was chosen because, as described by molecular modeling studies, it established an important interaction between the amide backbone and the amino acids Glu286 and Asp 381 of the Abl kinase pocket [33]. In addition, it was decided to further decorate the amino-benzamide chain with the phenolic and chlorine group, which are essential for obtaining a potent inhibitory activity in compound **9** [29]. Moreover, the benzamide moiety can be found in the structure of other TKIs such as Imatinib **1**, the first drug approved in CML therapy. The subsequent design of benzyl ether derivatives aims at molecular simplification of benzamides chain (Figure 3.7). Indeed, the amide bond was replaced by an ether group in order to increase the flexibility of the molecule in the *c*-Abl kinase site as well as water solubility.

Finally, the family of ureidic derivatives arises from hybridization of the Abl inhibitor **10** (compound **8b** in **chapter II**) with Sorafenib **1**, another TKIs which shows an ureidic moiety

into its chemical structure [21]. The structure of these new derivatives features the pyrazolo[3,4-*d*]pyrimidine scaffold connected by an ureidic bridge to phenyl ring in C4 position, as shown in Figure 3.7. This hydrogen bond donor group was chosen because it gives rise in Sorafenib to an important interaction to inhibit the Abl target [33].

▪ *Design of c-Src inhibitors*

Aminothiazole derivatives, which originate from merge-hybridization of Si192 **7** with SFK inhibitor Dasatinib **3** (Figure 3.8), are designed and synthesized with the aim of obtain potent c-Src inhibitors. The distinctive chain of Dasatinib, introduced at C4 position of pyrazolo[3,4-*d*]pyrimidine core, was decorated on the aniline ring with different functional groups.

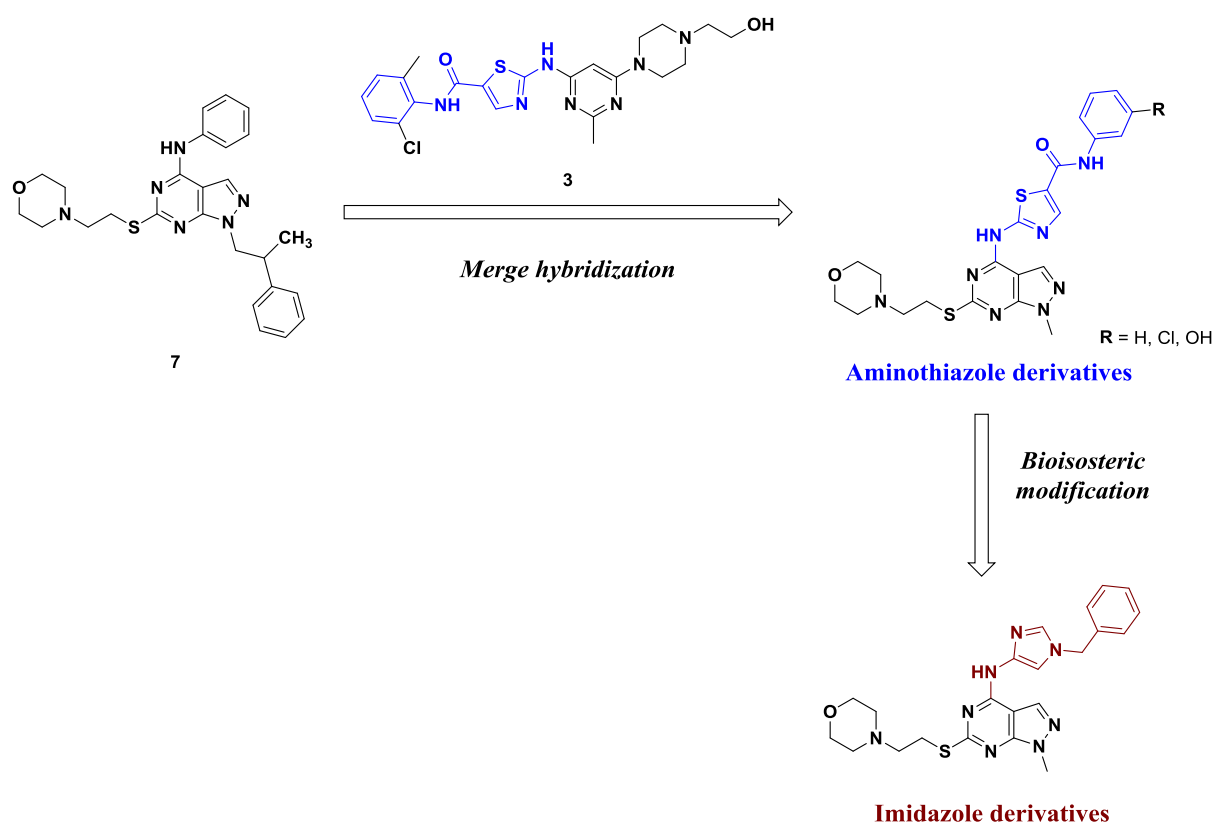


Figure 3.8 Design of aminothiazole and imidazole derivatives as c-Src inhibitors.

The family of imidazole originates from the molecular simplification of aminothiazole derivatives and was designed to targets c-Src. Imidazole is an aminothiazole bioisoster, therefore it is possible to observe a similar inhibitory activity if compared with aminothiazole analogue [34].

4.1.2 Synthesis

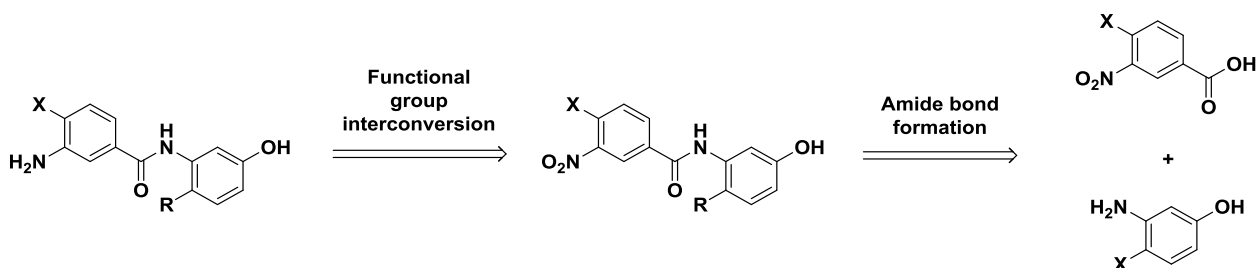
The preparation of the novel compounds follows the classic synthetic approach widely used by our research group which shows versatility to quickly generate different pyrazole[3,4-*d*]pyrimidine derivatives. However, the chains introduced in the C4 position of nucleus (Figure 3.5) were previously synthesized through the study and subsequent application of novel synthetic strategies.

Section I: preparation of synthons

▪ *Amino-benzamide and amino-benzylether synthons*

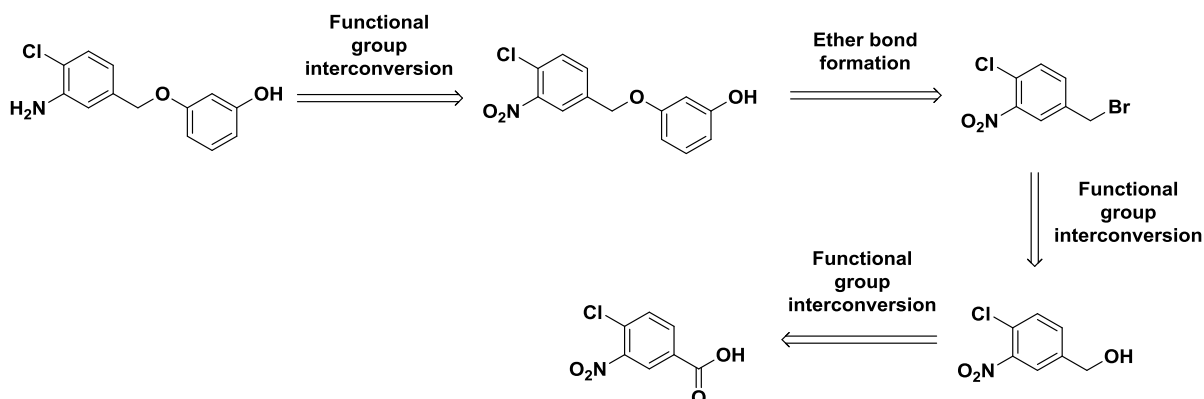
The amino-benzamide synthon was prepared using a precise retrosynthetic approach shown in scheme I.

Scheme I. Disconnection approach of amino-benzamide synthon



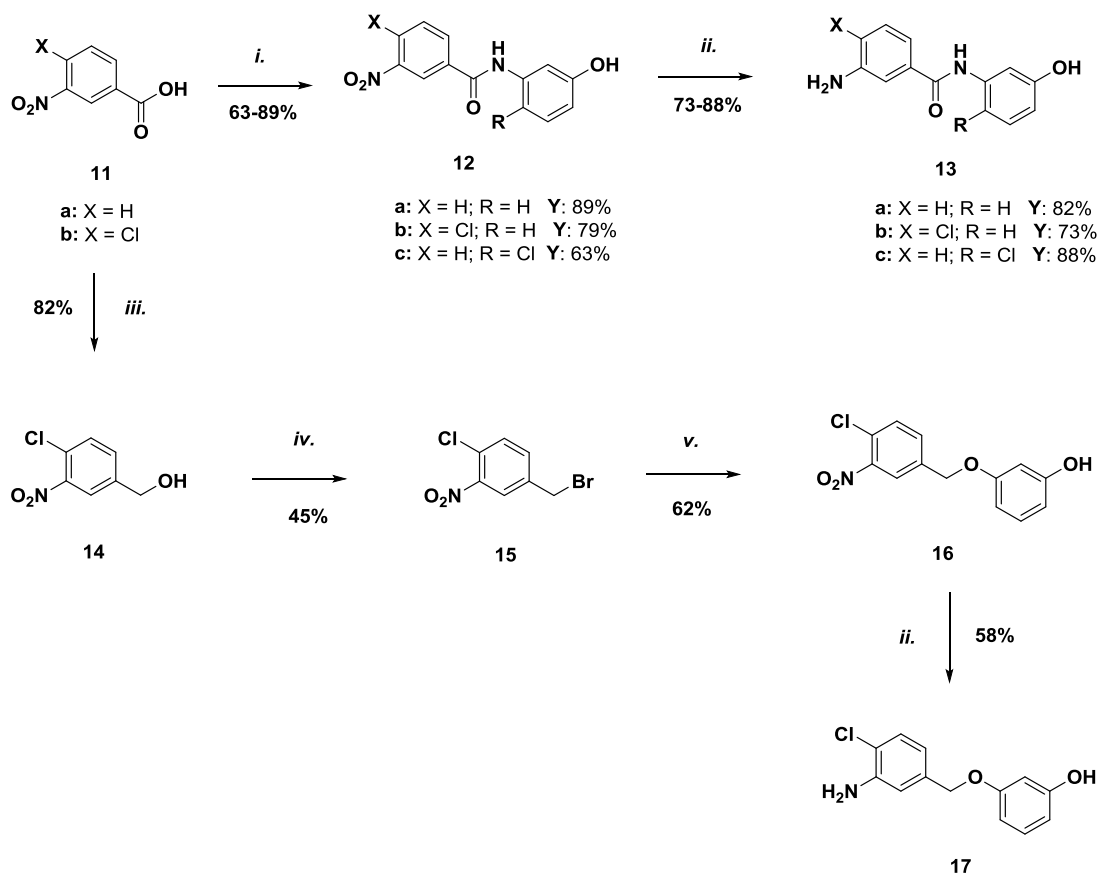
The nitro group interconversion (FGI) into amine is a first step of retrosynthesis (Scheme I) and avoids the cross-coupling reaction during the amide bond generation, which is caused by the simultaneous presence of two anilines into reaction mix. FGI of the amino into nitro group is also required in scheme II for ether synthon preparation in order to prevent aniline nucleophilic attack on benzyl halide during the reaction of ether bond formation.

Scheme II. Disconnection approach of amino-benzylether synthon



Furthermore, it is possible to observe in Scheme II that 3-nitro-4-chloro benzoic acid is the same starting material used in the synthesis of both synthons. Therefore, following the setting of these two retrosynthetic approaches, the synthons were prepared using specific reagents and reaction conditions as reported in Scheme III.

Scheme III. Synthesis of amino-benzamide **13a-c** and amino-benzyl ether **17** synthons



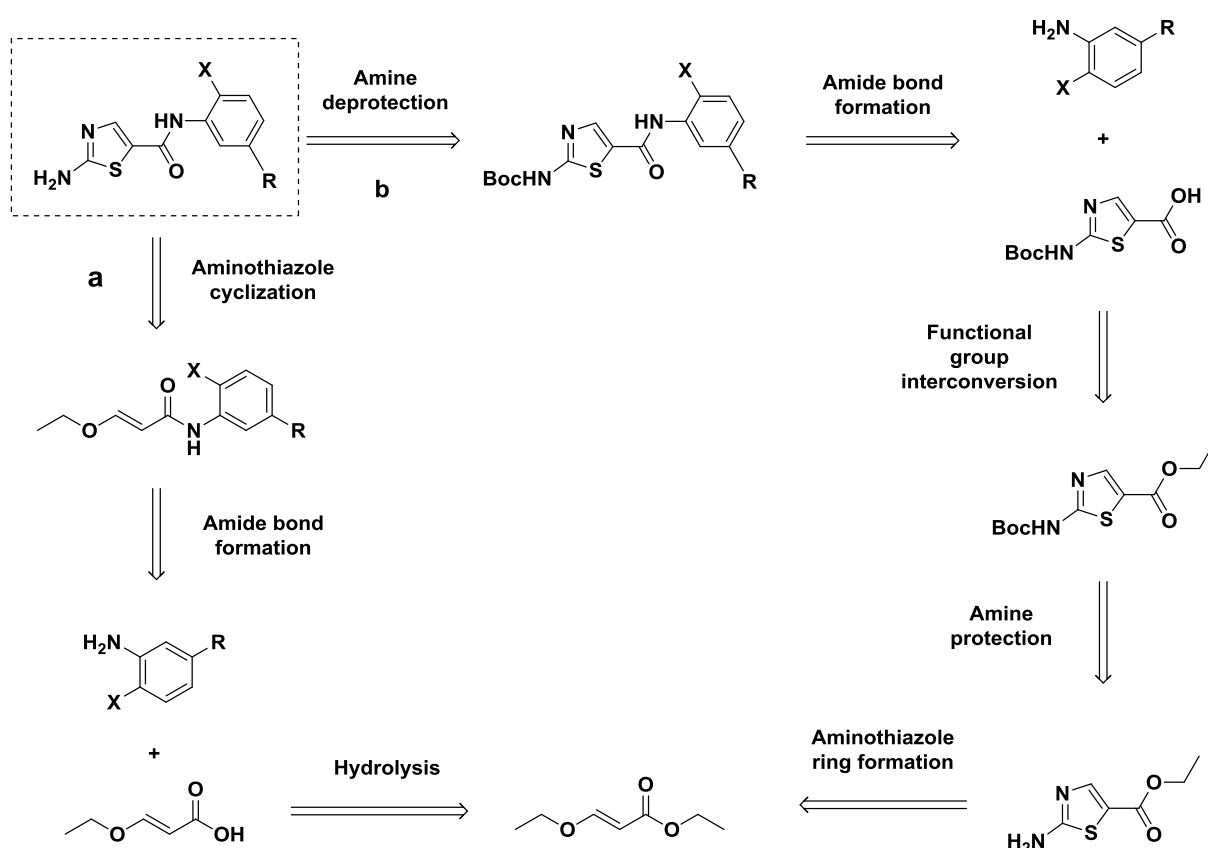
Reagent and conditions: *i.*) appropriate aniline, HOBt monohydrate, EDC·HCl, DMF, rt, 8-12 hours. *ii.*) Fe, NH₄Cl, EtOH/H₂O 3:1, 3 hours. *iii.*) BH₃S(CH₃)₂, dry THF, 0 °C to rt, 18 hours. *iv.*) PBr₃, dry DCM, 0 °C, 2 hours. *v.*) resorcinol, K₂CO₃, acetone, reflux, 4 hours.

Amide bond formation is achieved through the reaction between appropriate 3-nitrobenzoic acid **11a,b** and the suitable aniline using hydroxybenzotriazole (HOBt) as condensing agent in addition to EDC·HCl. The subsequent reduction of nitro into amino group, through selective reduction with iron, allows to obtain the desired synthon **13a,b,c**. Starting from the same compound **11b**, the selective reduction of the carboxy group to alcohol **14** was performed using borane dimethylsulphide in anhydrous THF with a yield of 82%. The conversion to benzyl bromide **15** and the subsequent nucleophilic reaction with resorcinol allows to obtain 3-((3-amino-4-chlorobenzyl)oxy)phenol (**17**).

▪ *Aminothiazole synthons*

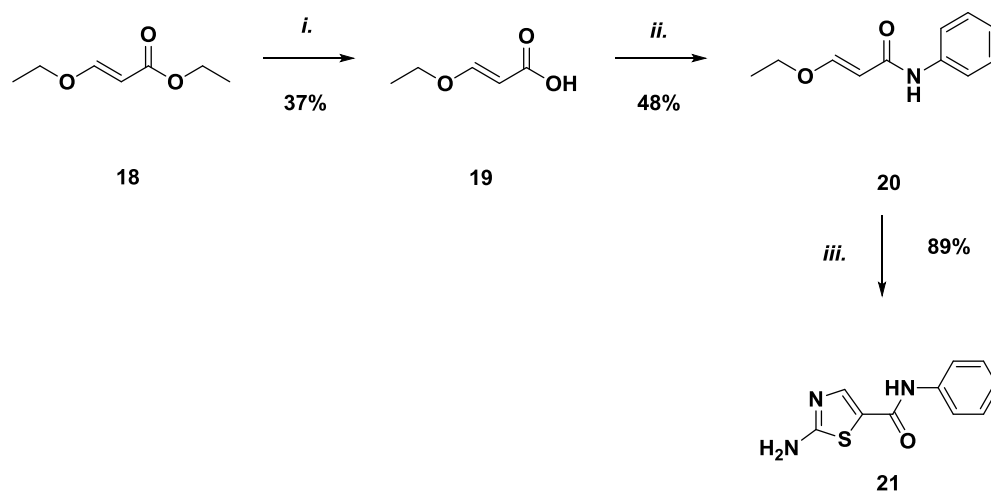
The aminothiazole chains are structurally characterized by the amide linkage between aminothiazole and benzene ring, and for their preparation two retrosynthetic approaches have been considered, which are shown in Scheme IV.

Scheme IV. Disconnection approach of aminothiazole synthons



The retrosynthetic pathway **a** (Scheme IV) involves a lower number of disconnections compared to the pathway **b** where the number of steps to obtain the desired compound is increased due to the protection-deprotection processes. Nevertheless, it has been experimentally observed that the path **a**, characterized by the final cyclization of the aminothiazole ring, is not very advantageous due to the low overall yield, as reported in Scheme V.

Scheme V. Synthesis of aminothiazole synthon **21**



Reagents and conditions: *i.*) 2 N NaOH, reflux, 2 hours; *ii.*) 1. oxalyl chloride, DMF, DCM, 0 °C to r.t., 8 hours; 2. aniline, TEA, DCM, r.t., 2 hours; *iii.*) 1. NBS, water/1,4-dioxane 1:1, -10 °C to 0 °C, 1 hour; 2. thiourea, 80 °C, 1 hour.

In this synthesis approach, a critical point was found in the hydrolysis of the acrylic ester **18** into the corresponding acrylic acid **19** since obtaining this compound sufficiently dry to be used in the next step has proved problematic.

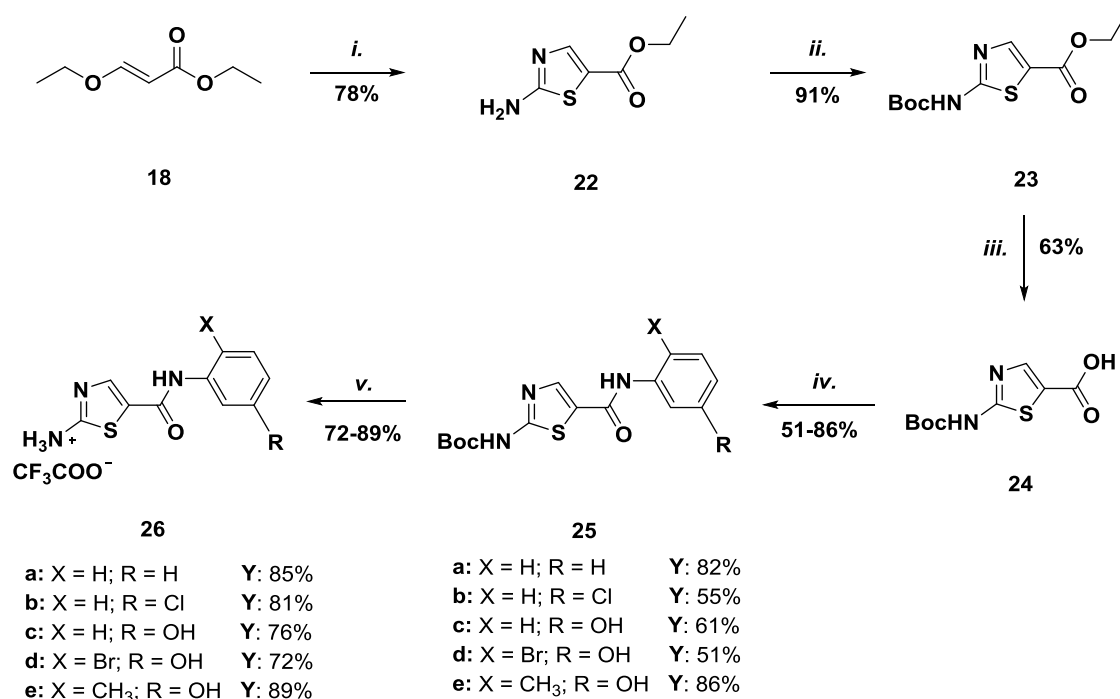
Table 1. Purification conditions of **19**

Test	Conditions
1	Remove water by added toluene and evaporation under reduce pressure (azeotropic solution)
2	Remove water by introducing in dryer with phosphorous pentoxide
3	Remove water with N ₂ or air flux

Despite attempts to completely remove the water by nitrogen flow (Table 1), azeotropic distillation with toluene, or the addition of a drying agent, such as phosphorus pentoxide, the

acid **19** was not obtained completely anhydrous. Nevertheless, it was chlorinated and reacted with aniline in the following step to give in moderate yield the intermediate **20**, which was finally cyclized with thiourea. Using the second synthesis route, which is characterized by the final amide condensation, this problem was not observed thus obtaining different synthons with a favorable reaction yield as reported in Scheme VI.

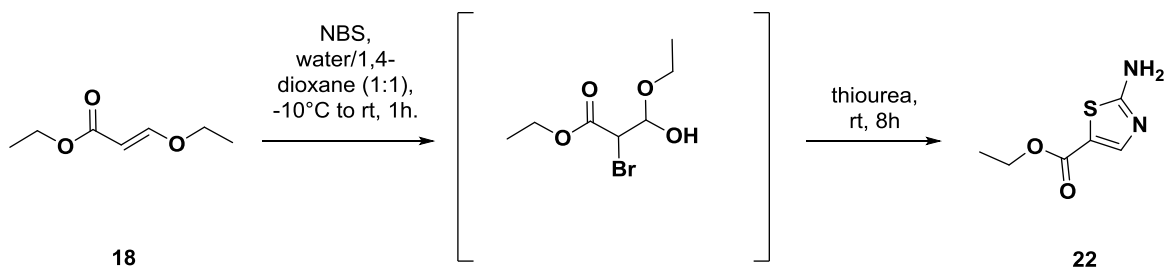
Scheme VI. Synthesis of aminothiazole synthons **26 a-e**



Reagents and conditions: *i.*) 1. NBS, 1,4-dioxane/H₂O 1:1, -10 °C to rt, 1 hours. 2. thiourea, 80 °C, 12 hours. *ii.*) Boc₂O, DMAP, dry THF, rt, 12 hours. *iii.*) 6 N KOH, EtOH/THF 1:1, 50 °C, 7 hours. *iv.*) appropriate aniline, HOBt monohydrate, EDC·HCl, DMF, rt, 11 hours. *v.*) TFA, dry DCM, rt, 6 hours.

The synthesis of the aminothiazole chains **26a-e** begins with the cyclization of the acrylic ester **18** with thiourea thus obtaining the intermediate **22** through a reaction that involves the pathway shown in Scheme VII.

Scheme VII. Cyclization mechanism of intermediate **22**

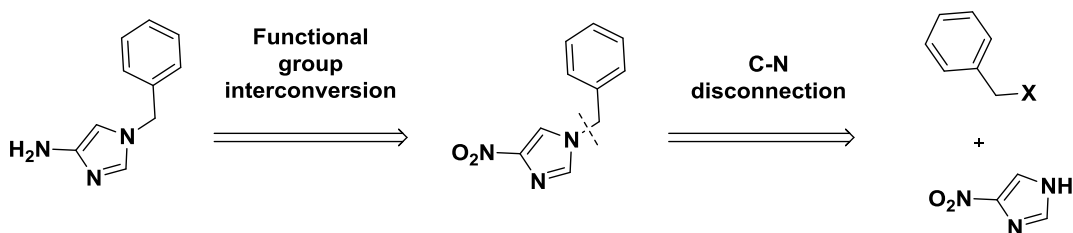


Monitoring the reaction by TLC revealed the formation of a brominated intermediate which subsequently was converted by thiourea at room temperature into the aminothiazole **22**. The free amino group was protected by reaction with di-*tert*-butyl dicarbonate to give compound **23**, which was hydrolyzed under basic conditions, thus generating the respective acid **24** as a completely dry white solid after evaporation with toluene. The condensation with the appropriate aniline was carried out using the same conditions used in the preparation of the amino-benzamide chains. Thus, it was possible to make use of different anilines to diversify the aminothiazole synthons. Finally, intermediates **25a-e** were deprotected using a 10% solution of TFA in dry DCM to give the desired final synthons **26a-e**.

• *Imidazole synthons*

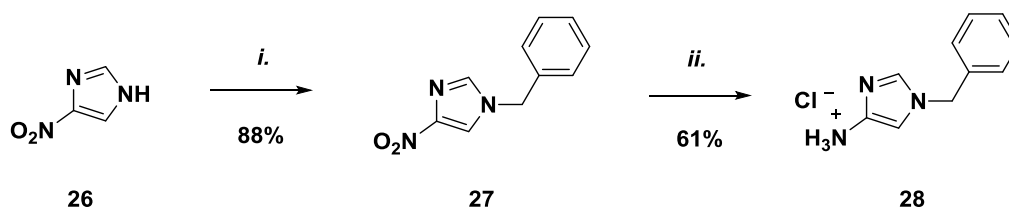
The retrosynthetic approach studied for the preparation of this synthon is shown in Scheme VIII.

Scheme VIII. Disconnection approach of imidazole derivatives



Scheme VIII shows the amine/nitro interconversion and the subsequent C-N connection to the aromatic nitrogen of the imidazole ring generating the two synthons. Following this retrosynthetic approach, the synthesis was developed using specific reagents and conditions (Scheme IX).

Scheme IX. Synthesis of imidazole synthon **28**



Reagents and conditions: *i*) benzyl bromide, K₂CO₃, CH₃CN, 60 °C, 7 hours. *ii*) 1. H₂, Pd/C, EtOH, rt, 12 hours; 2. 1.25 N HCl in EtOH, rt, 24 hours.

Starting from nitroimidazole **26**, intermediate **27** was obtained by alkylation reaction with benzyl bromide. The reduction of nitro derivative **27** to amine **28** led to a light sensitive compound, which was therefore quickly converted into its hydrochloride salt, as a stable, pale yellow solid.

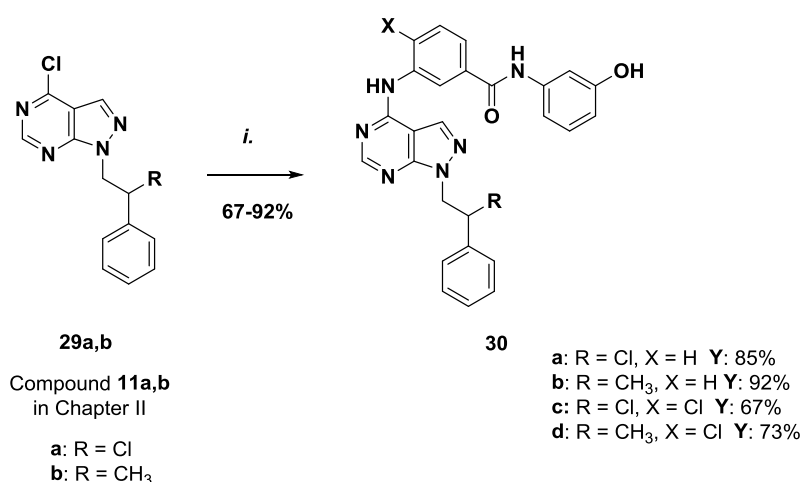
Section II: general synthesis of final compounds

The second part of the synthesis shows the final coupling reaction between the previously prepared synthons and the different chlorinated pyrazolo[3,4-*d*]pyrimidine nuclei, the synthesis of which is reported in chapter 2, to obtain the desired final compounds.

▪ Synthesis of C6-unsubstituted amino-benzamide derivatives

The C6-unsubstituted amino-benzamide derivatives were prepared through the classic aromatic nucleophilic substitution reaction between the amino group of the synthons **13a,b** and the appropriate chlorinated pyrazolo[3,4-*d*]pyrimidine intermediate **29a,b** (Scheme X).

Scheme X. Synthesis of C6-unsubstituted amino-benzamide derivatives **30a-d**



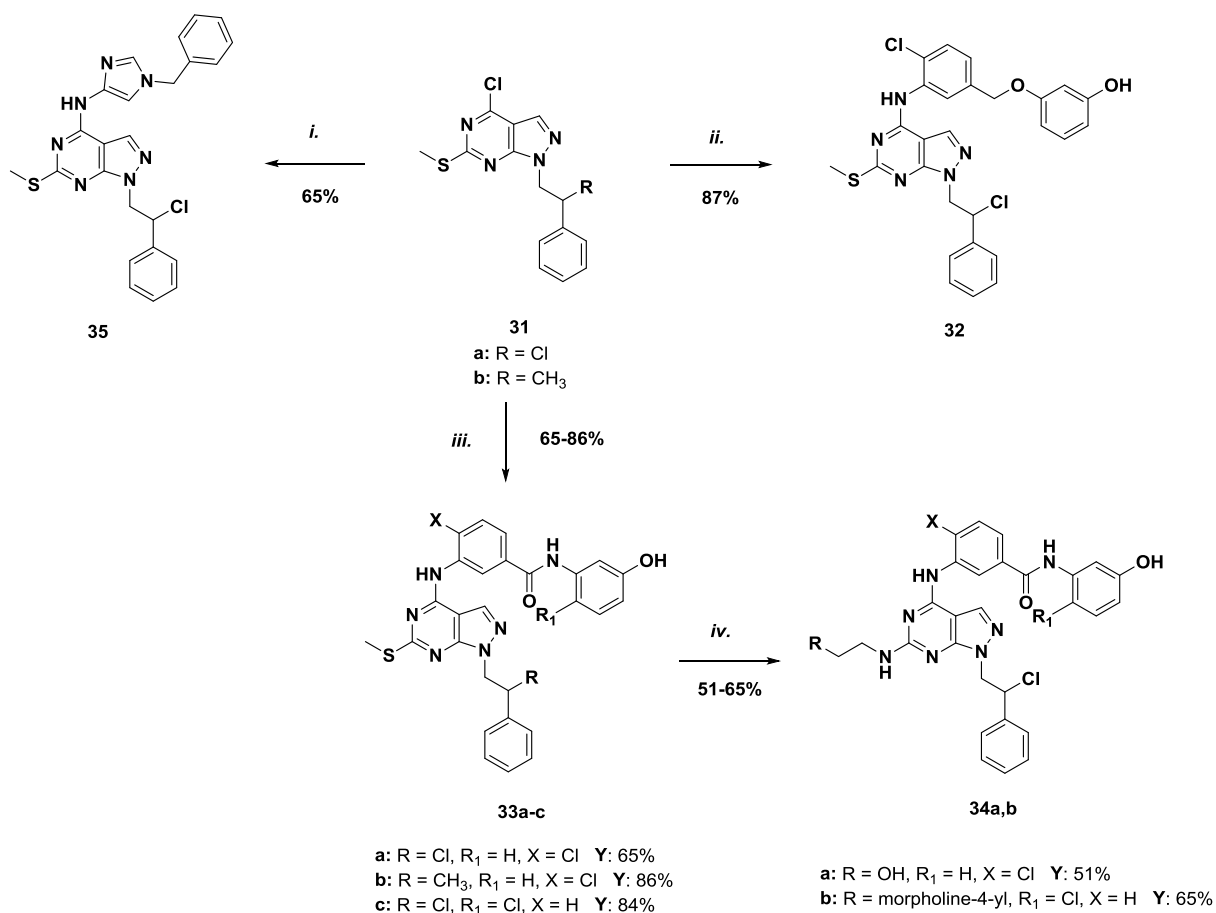
Reagents and conditions: *i*) **13a** or **13b**, EtOH, reflux, 3.5-12 hours.

The synthesis of intermediates **29a** and **29b** has already been described in chapter II. Analyzing specifically this synthesis step it was observed that the reaction times increase when using the synthon **13b** which bears, compared to **13a**, an additional *ortho* chlorine atom on aniline thus increasing its steric hindrance and reducing its nucleophilicity. Nevertheless, the final compounds **30** were obtained with satisfactory yields.

■ General synthesis of C6-substituted derivatives

C6-diversification of the pyrazolo[3,4-*d*]pyrimidine scaffold (see Figure 3.5) was achieved using the synthetic approach previously described by our research group [25,29]. Following this procedure, the desired compounds **32**, **33a-c**, **34a,b** and **35** were easily obtained in moderate to good yield (Scheme XI)

Scheme XI. Synthesis of C6-substituted compounds **32**, **33a-c**, **34a,b** and **35**



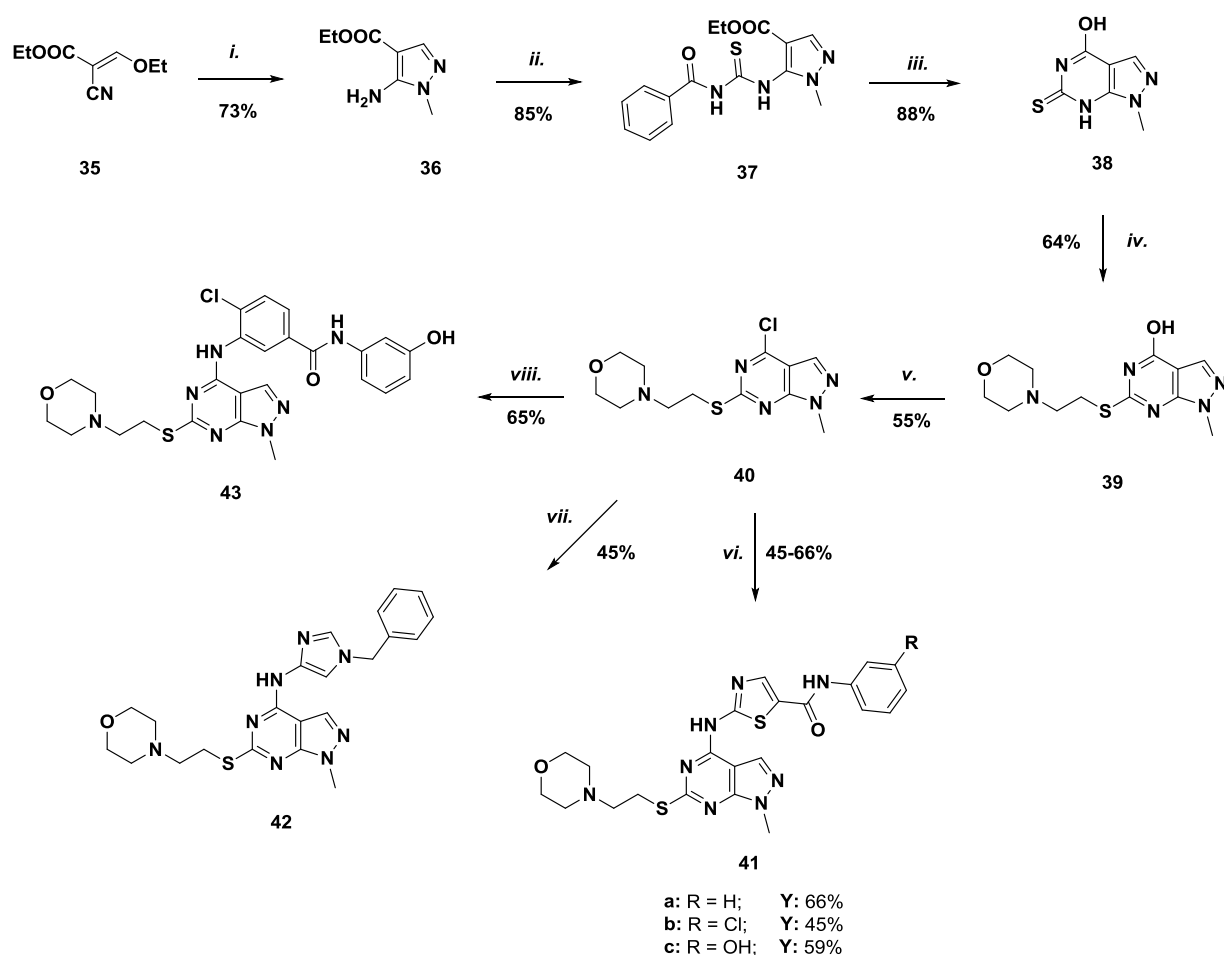
Reagents and conditions: *i.*) **28**, TEA, abs. EtOH, 6 hours, reflux. *ii.*) **17**, abs. EtOH, 3 hours, reflux; *iii.*) **13b,c**, abs. EtOH, 3-5 hours, reflux. *iv.*) 1. *m*-CPBA, dry DCM, dry DMF, rt, 2 hours; 2. ethanolamine or 4-(2-aminoethyl)morpholine, DMSO/butanol 1:2, reflux, 8-10 hours.

Synthesis of chlorinated intermediate **31** has already been described in chapter II (see compound **16a**), while the Scheme XI shows the last steps where the desired final compounds are generated. The preparation of compounds **32** and **33a,b** involved an aromatic nucleophilic substitution reaction in ethanol between the intermediate **31** and the appropriate amino derivatives **17** or **13a,b**. In addition, the final compounds **33a** and **33c** were further diversified

in C6-position by introducing the ethanolamine and 4-(2-aminoethyl)morpholine polar chains, respectively. Unlike the standard procedure used, in this case dry DMF was added dropwise as a cosolvent to allow the dissolution of the starting intermediate and favor the oxidation of the thiomethyl group, so as to obtain the final compounds **34a,b**. On the other hand, for the preparation of compound **35** the usual reaction conditions were adopted, with the only modification of adding fresh distilled TEA as a catalyst.

Another class of compounds, characterized by a pyrazolo[3,4-*d*]pyrimidine scaffold substituted in N1 position with a methyl group and in C6 with a 2-(4-morpholino)ethylthio moiety were obtained by introducing in C4 the desired chains previously synthesized, as reported in Scheme XII.

Scheme XII. Synthesis of C6-substituted compounds **41a-c**, **42** and **43**



Reagents and conditions: *i.*) methylhydrazine, EtOH, reflux, 8 hours. *ii.*) benzoyl isothiocyanate, dry THF, reflux, 6 hours. *iii.*) 2 N NaOH, reflux, 5 hours. *iv.*) chloroethyl morpholine hydrochloride, NaOH, EtOH, DMF, reflux, 8 hours. *v.*) POCl₃, dry DMF, dry CHCl₃, reflux, 4 hours. *vi.*) Pd₂(dba)₃, Xantphos, synthon **26a-e**, K₂CO₃, dry 1,4-dioxane, 4

hours, reflux. *vii.*) synthon **28**, TEA, abs. EtOH, 8 hours, reflux. *viii.*) Pd₂(dba)₃, Xantphos, synthon **13b**, K₂CO₃, dry 1,4-dioxane, 6 hours, reflux.

The approach used in the preparation of intermediate **40** follows the procedure used over the years by our research group. Thus, ethyl ethoxymethylenecyanoacetate **35** was cyclized with methylhydrazine in refluxing ethanol to afford the pyrazole compound **36**. The reaction with benzoyl isothiocyanate and the subsequent cyclization of intermediate **36** in basic conditions were carried out to give the thiol compound **37**, which was alkylated with 4-(2-chloroethyl)morpholine hydrochloride to obtain intermediate **38**. This was halogenated using the Vilsmeier reaction to give the intermediate **40**, which in turn was reacted with the appropriate synthons by replacing the chlorine atom in C4 position. Specifically, the synthesis of aminothiazole derivatives **41a-e** was optimized by testing different reaction conditions (Table 2), since the desired results were not obtained by simply refluxing the reaction mixture in ethanol.

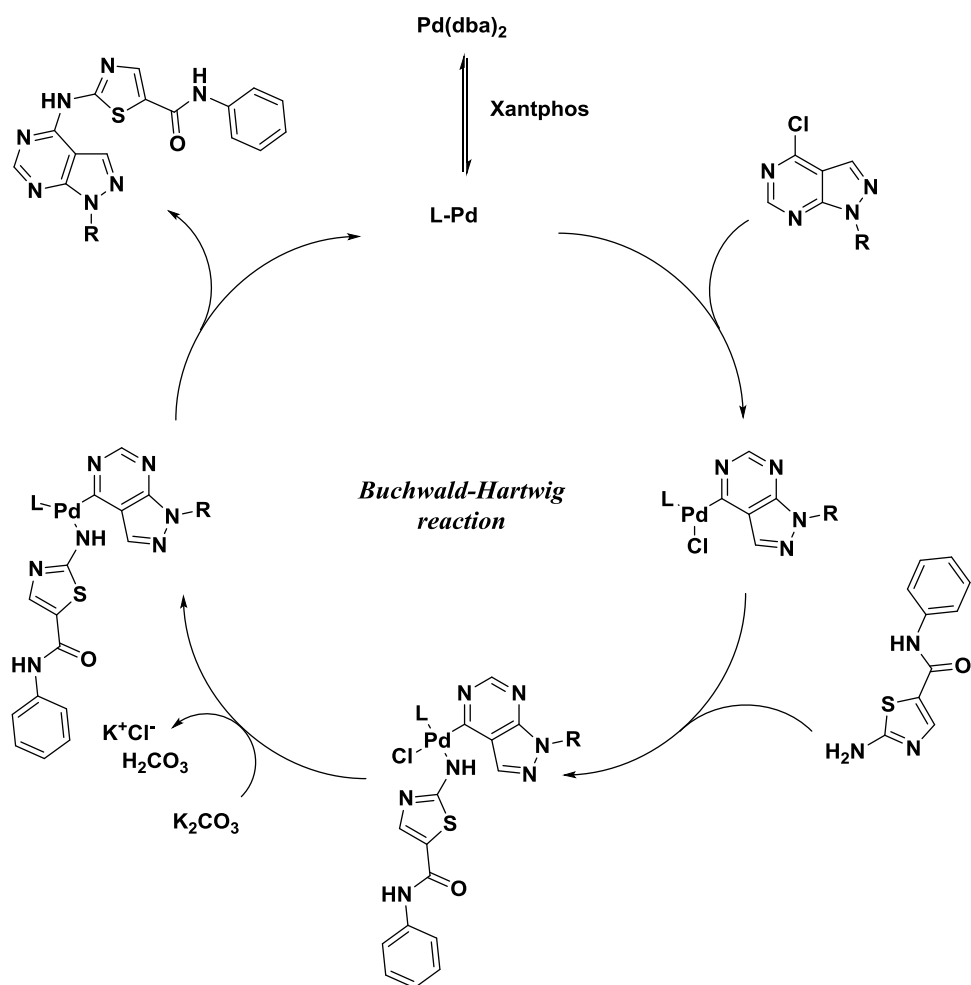
Table 2. Conditions for prepare aminothiazole derivatives **41a-e**

Test	Reagents and conditions	Yield %
1	41a , abs. EtOH, reflux, 24 hours	0
2	41a , TEA, abs. EtOH, reflux, 24 hours	0
3	41a , DMSO, reflux, 48 hours	0
4	41a , t-Bu-Xphos, Pd ₂ (dba) ₃ , dry 1,4-dioxane reflux, 8 hours	52
5	41a-e , Xantphos, Pd ₂ (dba) ₃ , dry 1,4-dioxane reflux, 3-5 hours	55-69

Neither the addition of a base (TEA) nor the change of solvent gave any result, so it was decided to use a novel reaction based on palladium chemistry. The Buchwald reaction, known for its wide use in the coupling of aromatic amines, was chosen for the preparation of these derivatives. Among the reagents, electron-rich phosphines play a key role since in the catalytic mechanism (see scheme XIII) they activate palladium and stabilize the amine bond. In fact, in absence of these particular ligands, the reversible bond between palladium and nitrogen is labile and the amine could be released before reacting with the substrate. However, there is no phosphine generally suitable for every need therefore, to select the appropriate ligand, a test was performed initially using t-Bu-Xphos and later Xantphos. Utilizing Xantphos the reaction

yield was increased (Table 2) and hence it was chosen as a ligand for the subsequent Buchwald reactions to obtain compounds **41** and **43**.

Scheme XIII. Mechanism of Buchwald-Hartwig reaction

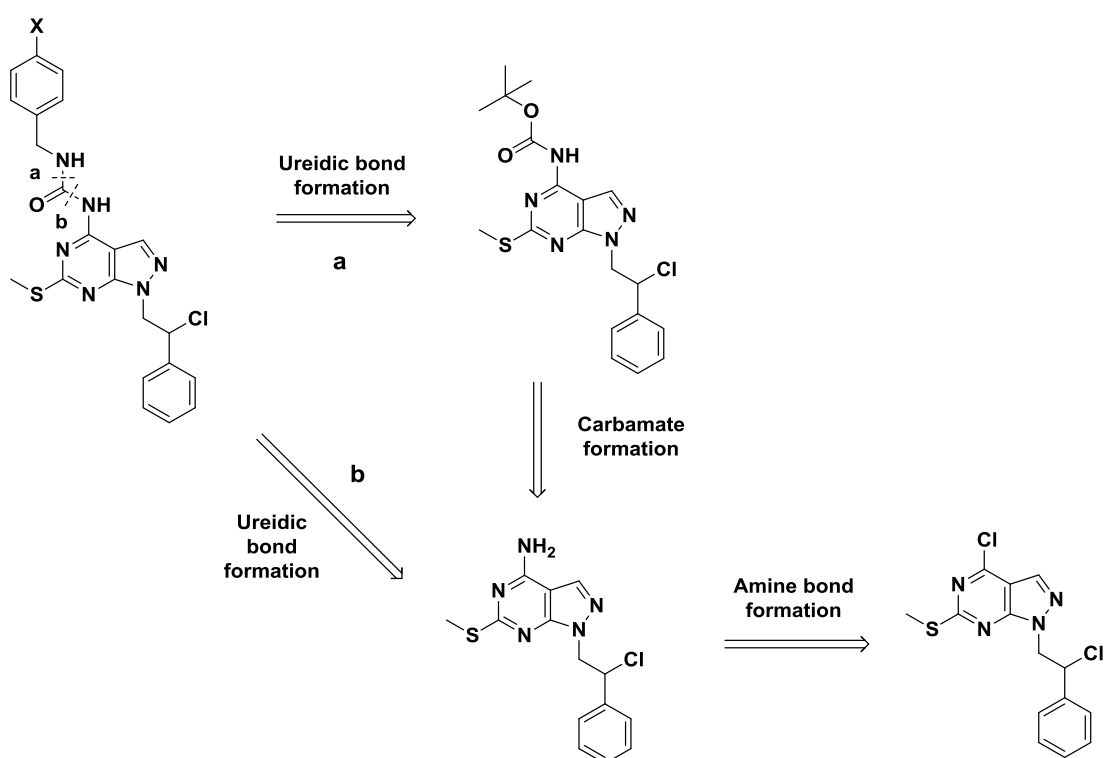


Conversely, the synthesis of compound **42** was accomplished in refluxing ethanol by adding a catalytic amount of TEA.

Section III: synthesis of ureidic derivatives

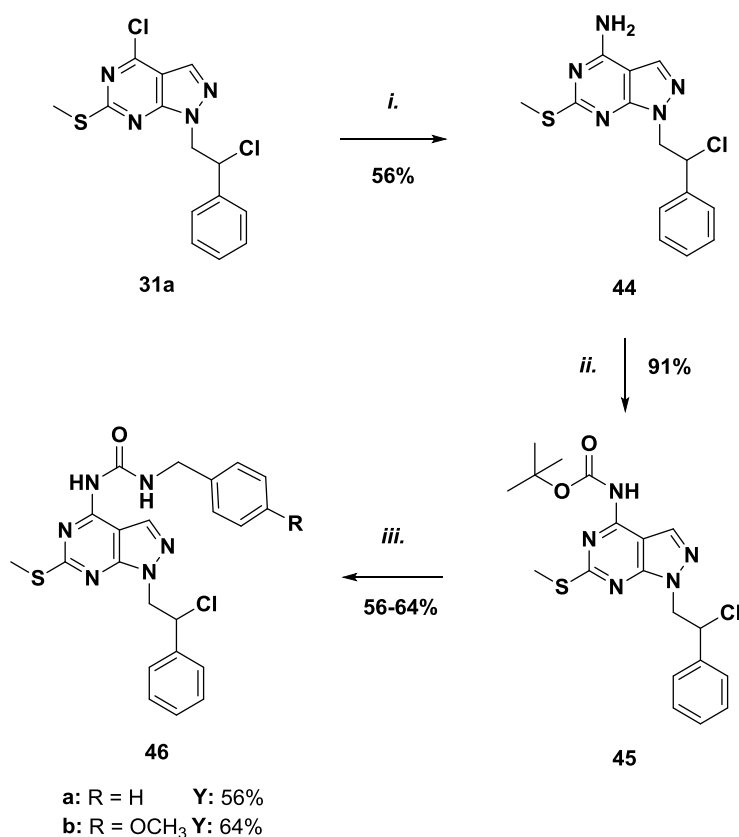
Ureidic derivatives are characterized by a urea bridge between the pyrazolo[3,4-*d*]pyrimidine nucleus and the benzyl ring. To obtain these compounds, two types of disconnections have been studied, reported in scheme XIV.

Scheme XIV. Disconnection approach of ureidic derivatives



Retrosynthetic pathway **a** shows the disconnection of the C-N bond at the distal nitrogen to the pyrazolopyrimidine nucleus to reach the carbamate, which originates from the aromatic amine of the pyrazolo[3,4-*d*]pyrimidine synthon. On the other hand, way **b** shows the disconnection of the C-N bond at the vicinal nitrogen to directly generate the same aromatic amine. Following these two disconnection approaches, different reactions were studied and applied to obtain the desired final compounds. The ureidic bridge between the pyrazolo[3,4-*d*]pyrimidine nucleus and the phenyl chain was constructed using different synthesis strategies reported in Scheme XV.

Scheme XV. Synthesis of ureidic derivatives **46a,b**



Reagents and conditions: *i*) NH₄OH, EtOH, reflux, 12 hours. *ii*) Boc₂O, DMAP, dry THF, 0 °C to rt, 7 hours. *iii*) appropriate benzylamine, DMAP, dry DMF, MS 5Å, 80 °C, 24 hours.

The first step of the synthetic process involves the nucleophilic reaction between ammonia and the intermediate **31a** to give the compound **44**. Following the disconnection **b** (Scheme XIII), the first synthesis strategy applied was the isocyanate generation on benzylamine. Although the formation of this chemical species was observed monitoring the reaction by TLC, only the undesired product was obtained, that is the symmetrical dibenzylurea. Even the use of commercial benzyl isocyanate failed to provide the expected product. Finally, through the reaction between intermediate **44** and di-*tert*-butyl dicarbonate, the carbamate **45** was obtained, which by reaction with the suitable benzylamine afforded the desired ureidic derivatives **46**.

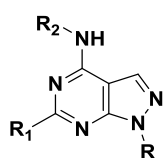
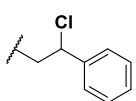
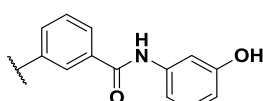
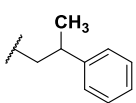
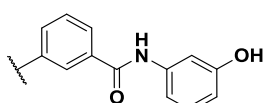
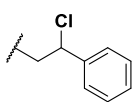
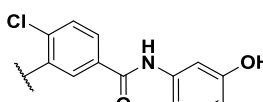
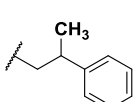
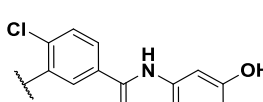
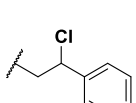
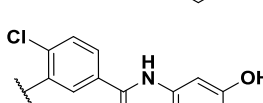
4.1.3 Biological data

The new derivatives **30-46** were subjected to enzymatic screening in order to evaluate their inhibitory potency on the corresponding Abl or c-Src target. This preliminary study allowed to select a family of derivatives on which to undertake further pharmacological studies in HCC.

▪ *Screening on c-Abl protein*

Benzamides, ethers and ureidics derivatives were designed to block Abl protein by introducing on the pyrazolo[3,4-*d*]pyrimidine scaffold specific chains or functional groups belonging to TKIs used in CML therapy as Bcr-Abl inhibitors. Therefore, these compounds were analyzed through an enzyme assay to evaluate the inhibitory potency on this target (Table 3).

Table 3. Screening of amino-benzamide, amino-benzylether and ureidic derivatives for c-Abl inhibition

Compd			Biological Data		
	R	R ₁	R ₂	c-Abl IC ₅₀ (μM) ^a	Inhibition % 10 μM
30a		H		n.d.	30
30b		H		n.d.	25
30c		H		n.d.	80
30d		H		n.d.	67
33a		SCH ₃		n.d.	40

33b		SCH ₃		n.d.	68
33c		SCH ₃		n.d.	13
34a				8.80	91
34b				n.d.	14
43	CH ₃			n.a	0
32		SCH ₃		n.a	0
46a		SCH ₃		n.d.	90
46b		SCH ₃		n.d.	44

^a Values are the means of two experiments; n.d. = not determinate; n.a. = no active versus c-Abl

These data demonstrated that all amino-benzamide derivatives show low inhibitory activity on c-Abl kinase. Although the inhibition percentage of compounds could be measured, it was not possible to calculate the IC₅₀ value, with the exception of derivative **34a**. However, even this compound shows low potency on Abl (IC₅₀ value = 8.80 μM), resulting very far from the inhibition values reported for compounds described in chapter II.

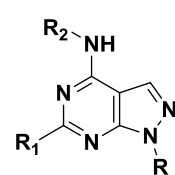
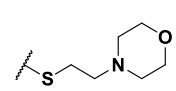
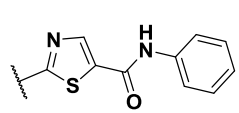
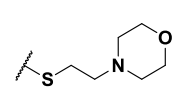
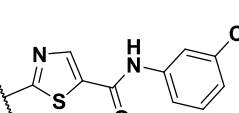
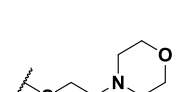
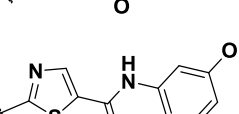
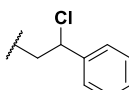
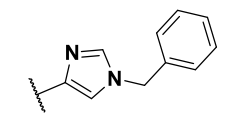
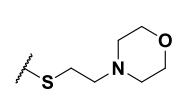
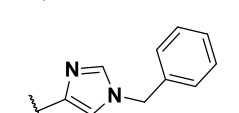
However, on the basis of the values of the percentages of inhibition, a favorable effect on potency is highlighted only in amino-benzamide derivatives which have a chlorine atom in the ortho position on the aniline ring (**30c-d**, **33a-b** and **34**) compared to the corresponding derivatives devoid of the chlorine atom (**30a,b**). Therefore, it is possible to envisage the generation of important hydrophobic interactions between chlorinated compounds and the pocket of the c-Abl kinase. The comparison between c-Abl inhibitory values of **32** and **33a** clearly highlights that the amide backbone establishes more relevant interactions with the Abl

kinase pocket than the ethereal backbone. Also derivatives **46a,b** proved to be very weak inhibitors of c-Abl kinase and similarly to the previous compounds they did not pass to further evaluation.

▪ *Screening on c-Src protein*

Aminothiazole and imidazole derivatives have been designed as possible inhibitors of the c-Src protein starting from the structure of the potent SFK inhibitor Dasatinib **3** and Si192 **7**. The new synthesized compounds were analyzed through enzymatic inhibitory assay on the specific target.

Table 4. Screening of aminothiazole and imidazole derivatives for c-Src inhibition

Compd				Biological Data	
	R	R ₁	R ₂	c-Src IC ₅₀ (μM) ^a	Inhibition % 10 μM
41a	CH ₃			0.134 ± 0.014	92
41b	CH ₃			n.d.	11
41c	CH ₃			0.024 ± 0.004	99
35		SCH ₃		n.d.	25
42	CH ₃			1.000 ± 0.001	75

^a Values are the means of two experiments; n.d. = not determinate;

Overall, data from Table 4 point out significant c-Src inhibition by aminothiazole derivatives **41a,c**, comparable to that obtained with other potent pyrazolo[3,4-*d*]pyrimidine [29]. In particular, the presence of a hydroxy group in the meta position of the aniline ring (compound **41c**) gives rise to an appreciable increase of the inhibitory activity compared to the

unsubstituted analog **41a**. Therefore, a polar interaction between this OH group and the Glu310 residue of c-Src kinase pocket can be envisioned, as reported in Tintori *et al* (Figure 3.9) [28].

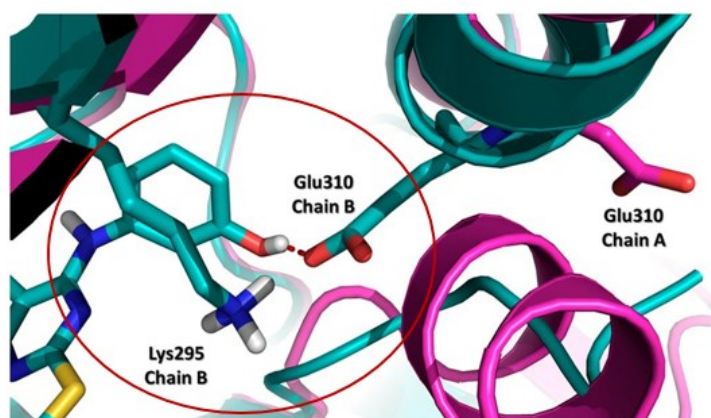


Figure 3.9 Phenol-Glu310 interaction on c-Src kinase pocket.

Finally, low inhibitory effect on c-Src was exerted by imidazole derivatives **35** and **42** (Table 4). Although the IC_{50} value on the target has been determined, compound **42** is approximately ten-fold less active than the aminothiazole precursor **41a** suggesting that the imidazole chain gives rise to weak interactions within the c-Src pocket.

In spite of these rather disappointing initial results, it was decided to continue investigating aminothiazoles through the synthesis of other novel derivatives designed with the objective to increase the inhibitory potency on c-Src and to study their *in vitro* pharmacological properties for use in hepatocellular carcinoma treatment.

4.2 Part II

4.2.1 C4 optimization of **41c**: design, synthesis and biological evaluation

From the analysis of the biological data reported in part I, it is clear that the aminothiazole derivatives revealed a notable inhibition of c-Src. Specifically, among these the most potent compound was **41c**, which was analyzed through molecular modelling techniques to investigate the mechanism of action on c-Src and to evaluate which of the possible conformational states of the protein is stabilized by the inhibitor [28]. The information obtained from this study was then used for the rational design of **41c** derivatives with potentially better pharmacodynamic

properties. Therefore, from the different **41c** derivatives designed by computational methods, two compounds were synthesized, which are characterized by a methyl group or a bromine atom in the ortho position of the aminophenol ring (Figure 3.10).

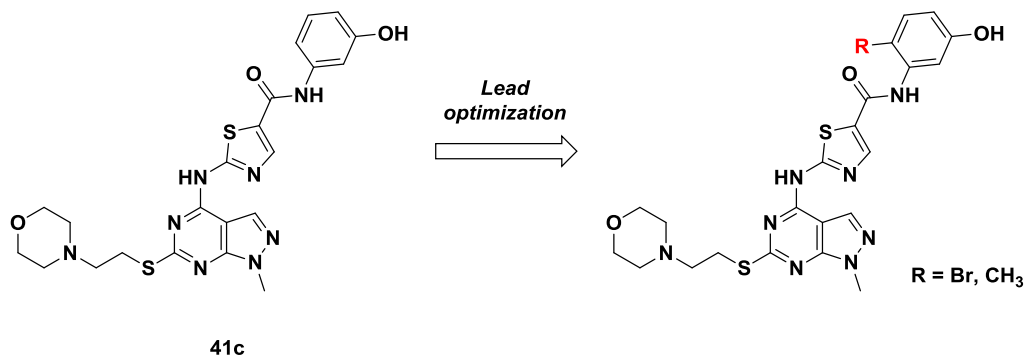
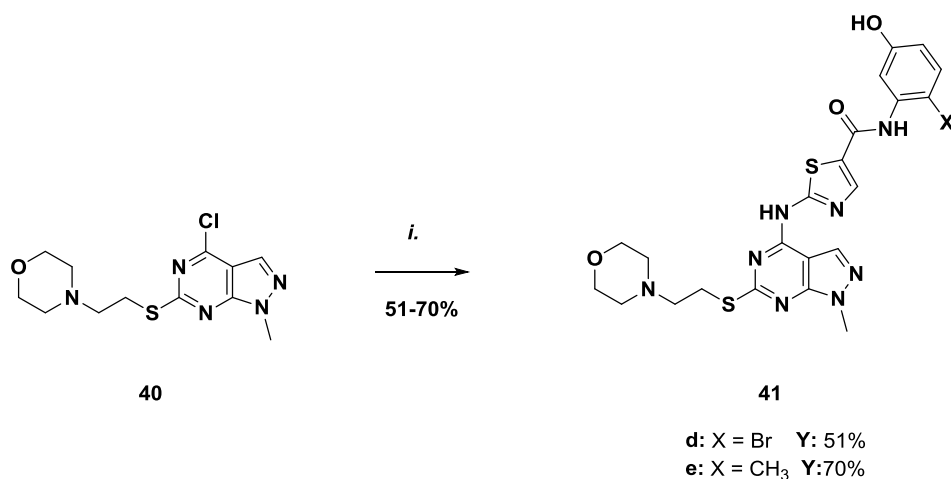


Figure 3.10 Optimization of **41c** by hydrogen replacement with bromine or methyl group.

The synthesis of new aminothiazole derivatives **41d,e** was performed using the same experimental conditions previously described for the preparation of the compounds **41a-c** (scheme XVI).

Scheme XVI. Synthesis of novel aminothiazole derivatives **41d,e**

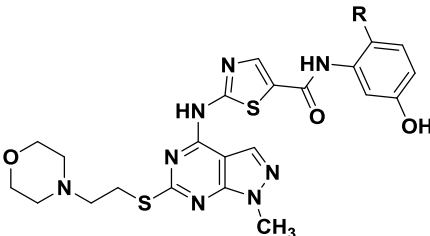


Reagents and conditions: *i.*) appropriate synthon **26d,e**, Pd₂(dba)₃, Xantphos, K₂CO₃, dry 1,4-dioxane, 4 hours, reflux.

Compounds **41d** and **41e** were obtained with a yield of 51 and 70%, respectively, as a white solid after crystallization from DCM. Conversely, purification by flash chromatography was not satisfactory, especially for the separation of the phosphine oxide by-product. Compounds

41d,e were subjected to the c-Src enzymatic assay to investigate the effect of their bromine or methyl substituent on inhibitory potency.

Table 5. Inhibition assay on c-Src of compounds **41d,e**

Compd		c-Src IC ₅₀ (μM) ^a
	R	
41d	CH ₃	0.2577 ± 0.0254
41e	Br	0.0007 ± 0.0001

^a Values are the means of two experiments

As can be seen from the data reported in Table 5, the introduction of a bromine atom on the aminophenolic portion of the precursor **41c** led to a very considerable increase in activity for the compound **41e**, which, in accordance with the preliminary prediction of molecular modeling, is resulted capable of blocking this target at a concentration of 0.7 nM (IC₅₀ value) comparable to that of Dasatinib. Therefore, **41e** ranks among the most potent pyrazolo[3,4-*d*]pyrimidines produced in our research group.

4.2.2 C6 and N1 optimization of **41c**: design, synthesis and biological evaluation

The following step in preclinical development of aminothiazole derivative was the evaluation of the antiproliferative activity of compound **41c** on Hepg-2 cell line, typical of HCC where c-Src results overexpressed. Despite its potent c-Src inhibition, **41c** affects to a moderate extent the cell viability of Hepg-2 (IC₅₀ value >50 μM), as reported in Table 6. In order to investigate this unexpected pharmacological effect, some *in vitro* ADME properties have been evaluated.

Table 6. *In vitro* ADME of compound **41c**

Compd	Hepg-2 IC ₅₀ (μM)	Water solubility μg mL ⁻¹	Metabolic Stab. %	GI P _{app} (10 ⁻⁶ cm s ⁻¹) (MR) %
41c	>50	0.03	99.4	0.1 (3.1)

As a result, low water solubility and poor passive membrane permeability were observed, suggesting that the lowly antiproliferative activity could be due to these unfavorable properties which negatively influence the intracellular target achievement. Furthermore, compound **41c** proved to precipitate in the aqueous buffer of cell culture medium. For these reasons, it was decided to further modulate the structure of **41c** by C6 and N1 functionalization of the pyrazolo[3,4-*d*]pyrimidine core (Figure 3.11).

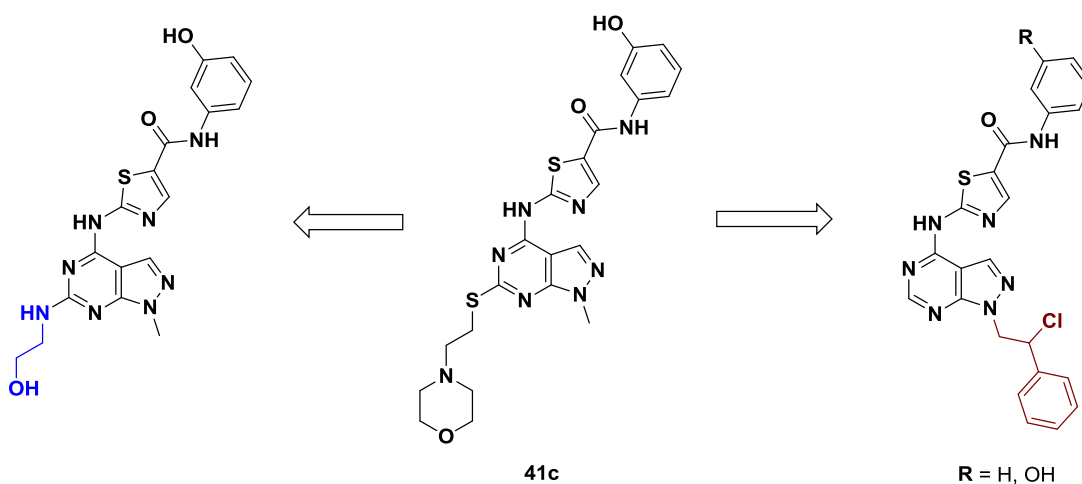
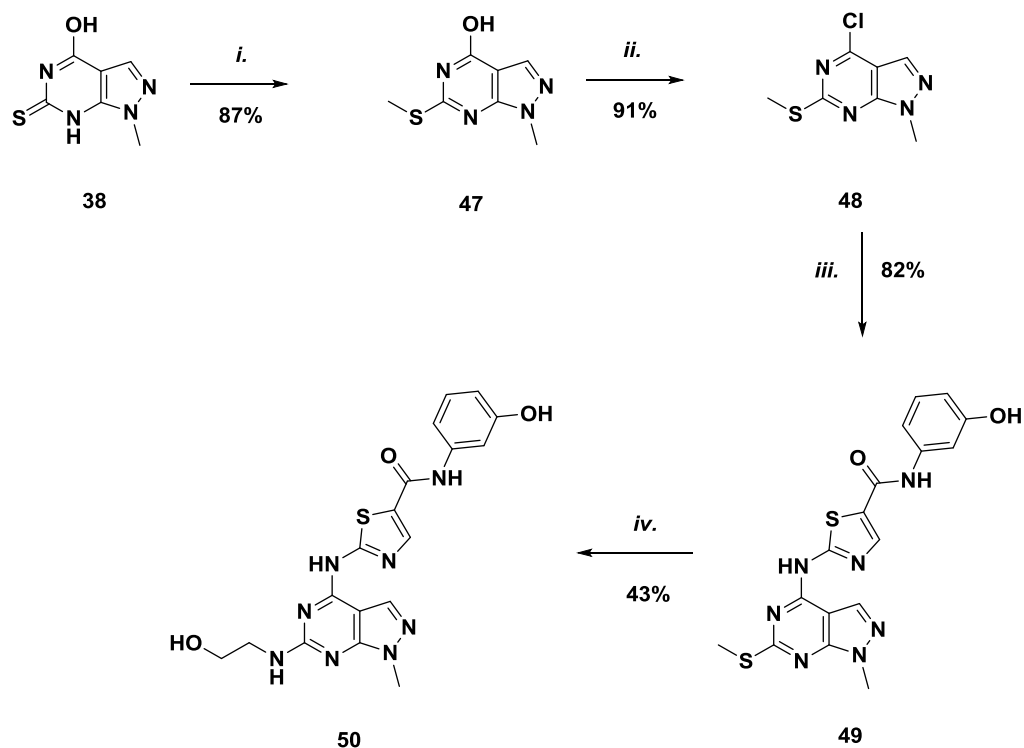


Figure 3.11 C6 and N1 substitution of hit compound **41c**.

C6 substitution, using ethanolamine chain, was realized with the objective of increasing water solubility and to allow dissolution in the aqueous buffers used in biological assays. On the other hand, N1 diversification was performed, introducing the wont chlorophenylethyl chain, in order to increase lypophilicity and to improve membrane permeability.

For the synthesis of aminothiazole derivative **50** (Scheme XVII) the usual procedure reported in the first part of the project was leveraged.

Scheme XVII. Synthesis of novel aminotiazole derivative **50**

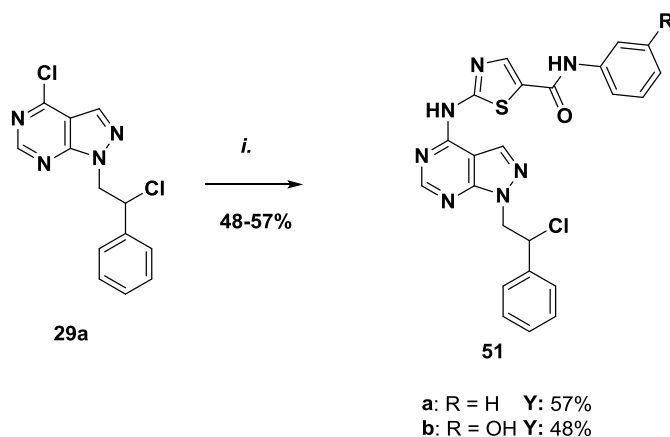


Reagents and conditions: *i.*) iodomethane, dry THF, reflux, 12 hours. *ii.*) POCl₃, dry DMF, dry CHCl₃, reflux, 4 hours. *iii.*) Pd₂(dba)₃, Xantphos, synthon **26c**, K₂CO₃, dry 1,4-dioxane, 4 hours, reflux. *iv.*) 1. *m*-CPBA, dry DCM, dry DMF, rt, 2 hours; 2. ethanolamine, DMSO/butanol 1:2, reflux, 11 hours.

The synthesis of derivative **50** starts from the alkylation of intermediate **38** with iodomethane to give compound **47**, which has been halogenated through Vilsmeier chlorination, thus obtaining intermediate **48** as a white solid. The subsequent Buchwald coupling between chain **26c** and compound **48**, using Xantphos as ligand, was performed to give the thiomethyl intermediate **49**. This was oxidized to sulfone using *m*-CPBA and replaced with ethanolamine, thus obtaining the desired compound **50**.

Finally, compounds **51a,b** unsubstituted at C6 but bearing the chlorophenylethyl chain at N1 were synthesized by Buchwald reaction between the intermediate **29a** and the **26a,b** chains (Scheme XVIII).

Scheme XVIII. Synthesis of C6-unsubstituted novel aminotiazole derivatives



Reagents and conditions: Pd₂(dba)₃, Xantphos, synthon **26a,c**, K₂CO₃, dry 1,4-dioxane, 4 hours, reflux.

The purification of compounds **51a,b** by flash chromatography proved problematic due to the presence of the oxidation products of the phosphines. Therefore, the compounds were purified by crystallization from hexane, thus obtaining the desired derivatives **51a** and **51b** as white solids. Subsequently, compounds **50** and **51a,b** were analyzed to evaluate their c-Src inhibitory properties through the appropriate enzymatic assay.

Table 7. Inhibition assay of **50** and **51a,b** on c-Src

Compd				c-Src IC ₅₀ (μM) ^a
	R	R ₁	R ₂	
50	CH ₃		OH	0.0025 ± 0.0014
51a		H	H	0.6000 ± 0.1270
51b		H	OH	0.0743 ± 0.0142

^a Values are the means of two experiments

The data reported in Table 7 show a powerful inhibitory activity in compound **50**, which is characterized by the presence of an ethanolamine chain in C6 position, thus replacing the morpholine chain in the structure of precursor **41c**. On the other hand, the introduction of a chlorinated phenylethyl chain in N1 position (**51a,b**) decreases to some extent the inhibitory potency, though it still remains significant. Finally, although compound **51a** exhibits the lowest inhibitory potency among the molecules in the set (see Table 7) it was decided to test it first on the HepG-2 cell line, because compound **51a**, compared with **50** and **51b**, results to be more lipophilic due to the absence of hydroxyl groups in the structure. Therefore, based on this consideration, a preliminary cellular assay was performed on compound **51a**.

Table 8. Cell viability of **51a** on HepG-2

Cell viability on HepG-2			
Compd	12h μ M	24h μ M	72h μ M
51a	8.4	3.4	2.21

As shown in Table 8, compound **51a** shows potent antiproliferative activity on the HepG-2 cell line (IC_{50} value = 2.21 μ M, 72h), significantly higher than derivative **41c** (IC_{50} value >50 μ M, 72h). Moreover, compound **51a** is also more potent than Dasatinib (IC_{50} value = 4.7 μ M, 72h), which was used as an internal reference standard in the experiment.

Compounds **50** and **51b** were also analyzed to evaluate the antiproliferative activity on HepG-2 cell line, but to date the experiments are still ongoing. In addition, it was decided to analyze the *in vitro* ADME profile in compounds in order to outline to which parameters, such as water solubility, biological membranes permeability and liver microsomes metabolism, the observed pharmacological effect was mainly due. These experiments are also ongoing and hence are not reported in this thesis.

5. Conclusion

The design of novel pyrazolo[3,4-*d*]pyrimidines using the merge-hybridization process has allowed us to obtain novel potent tyrosine kinase inhibitors with favorable pharmacological properties. The preliminary synthesis of synthons introduced in C4-position (**13a-c**, **17**, **26a-e**, and **28**) of the pyrazolo[3,4-*d*]pyrimidine nucleus was successfully performed in good overall yield. On the other hand, the synthetic approach used in the preparation of all final compounds

reported in this chapter, has shown remarkable versatility, allowing to obtain a considerable number of molecules through the crossing between the appropriate nucleus and the various chains. Among all compounds prepared in this project, aminothiazole derivatives have emerged as highly efficient in c-*Src* inhibition, showing a potency comparable to that of Dasatinib. Specifically, a surprisingly high inhibitory activity was observed in compound **41c** and its derivatives **41d,e** and **50**, which were obtained by lead optimization process. Nevertheless, compound **41c** did not show a favorable antiproliferative activity on the HepG-2 cell line, therefore it was hypothesized that this behavior may be due to limitations in terms of water solubility or biological membranes permeability, as reported by the *in vitro* ADME data. For these reasons, derivative **51a** was designed and synthesized, which exhibits a potent inhibition of cell viability on HepG-2, surpassing Dasatinib value. However, cell assays and the subsequent ADME properties analysis of other compounds **41d,e**, **50** and **51b** are still ongoing and, based on the next results, decisions will be made on the future development of these novel derivatives, which are promising agents for the HCC treatment.

6. Materials and methods

All commercially available chemicals were used as purchased. DCM was dried over sodium hydride, THF was dried over Na/benzophenone prior to use, while DMF was bought already anhydrous. Anhydrous reactions were run under a positive pressure of dry N₂ or argon. TLC was carried out using Merck TLC plates silica gel 60 F254. Chromatographic purifications were performed on columns packed with Merk 60 silica gel, 23-400 mesh, for flash technique. ¹H NMR and ¹³C NMR spectra were recorded on a Bruker Avance DPX400 (at 400 MHz for ¹H and 101 MHz for ¹³C). Chemical shifts are reported relative to tetramethylsilane at 0.00 ppm. Mass spectra (MS) data were obtained using an Agilent 1100 LC/MSD VL system (G1946C) with a 0.4 mL/min flow rate using a binary solvent system of 95:5 methanol/water. UV detection was monitored at 254 nm. MS were acquired in positive and negative mode scanning over the mass range 50-1500. The following ion source parameters were used: drying gas flow, 9 mL/min; nebulizer pressure, 40 psig; drying gas temperature, 350 °C.

Procedures

General procedure for preparation of 12a-c

To a solution of appropriate nitrobenzoic acid **11a** (414 mg, 2.48 mmol) or **11b** (500 mg, 2.48 mmol) in anhydrous DMF (25 mL), EDC·HCl (418 mg, 2.97 mg), HOBt monohydrate (418 mg, 2.72 mmol) and appropriate aminophenol (270 mg, 2.48 mmol) was added and the reaction mixture stirred for 8-12 hours at room temperature. Then, water (15 mL) was added and the crude product was extracted in EtOAc (20 mL x 3). The organic layer was washed with LiCl 5% solution (50 mL x 3) and brine, dried on Na₂SO₄ and concentrated under reduced pressure. The product was purified by flash chromatography using a proper mixture of DCM/MeOH as eluent (99:1 to obtain compounds **12a** and **12b**, 97:3 to obtain compounds **12c**) to afford compounds **12a-c**.

N-(3-Hydroxyphenyl)-3-nitrobenzamide (12a)

Yield: 89%. ¹H NMR (400 MHz, MeOD) δ 10.11 (bs, 1H), 8.76 (bs, 1H), 8.40 (d, *J* = 8.0 Hz, 1H), 8.29 (d, *J* = 8.0 Hz, 1H), 7.75 (t, *J* = 8.0 Hz, 1H), 7.18-7.09 (m, 4H), 6.60 (d, *J* = 8.0 Hz, 1H). MS: 257.1 m/z [M-1]⁻.

4-Chloro-N-(3-Hydroxyphenyl)-3-nitrobenzamide (12b)

Yield: 79%. ¹H NMR (400 MHz, DMSO-d₆) δ 10.37 (s, 1H), 9.45 (bs, 1H), 8.62 – 8.51 (m, 1H), 8.21 (d, *J* = 8.0 Hz, 1H), 7.93 (t, *J* = 7.0 Hz, 1H), 7.29 (s, 1H), 7.11 (d, *J* = 7.0 Hz, 2H), 6.51 (s, 1H). MS: 291.2 m/z [M-1]⁻.

N-(2-Chloro-5-Hydroxyphenyl)-3-nitrobenzamide (12c)

Yield: 63%. ¹H NMR (400 MHz, Acetone-d₆) δ 9.26 (bs, 1H), 8.97 – 8.63 (m, 2H), 8.50 – 8.40 (m, 2H), 8.04 – 7.81 (m, 1H), 7.79 – 7.60 (m, 1H), 7.47 – 7.18 (m, 1H), 6.90 – 6.58 (m, 1H). MS: 291.0 m/z [M-1]⁻.

General procedure for preparation of 13a-c

The suitable nitro-benzamidic compounds **12a-c** (**12a**: 292 mg, 1.13 mmol; **12b-c**: 330 mg, 1.13 mmol) was suspended in EtOH/Water 3:1 (12 mL) and NH₄Cl (30.2 mg, 0.56 mmol) was added. After the iron powder addition (315 mg, 5.65 mmol), the black suspension was heated at reflux for about 2 hours until finished start material, monitoring by TLC. The reaction mixture was cooled at room temperature and filtered on celite. The product was purified by

flash chromatography using DCM/MeOH (98:2 to obtain compounds **13a** and **13b**, 96:4 to obtain compounds **13c**) as eluent to give compounds **13a-c** as a pale-yellow solid.

3-Amino-N-(3-Hydroxyphenyl)benzamide (13a)

Yield: 82%. ¹H NMR (400 MHz, MeOD) δ 10.1 (bs, 1H), 7.28 (m, 1H), 7.20-7.11 (m, 5H), 7.05 (d, *J* = 8 Hz, 1H), 6.88 (d, *J* = 8Hz, 1H), 6.57 (d, *J* = 8Hz, 1H), 5.01 (bs, 2H). MS: 228.3 m/z [M-1]⁻.

3-Amino-4-chloro-N-(3-Hydroxyphenyl)benzamide (13b)

Yield: 73%. ¹H NMR (400 MHz, MeOD) δ 9.91 (bs, 1H), 7.30 (bs, 1H), 7.22 (d, *J* = 1.6 Hz, 1H), 7.20 (s, 1H), 7.17 (d, *J* = 1.6 Hz, 1H), 7.05 – 6.99 (m, 2H), 6.96 (d, *J* = 7.9 Hz, 1H), 6.48 (d, *J* = 7.9 Hz, 1H), 5.08 (bs, 2H). MS: 262.0 m/z [M-1]⁻.

3-Amino-N-(2-Chloro-5-hydroxyphenyl)benzamide (13c)

Yield: 88%. ¹H NMR (400 MHz, Acetone-d₆) δ 8.71 (bs, 1H), δ 8.61 (bs, 1H), 7.96 (d, *J* = 2.7 Hz, 1H), 7.27 – 7.25 (m, 2H), 7.23 – 7.15 (m, 2H), 6.87 (d, *J* = 7.6, 1H), 6.63 (dd, *J* = 8.3, 2.7 Hz, 1H), 4.93 (bs, 2H). MS: 262.1 m/z [M-1]⁻.

(4-Chloro-3-nitrophenyl)methanol (14)

Borane dimethyl sulfide (659 mg, 8.68 mmol) was added dropwise to a solution of 3-nitro-4-chlorobenzoic acid (500 mg, 2.48 mmol) **11b** in dry THF (5 mL) at 0 °C and the reaction stirred at room temperature for 18 hours under nitrogen atmosphere. After removing the solvent *in vacuo*, the crude product was dissolved in DCM and silica was added. The mixture stirred at room temperature for 1 hours, then filtered on Gooch and the product was purified by flash chromatography using DCM/MeOH (99.7:0.3) as eluent. Yield: 82%. ¹H NMR (400 MHz, Acetone-d₆) δ 7.95 – 7.93 (m, 1H), 7.67 – 7.65 (m, 2H), 4.73 (d, 2H), 4.65 – 4.59 (m, 1H). MS: 188.5 m/z [M+1]⁺.

4-(Bromomethyl)-1-chloro-2-nitrobenzene (15)

A 1.0 M solution of phosphorus tribromide in methylene chloride (797 mg, 2.95 mmol) was added dropwise to a reaction mixture of (4-chloro-3-nitrophenyl)methanol **14** (425 mg, 2.26 mmol) in dry DCM (10 mL) precooled at 0 °C. The red solution was stirred at 0 °C for 2 hours, until the complete transformation of alcohol to the corresponding bromide. Saturated solution of NaHCO₃ (10 mL) was added and the crude product was extracted in DCM (30 mL x 3), then dried and concentrated under reduce pressure. Finally, flash chromatography using E.P./EtOAc

(95:5) as eluent allowed to obtain the compound **15** as a brown oil. Yield: 45%. ¹H NMR (400 MHz, CDCl₃) δ 7.89 (s, 1H), 7.56 – 7.48 (m, 2H), 4.45 (s, 2H). MS: 251.2 m/z [M+1]⁺.

3-((4-Chloro-3-nitrobenzyl)oxy)phenol (16)

To a solution of resorcinol (454 mg, 4.13 mmol) and K₂CO₃ (171 mg, 1.24 mmol) in acetone (7 mL), previously stirred for 20 min at room temperature, 4-(bromomethyl)-1-chloro-2-nitrobenzene **15** (207 mg, 0.83 mmol) was added and the mixture was led to reflux for 3 hours. The solvent was removed under reduced pressure and the crude product was purified by flash chromatography using DCM/MeOH (99.5:0.5) as eluent, obtaining a yellow pale solid. Yield: 62%. ¹H NMR (400 MHz, CDCl₃) δ 10.51 (bs, 1H), 7.92 (s, 1H), 7.61 – 7.47 (m, 2H), 7.13 (td, 1H), 6.51 (d, *J* = 8.6, 1H), 6.49 – 6.43 (m, 2H), 5.03 (s, 2H). MS: 278.4 m/z [M-1]⁻.

3-((3-Amino-4-chlorobenzyl)oxy)phenol (17)

Nitrobenzyl ether intermediate **16** (200 mg, 0.72 mmol) was suspended in EtOH/Water 3:1 (7 mL) and NH₄Cl (20 mg, 0.36 mmol) was added. After the iron powder addition (199 mg, 3.58 mmol), the black suspension was heated at reflux for about 2 hours until start material finished, monitoring by TLC. The reaction mixture was cooled at room temperature and filtered on celite. The product was purified by flash chromatography using as eluent DCM/MeOH 97:3 to obtain compound **17**. **Yield:** 58%. ¹H NMR (400 MHz, Acetone-d₆) δ 8.26 (s, 1H), 7.24 - 7.16 (m, 1H), 7.14 – 7.01 (m, 1H), 6.92 (s, 1H), 6.75 – 6.61 (m, 1H), 6.54 – 6.36 (m, 3H), 4.94 - 4.92 (m, 4H). MS: 248.2 m/z [M-1]⁻.

Ethyl 2-aminothiazole-5-carboxylate (22)

To a mixture of ethyl-3-ethoxyacrylate **18** (1.00 g, 0.007 mol) in H₂O/1,4-Dioxane 1:1 (30 mL), precooled at -10 °C, NBS (1.36 g, 0.008 mol) was added and the reaction stirred for about 1 hour at room temperature until starting material finished. Thiourea (0.527 g, 0.007 mol) was added and the mixture stirred at 80 °C for 12 hours. The green-yellow solution was concentrated in vacuo, then treated with saturated NaHCO₃ solution until pH = 7. Extraction in EtOAc (50 mL x 3) and subsequent purification using DCM/MeOH (98.5:1.5) as eluent allowed to obtain compound **22** as a white solid. Yield: 78%. ¹H NMR (400 MHz, DMSO-d₆) δ 7.83 (s, 2H), 7.65 (s, 1H), 4.20 – 4.09 (m, 2H), 1.20 (s, 3H). MS: 173.3 m/z [M+1]⁺.

Ethyl 2-((tert-Butoxycarbonyl)amino)thiazole-5-carboxylate (23)

Ethyl 2-aminothiazole-5-carboxylate **22** (0.975 g, 0.006 mol) and DMAP (34 mg, 0.283 mmol) were dissolved in dry THF (15 mL), then di-*tert*-butyl dicarbonate (1.482 g, 0.007 mol) was added. After 15 minutes, a white suspension was generated and the reaction mixture stirred for 12 hours at room temperature. The solvent was removed *in vacuo* and the crude product was extracted with EtOAc (50 mL x 3). The organic layer was washed with 1 N HCl (70 mL), brine, then dried on Na₂SO₄ and concentrated under reduce pressure. To obtain a white solid **23**, the product was triturated with Hexane. Yield: 91%. ¹H NMR (400 MHz, CDCl₃) δ 7.76 (s, 1H), 5.12 (bs, 1H), 4.22 (q, J = 7.1 Hz, 2H), 1.30 (t, J = 7.1 Hz, 3H), 1.25 (s, 9H). MS: 272.6 m/z [M+1]⁺.

2-((tert-Butoxycarbonyl)amino)thiazole-5-carboxylic acid (24)

To a suspension of ethyl 2-((tert-butoxycarbonyl)amino)thiazole-5-carboxylate **23** (1.23 g, 0.005 mol) in EtOH/THF 3:2 (15 mL), KOH 6N (30 mL) was added and the mixture stirred for 7 hours at 50 °C. After cooling, the yellow pale solution was concentrated under reduced pressure and HCl 3N was added until pH = 1. Then, the suspension was filtered on Gooch and the white solid washed with water. The wet product was suspended in Toluene (25 mL x3) and concentrated under *vacuum* obtaining the compound **24**. Yield: 63%. ¹H NMR (400 MHz, DMSO-d₆) δ 11.99 (bs, 1H), 8.01 (s, 1H), 1.55 (s, 9H). MS: 242.0 m/z [M-1]⁻.

General procedure for preparation of 25a-e

2-((tert-Butoxycarbonyl)amino)thiazole-5-carboxylic acid **24** (300 mg, 1.23 mmol) was dissolved into a solution of EDC·HCl (282 mg, 1.48 mmol) in DMF (20 mL) and the mixture was stirred for 20 minutes at room temperature. HOBt monohydrate (207 mg, 1.35 mmol) and the suitable aniline (1.23 mmol) were added, then the reaction mixture stirred for about 11 hours at room temperature. Water (10 mL) was added at the solution and the crude product was extracted in EtOAc (40 mL x 3). The organic layer was washed with LiCl 5% solution (50 mL x 3), brine, then dried with Na₂SO₄ and concentrated under reduced pressure. Purification by flash chromatography using DCM/MeOH 98:2 as eluent allowed to obtain the respective compound **25a-e**.

tert-Butyl (5-(Phenylcarbamoyl)thiazol-2-yl)carbamate (25a)

Yield: 82%. ¹H NMR (400 MHz, DMSO-d₆) δ 10.10 (s, 1H), 9.50 (bs, 1H), 8.19 (s, 1H), 7.65 (d, J = 7.9 Hz, 2H), 7.31 (t, J = 7.9 Hz, 2H), 7.06 (t, J = 7.9 Hz, 1H), 1.48 (s, 9H). MS: 318.1 m/z [M-1]⁻.

tert-Butyl (5-((3-Chlorophenyl)carbamoyl)thiazol-2-yl)carbamate (25b)

Yield: 55%. ¹H NMR (400 MHz, DMSO-d₆) δ 10.12 (s, 1H), 9.42 (s, 1H), 8.21 (s, 1H), 7.31 (s, 1H), 7.20 – 7.01 (m, 2H), 6.53 – 6.48 (m, 1H), 1.46 (s, 9H). MS: 353.0 m/z [M-1]⁻.

tert-Butyl (5-((3-Hydroxyphenyl)carbamoyl)thiazol-2-yl)carbamate (25c)

Yield: 61%. ¹H NMR (400 MHz, DMSO-d₆) δ 9.97 (s, 1H), 9.37 (s, 1H), 8.28 (s, 1H), 8.17 (s, 1H), 7.23 (s, 1H), 7.15 – 6.96 (m, 2H), 6.50 – 6.44 (m, 1H), 1.48 (s, 9H). MS: 334.1 m/z [M-1]⁻.

tert-Butyl (5-((2-Bromo-5-hydroxyphenyl)carbamoyl)thiazol-2-yl)carbamate (25d)

Yield: 51%. ¹H NMR (400 MHz, DMSO-d₆) δ 11.80 (bs, 1H), 10.27 (s, 1H), 10.12 (s, 1H), 8.19 (s, 1H), 7.53 (s, 1H), 7.38 (d, *J* = 8.6 Hz, 1H), 7.01 (d, *J* = 8.6 Hz, 1H), 1.49 (s, 9H). MS: 414.3 m/z [M-1]⁻.

tert-Butyl (5-((5-Hydroxy-2-methylphenyl)carbamoyl)thiazol-2-yl)carbamate (25e)

Yield: 86%. ¹H NMR (400 MHz, DMSO-d₆) δ 11.76 (bs, 1H), 9.62 (s, 1H), 9.24 (s, 1H), 8.13 (s, 1H), 7.01 (d, *J* = 8.2 Hz, 1H), 6.76 (s, 1H), 6.55 (d, *J* = 8.2 Hz, 1H), 2.08 (s, 3H), 1.48 (s, 9H). MS: 348.0 m/z [M-1]⁻.

General procedure for preparation of 26a-e

To a solution of TFA 10% in anhydrous DCM (5 mL) was added the opportune compound **25a-e** (0.313 mmol) and the mixture was stirred for 6 hours at room temperature. The solution was concentrated with reduced pressure and dried by washing with toluene.

5-(Phenylcarbamoyl)thiazol-2-ammonium trifluoroacetate (26a)

Yield: 85%. ¹H NMR (400 MHz, MeOD) δ 9.40 (bs, 1H), 8.10 (s, 1H), 7.45-7.29 (m, 3H), 7.08-7.06 (m, 2H), 6.30 (bs, 3H). MS: 333.1 m/z [M+1]⁺.

5-((3-Chlorophenyl)carbamoyl)thiazol-2-ammonium trifluoroacetate (26b)

Yield: 81%. ¹H NMR (400 MHz, MeOD) δ 9.42 (bs, 1H), 8.18 (s, 1H), 7.28-7.06 (m, 3H), 6.48 – 6.40 (m, 1H), 6.22 (bs, 3H). MS: 367.5 m/z [M+1]⁺.

5-((3-Hydroxyphenyl)carbamoyl)thiazol-2-ammonium trifluoroacetate (26c)

Yield: 76%. ¹H NMR (400 MHz, MeOD) δ 9.30 (bs, 1H), 8.18 (bs, 1H), 8.09 (s, 1H), 7.21-6.94 (m, 3H), 6.46 – 6.41 (m, 1H) 6.18 (bs, 3H). MS: 349.4 m/z [M+1]⁺.

5-((2-Bromo-5-hydroxyphenyl)carbamoyl)thiazol-2-ammonium trifluoroacetate (26d)

Yield: 72%. ¹H NMR (400 MHz, MeOD) δ 9.35 (bs, 1H), 8.54 (bs, 1H), 8.21 (s, 1H), 7.27-6.99 (m, 2H), 6.72-6.64 (m, 1H), 6.18 (bs, 3H). MS: 428.1 m/z [M+1]⁺.

5-((5-Hydroxy-2-methylphenyl)carbamoyl)thiazol-2-ammonium trifluoroacetate (26e)

Yield: 89%. ¹H NMR (400 MHz, MeOD) δ 9.31 (bs, 1H), 8.30 (bs, 1H), 8.15 (s, 1H), 7.17 – 6.98 (m, 2H), 6.55-6.53 (m, 1H), 6.15 (bs, 3H), 2.15 (s, 3H). MS: 363.2 m/z [M+1]⁺.

1-Benzyl-4-nitro-1H-imidazole (27)

To a suspension of 4-nitroimidazole (500 mg, 4.42 mmol) **26** and K₂CO₃ (977 mg, 7.07 mmol) in CH₃CN (7 mL), previously stirred at room temperature for 25 minutes, benzyl bromide (831 mg, 4.86 mmol) was added dropwise and the reaction mixture stirred for 7 hours at reflux. After removing the solvent under reduced pressure, the crude product was purified by flash chromatography using a mix of E.P./Acetone/MeOH (8:1.9:0.1) as eluent to obtaining the intermediate **27**. Yield: 88%. ¹H NMR (400 MHz, DMSO-d₆) δ 8.45 (s, 1H), 7.97 (s, 1H), 7.46 – 7.24 (m, 5H), 5.28 (s, 2H). MS: 204.1 m/z [M+1]⁺.

1-Benzyl-1H-imidazol-4-amine hydrochloride (28)

1.) 1-benzyl-4-nitro-1H-imidazole **27** (300 mg, 1.47 mmol) was dissolved in EtOH (20 mL) and Pd/C (0.3 mg, 0.245 mmol) was added in small batches. The mixture stirred for about 12 hours at room temperature under H₂ atmosphere, until the end of reaction, monitoring by TLC. The black suspension was filtered on celite obtaining a yellow pale solution.

2.) In order to preserve the crude product from the light, it was introduced into an aluminium-coated reaction flask and a solution of HCl 1.25 N in EtOH (20 mL) was added. The mixture stirred for 24 hours at room temperature, then concentrated under reduced pressure obtaining a yellow oil. Trituration with DCM/E.P. give the chloro ammonium salt **27** as a yellow pale solid. Yield: 61%. ¹H NMR (400 MHz, DMSO-d₆) δ 8.61 (d, *J* = 6.7 Hz, 1H), 7.42 – 7.30 (m, 5H), 6.58 (d, *J* = 6.8 Hz, 1H), 5.42 (s, 3H), 5.23 (s, 2H). MS: 209.3 m/z [M+1]⁺.

General procedure for preparation of compounds 30a-d, 32 and 33a-c.

The appropriate halo-compound **29a,b** or **31a,b** (0.183 mmol) was dissolved in absolute EtOH (8 mL) and the suitable chain **13a-c** or **17** (0.366 mmol) was added. The reaction mixture stirred for about 6 hours at reflux, monitoring the end by TLC. After cooling at room temperature,

EtOH was removed under vacuum and the residue was purified by flash chromatography using a proper mix of DCM/MeOH (99.5:0.5 for **30a-b**, 98:2 for **30c-d**, and 99:1 for **32** and **33a-c**) as eluent. Subsequent trituration using E.P. allowed to obtain a white solids **30a-d**, **32** and **33a-c**.

3-((1-(2-Chloro-2-phenylethyl)-1H-pyrazolo[3,4-d]pyrimidin-4-yl)amino)-N-(3-hydroxyphenyl) benzamide (30a)

Yield: 85%. ¹H NMR (400 MHz, Acetone-d₆) δ 9.41 (bs, 1H), 9.37 (bs, 1H), 8.45 (s, 1H), 8.35 (s, 1H), 8.32 (bs, 1H), 8.19 – 8.16 (m, 2H), 7.68 (d, *J* = 7.3 Hz, 1H), 7.59 – 7.44 (m, 4H), 7.42 – 7.29 (m, 3H), 7.24 (d, *J* = 7.3 Hz, 1H), 7.13 (t, *J* = 8.0 Hz, 1H), 6.59 (d, *J* = 8.0 Hz, 1H), 5.74 – 5.62 (m, 1H), 5.02 (dd, *J* = 14.1, 8.6 Hz, 1H), 4.85 (dd, *J* = 14.1, 8.6 Hz, 1H). ¹³C NMR (100 MHz, Acetone-d₆) δ 165.22, 157.75, 155.30, 154.73, 154.01, 140.57, 139.69, 138.34, 136.37, 131.69, 129.33, 128.90, 128.76, 128.67, 127.54, 123.98, 122.17, 120.37, 111.27, 110.80, 107.33, 101.33, 60.38, 53.16. MS: 485.2 m/z [M+1]⁺.

N-(3-Hydroxyphenyl)-3-((1-(2-phenylpropyl)-1H-pyrazolo[3,4-d]pyrimidin-4-yl)amino)benzamide (30b)

Yield: 92%. ¹H NMR (400 MHz, Acetone-d₆) δ 9.42 (s, 1H), 9.34 (s, 1H), 8.41 (s, 1H), 8.34 (s, 1H), 8.32 (s, 1H), 8.18 (d, *J* = 8.0 Hz, 1H), 8.11 (s, 1H), 7.67 (d, *J* = 7.9 Hz, 1H), 7.54-7.52 (m, 1H), 7.47 (t, *J* = 7.9 Hz, 1H), 7.31 – 7.18 (m, 5H), 7.13 (t, *J* = 8.0 Hz, 2H), 6.59 (d, *J* = 8.0 Hz, 1H), 4.56 (dd, *J* = 13.6, 7.4 Hz, 1H), 4.49 (dd, *J* = 13.6, 7.4 Hz, 1H), 3.67 – 3.46 (m, 1H), 1.22 (d, *J* = 7.0 Hz, 3H). ¹³C NMR (100 MHz, Acetone-d₆) δ 165.3, 157.7, 155.1, 154.6, 153.8, 143.7, 140.6, 139.8, 136.3, 130.8, 129.3, 128.7, 128.3, 127.2, 126.5, 123.9, 122, 120.3, 111.3, 110.8, 107.4, 101.3, 53.1, 39.9, 18.5. MS: 465.2 m/z [M+1]⁺.

4-Chloro-3-((1-(2-chloro-2-phenylethyl)-1H-pyrazolo[3,4-d]pyrimidin-4-yl)amino)-N-(3-hydroxyphenyl) benzamide (30c)

Yield: 67%. ¹H NMR (400 MHz, Acetone-d₆) δ 9.57 (bs, 1H), 9.48 (bs, 1H), 8.50 (d, *J* = 8.2 Hz, 1H), 8.39 – 8.31 (m, 1H), 8.11 – 8.03 (m, 1H), 8.01 – 7.85 (m, 2H), 7.69-7.64 (m, 1H), 7.57 – 7.43 (m, 3H), 7.41 – 7.30 (m, 3H), 7.20 (d, *J* = 8.2 Hz, 1H), 7.17 – 7.06 (m, 1H), 6.60 (t, *J* = 8.2 Hz, 1H), 5.71 – 5.63 (m, 1H), 5.09 – 4.96 (m, 1H), 4.89 – 4.79 (m, 1H). ¹³C NMR (100 MHz, Acetone-d₆) δ 165.11, 162.42, 157.57, 154.89, 153.24, 143.05, 139.36, 134.85, 131.48, 130.02, 129.13, 129.06, 128.85, 128.06, 127.62, 126.86, 126.48, 126.38, 116.23, 114.42, 111.91, 111.39, 111.21, 107.90, 52.72, 38.64. MS: 519.1 m/z [M+1]⁺.

4-Chloro-N-(3-Hydroxyphenyl)-3-((1-(2-phenylpropyl)-1H-pyrazolo[3,4-d]pyrimidin-4-yl)amino) benzamide (30d)

Yield: 73%. ¹H NMR (400 MHz, MeOD) δ 9.38 (bs, 1H), 9.32 (bs, 1H), 8.22 (bs, 1H), 8.20 (s, 1H), 7.90 (s, 1H), 7.84 (d, *J* = 8.4, 1H), 7.68 (d, *J* = 8.4 Hz, 1H), 7.35 – 7.24 (m, 2H), 7.23 – 7.03 (m, 7H), 6.59-6.52 (m, 1H), 4.52 – 4.49 (m, 2H), 3.56 – 3.44 (m, 1H), 1.34 – 1.20 (m, 3H). ¹³C NMR (100 MHz, MeOD) δ 165.68, 163.42, 157.57, 154.89, 153.24, 143.05, 139.36, 134.85, 131.48, 130.02, 129.13, 129.06, 128.85, 128.06, 127.62, 126.86, 126.48, 126.38, 116.23, 114.42, 111.91, 111.39, 111.21, 107.90, 53.14, 40.10, 17.69. MS: 499.5 m/z [M+1]⁺.

3-((4-Chloro-3-((1-(2-chloro-2-phenylethyl)-6-(methylthio)-1H-pyrazolo[3,4-d]pyrimidin-4-yl)amino) benzyl)oxy)phenol (32)

Yield: 87%. ¹H NMR (400 MHz, Acetone-d₆) δ 8.87 (bs, 1H), 8.35 (s, 1H), 8.04 (s, 1H), 7.71 (s, 1H), 7.57 – 7.47 (m, 3H), 7.42 – 7.26 (m, 4H), 7.06 (t, 1H), 6.52 – 6.40 (m, 3H), 5.65 – 5.57 (m, 1H), 5.09 (s, 2H), 4.91 (dd, *J* = 14.1, 8.3 Hz, 1H), 4.79 (dd, *J* = 14.1, 8.3 Hz, 1H), 2.50 (s, 3H). ¹³C NMR (100 MHz, Acetone-d₆) δ 169.26, 160.08, 158.71, 155.14, 154.63, 138.26, 137.61, 135.23, 132.01, 129.94, 129.76, 128.89, 128.57, 127.55, 126.73, 126.15, 108.15, 105.87, 102.24, 98.45, 68.50, 60.17, 53.08, 13.27. MS: 551.0 m/z [M-1]⁻.

4-Chloro-3-((1-(2-chloro-2-phenylethyl)-6-(methylthio)-1H-pyrazolo[3,4-d]pyrimidin-4-yl)amino)-N-(3-hydroxyphenyl)benzamide (33a)

Yield: 87%. ¹H NMR (400 MHz, DMSO-d₆) δ 10.17 (bs, 1H), 10.14 (bs, 1H), 9.38 (s, 1H), 8.21 (s, 1H), 7.91-7.87 (m, 2H), 7.76-7.70 (m, 1H), 7.52-7.46 (m, 2H), 7.38 – 7.28 (m, 4H), 7.10 (t, *J* = 6.9 Hz, 2H), 6.48 (d, *J* = 6.9 Hz, 1H), 5.68 – 5.59 (m, 1H), 4.89 (dd, *J* = 14.3, 8.5 Hz, 1H), 4.76 (dd, *J* = 14.3, 8.5 Hz, 1H), 2.39 (s, 3H). ¹³C NMR (100 MHz, DMSO-d₆) δ 169.44, 169.06, 163.84, 158.00, 155.13, 154.57, 140.29, 138.38, 135.44, 134.90, 132.19, 129.79, 129.23, 128.92, 128.62, 127.53, 127.39, 126.24, 111.19, 111.00, 107.53, 98.48, 60.12, 53.13, 13.32. MS: 564.2 m/z [M-1]⁻.

4-Chloro-N-(3-Hydroxyphenyl)-3-((6-(methylthio)-1-(2-phenylpropyl)-1H-pyrazolo[3,4-d]pyrimidin-4-yl)amino)benzamide (33b)

Yield: 87%. ¹H NMR (100 MHz, acetone-d₆) δ 9.51 (bs, 1H), 8.97 (bs, 1H), 8.55 (s, 1H), 8.35 (bs, 1H), 7.87 (d, *J* = 6.1 Hz, 1H), 7.81 (s, 1H), 7.68 – 7.65 (m, 1H), 7.49 (s, 1H), 7.27-7.10 (m, 7H), 6.58 (d, *J* = 6.1 Hz, 1H), 4.51 (dd, *J* = 8.0 Hz, 1H), 4.41 (dd, *J* = 8.0 Hz, 1H), 3.53 (sxt, 1H), 2.48 (s, 3H), 1.22 (s, 3H). ¹³C NMR (100 MHz, acetone-d₆) δ 164.2, 158.1, 154.6,

143.9, 140.4, 135.6, 132.35, 130.30, 129.7, 128.8, 128.5, 127.6, 127.3, 126.9, 111.6, 111.5, 108.1, 98.6, 53.2, 46.2, 19.5, 13.9, 8.9. MS: 544.1 m/z [M-1].

3-((1-(2-Chloro-2-phenylethyl)-6-(methylthio)-1H-pyrazolo[3,4-d]pyrimidin-4-yl)amino)-N-(2-chloro-5-hydroxyphenyl)benzamide (33c)

Yield: 87%. ¹H NMR (400 MHz, Acetone-d₆) δ 9.44 (bs, 1H), 8.83 (s, 1H), 8.76 (bs, 1H), 8.47 (s, 1H), 8.07 (d, *J* = 8.3 Hz, 2H), 7.90-7.87 (m, 1H), 7.71 (d, *J* = 7.4 Hz, 1H), 7.62 – 7.45 (m, 3H), 7.44 – 7.22 (m, 4H), 6.67 (d, *J* = 7.4 Hz, 1H), 5.65-5.62 (m, 1H), 4.91 (dd, *J* = 14.1, 8.2 Hz, 1H), 4.81 (dd, *J* = 14.1, 6.7 Hz, 1H), 2.59 (s, 3H). ¹³C NMR (100 MHz, Acetone-d₆) δ 169.64, 164.71, 156.80, 154.72, 153.56, 139.73, 138.35, 135.59, 135.26, 131.90, 129.51, 129.16, 128.89, 128.60, 127.55, 124.38, 122.01, 120.07, 114.83, 112.66, 110.46, 98.95, 59.95, 53.09, 13.50. MS: 563.0 m/z [M-1].

General procedure for preparation of 34a-b

3-Chloroperbenzoic acid (23 mg, 0.136 mmol) was added to a solution, precooled at 0° C, of suitable compound **33a** or **33c** (35 mg, 0.061 mmol) in anidrous DCM (5 mL) and the mixture stirred at room temperature for 2 h. Saturated solution of NaHCO₃ was added in ice bath dropwise until pH = 7 and the mixture was extracted with EtOAc(40 mL x 3). Organic phase was dried on Na₂SO₄, filtered and concentrated under reduce pressure. The crude product was employed in the next step without additional purification. The resulting mix of sulfone and sulfoxide was dissolved in DMSO/butan-1-olo 1:2 (6 mL). 4-(2-aminoethyl)morpholine or ethanolamine (0.146 mmol) was added and the reaction mixture stirred at 120° C for 8-10 hours. Water was added and the product was extracted in EtOAc (40 mL x 5), washed with brine, then dried on Na₂SO₄, filtered and concentrated *in vacuo*. The residual 1-butanolo and DMSO was removed under nitrogen flux. Brown solid was purified by Flash Chromatography, using a proper mix of P.E./Acetone (7:3 for **34a** and 8:2 for **34b**) as eluent, then crystallized in DCM to obtain a white solid.

4-Chloro-3-((1-(2-chloro-2-phenylethyl)-6-((2-hydroxyethyl)amino)-1H-pyrazolo[3,4-d]pyrimidin-4-yl)amino)-N-(3-hydroxyphenyl)benzamide (34a)

Yield: 51%. ¹H NMR (400 MHz, DMSO-d₆) δ 10.13 (s, 1H), 9.57 (bs, 1H), 9.39 (s, 1H), 8.18 (s, 1H), 7.83 – 7.78 (m, 2H), 7.68 (d, *J* = 8.4 Hz, 1H), 7.50-7.46 (m, 2H), 7.37 – 7.31 (m, 4H), 7.16 – 7.03 (m, 2H), 6.64 (s, 1H), 6.49 (d, *J* = 8.4 Hz, 1H), 5.69-5.60 (m, 1H), 4.81 – 4.56 (m, 2H), 3.48 (s, 2H), 3.32 (s, 2H), 3.15 (bs, 1H). ¹³C NMR (100 MHz, DMSO-d₆) δ 164.46, 161.42, 157.88, 156.84, 155.54, 140.32, 138.60, 136.18, 134.51, 132.92, 130.14, 129.59,

129.36, 129.09, 127.95, 126.52, 119.77, 111.64, 111.33, 107.97, 107.42, 95.82, 60.88, 60.46, 52.62, 29.47. MS: 577.3 m/z [M-1]⁻.

3-((1-(2-Chloro-2-phenylethyl)-6-((2-morpholinoethyl)amino)-1H-pyrazolo[3,4-d]pyrimidin-4-yl)amino)-N-(2-chloro-5-hydroxyphenyl)benzamide (34b)

Yield: 65%. ¹H NMR (400 MHz, Acetone-d₆) δ 9.08 (bs, 1H), 8.84 (bs, 1H), 8.78 (bs, 1H), 8.58 (s, 1H), 8.09 (d, *J* = 7.8 Hz, 1H), 7.92-7.88 (m, 2H), 7.66 (d, *J* = 7.8 Hz, 1H), 7.50 (s, 3H), 7.39 – 7.21 (m, 4H), 6.68 (d, *J* = 8.6 Hz, 1H), 6.20 (s, 1H), 5.67 – 5.61 (m, 1H), 4.90 – 4.56 (m, 2H), 3.60 (s, 4H), 2.85 (s, 2H), 2.61 (s, 2H), 2.47 (s, 4H). ¹³C NMR (100 MHz, acetone-d₆) δ 164.99, 161.34, 156.86, 156.41, 154.67, 140.43, 138.27, 136.42, 135.00, 134.94, 132.70, 129.15, 128.98, 128.66, 128.50, 127.42, 127.23, 125.68, 123.86, 120.99, 119.34, 112.36, 109.31, 96.69, 60.06, 57.28, 53.23, 48.29, 41.02, 30.64. MS: 646.0 m/z [M-1]⁻.

General procedure for preparation of compounds 35 and 42

The intermediate **31a** or **40** (0.058 mmol) was suspended in absolute ethanol (2 mL) and fresh distilled TEA (11 mg, 0.118 mmol) was added dropwise. Compound **28** (16 mg, 0.086 mmol) was added in the mixture and the reaction stirred for 6 hours at reflux. Then, after cooling to room temperature, the solution was concentrated under vacuum. Purification by flash chromatography using a gradient of DCM/MeOH (99.5:0.5 to 98:2) allowed to obtain compound **35** or **42** as a white solid.

N-(1-Benzyl-1H-imidazol-4-yl)-1-(2-chloro-2-phenylethyl)-6-(methylthio)-1H-pyrazolo[3,4-d]pyrimidin-4-amine (35)

Yield: 65%. ¹H NMR (400 MHz, CDCl₃) δ 9.59 (bs, 1H), 7.81 (s, 1H), 7.50 (s, 1H), 7.44 – 7.31 (m, 5H), 7.31 – 7.17 (m, 5H), 5.54-5.48 (m, 1H), 5.12 (s, 2H), 4.88 (dd, *J* = 14.0, 8.0 Hz, 1H), 4.77 (dd, *J* = 14.0, 8.0 Hz, 1H), 2.52 (s, 3H). ¹³C NMR (100 MHz, CDCl₃) δ 165.35, 161.11, 156.80, 154.72, 152.23, 146.97, 139.34, 139.21, 135.99, 134.37, 130.93, 130.77, 129.09, 128.48, 127.25, 98.95, 66.74, 58.96, 52.09, 13.50. MS: 476.4 m/z [M+1]⁺.

N-(1-Benzyl-1H-imidazol-4-yl)-1-methyl-6-((2-morpholinoethyl)thio)-1H-pyrazolo[3,4-d]pyrimidin-4-amine (42)

Yield: 45%. ¹H NMR (400 MHz, CDCl₃) δ 9.46 (bs, 1H), 7.81 (s, 1H), 7.56 (s, 1H), 7.44 – 7.29 (m, 4H), 7.29 – 7.19 (m, 2H), 5.13 (s, 2H), 3.94 (s, 3H), 3.72 (d, 4H), 3.40 – 3.27 (m, 2H), 2.82 – 2.69 (m, 2H), 2.55 (d, 4H). ¹³C NMR (100 MHz, CDCl₃) δ 168.91, 163.14, 146.97, 139.62, 139.22, 135.99, 134.37, 130.93, 130.77, 129.09, 128.48, 127.25, 66.74, 58.22, 53.43, 51.34, 33.53, 27.63. MS: 272.1 m/z [M+1]⁺.

Ethyl 5-amino-1-methyl-1H-pyrazole-4-carboxylate (36)

To a solution of compound **35** (7.00 g, 0.041 mol) in absolute ethanol (30 mL) methyl hydrazine (1.91 g, 0.041 mol) was added and the reaction mixture stirred for 8 hours at reflux. The solvent was removed under reduced pressure and the crude product was purified by flash chromatography using a gradient of DCM/MeOH (99:1 to 96:4) as eluent to obtain the intermediate **36** as a yellow pale solid. Yield: 73%. ¹H NMR (400 MHz, DMSO-d₆) δ 7.39 (s, 1H), 6.16 (s, 2H), 4.14 (q, *J* = 7.0 Hz, 2H), 3.51 (s, 3H), 1.22 (t, *J* = 7.0 Hz, 3H). MS: 170.2 m/z [M+1]⁺.

Ethyl 5-(3-benzoylthioureido)-1-methyl-1H-pyrazole-4-carboxylate (37)

Ethyl 5-amino-1-methyl-1H-pyrazole-4-carboxylate **36** (5.70 g, 0.034 mol) was dissolved in dry THF (30 mL) and benzoyl isothiocyanate (6.32 g, 0.039 mol) was added dropwise. The reaction mixture was stirred for 6 hours at reflux and, after cooling, it was concentrated *in vacuo*. The residue was resolubilized in DCM and triturated with E.P., then filtered on Gooch obtaining a white solid. Yield: 85%. ¹H NMR (400 MHz, CDCl₃) δ 10.6 (bs, 1H), 9.33 (s, 1H), 7.97 – 7.87 (m, 2H), 7.72 – 7.63 (m, 1H), 7.59 – 7.55 (m, 2H), 7.25 (s, 1H), 4.30 – 4.25 (m, 2H), 3.87 (s, 3H), 1.32 – 1.28 (m, 3H). MS: 331.0 m/z [M-1]⁻.

6-Mercapto-1-methyl-1H-pyrazolo[3,4-d]pyrimidin-4-ol (38)

Compound **37** (10.23 g, 0.057 mol) was suspended in 2 N NaOH (80 mL) and the reaction mixture stirred for 5 hours at reflux. Then, the limpid solution was cooled into an ice-bath and acetic acid was added dropwise to form a white precipitate. The solid compound was filtered on Gooch and washed with toluene to remove the excess of acetic acid, thus obtaining a white solid **38**. Yield: 88%. ¹H NMR (400 MHz, DMSO-d₆) δ 11.12 (bs, 1H), 10.31 (bs, 1H), 7.85 (s, 1H), 3.82 (s, 3H). MS: 180.1 m/z [M-1]⁻.

1-Methyl-6-((2-morpholinoethyl)thio)-1H-pyrazolo[3,4-d]pyrimidin-4-ol (39)

To a solution of 6-Mercapto-1-methyl-1H-pyrazolo[3,4-*d*]pyrimidin-4-ol **38** (1.02 g, 0.011 mol) in DMF (10 mL), NaOH (0.356 g, 0.018 mol) previously dissolved in EtOH (10 mL) was added dropwise. Then, chloroethyl morpholine hydrochloride (1.035 g, 0.011 mol) was added in the mixture and the reaction stirred for 8 hours at reflux. After cooling at room temperature, the solution was concentrated under vacuum and water was added. The crude product was extracted with EtOAc (50 mL x 3), then the organic layer was washed with LiCl 5% solution (60 mL x 3), brine, dried with Na₂SO₄ and concentrated under reduced pressure. The residue was crystallized in diethyl ether obtaining the compound **39** as a white solid. Yield: 64%. ¹H

NMR (400 MHz, CDCl₃) δ 10.21 (bs, 1H), 7.97 (s, 1H), 3.91 (s, 3H), 3.84 (m, 4H), 3.29 (m, 2H), 2.82 (m, 2H), 2.61 (m, 4H). MS: 294.2 m/z [M-1]⁻.

4-(2-((4-Chloro-1-methyl-1H-pyrazolo[3,4-d]pyrimidin-6-yl)thio)ethyl)morpholine (40)

The Vilsmeier complex, previously prepared from fresh distilled POCl₃ (3.89 g, 0.025 mol) and dry DMF (1.85 g, 0.025 mol) at 0°C, was added into a solution of compound **39** (0.750 g, 0.025 mol) in dry CHCl₃ (25 mL) and the reaction mixture stirred for 4 hours at reflux. After cooling at room temperature, water was added and the crude product was extracted in CHCl₃ (40 mL x 3). The organic layer was washed with LiCl 5% solution (50 mL x 3), brine, then dried with Na₂SO₄ and concentrated under reduced pressure. Purification using DCM/MeOH (95:5) as eluent allowed to obtain halogenated compound **40** as a white solid. Yield: 55%. ¹H NMR (400 MHz, CDCl₃) δ 7.96 (s, 1H), 4.01 (s, 3H), 3.70 (m, 4H), 3.35 (t, *J* = 7.0 Hz, 2H), 2.74 (t, *J* = 7.0 Hz, 2H), 2.56 (m, 4H). MS: 314.3 m/z [M+1]⁺.

General procedure for preparation of compounds 41a-e and 43

To a black solution of Pd₂(dba)₃ (35 mg, 0.038 mmol) and Xantphos (22 mg, 0.038 mmol) in dry 1,4-dioxane (5 mL), compound **40** (40 mg, 0.166 mmol) was added and the mixture stirred for about 30 minutes at room temperature. After a little solution color change to black/orange, K₂CO₃ (70 mg, 0.508 mmol) and the suitable aminothiazole chain **26a-e** (0.228 mmol) were added, and the mixture stirred for about 4 hours at reflux. The reaction was cooled at room temperature and palladium was filtered on a pad of celite. Purification by flash chromatography of crude product using a proper gradient mix of DCM/MeOH (99.5:0.5 to 97:3) as eluent and subsequent crystallization in MeOH allowed to obtain compounds **41a-e** and **43**.

2-((1-Methyl-6-((2-morpholinoethyl)thio)-1H-pyrazolo[3,4-d]pyrimidin-4-yl)amino)-N-phenylthiazole-5-carboxamide (41a)

Yield: 66%. ¹H NMR (400 MHz, CDCl₃) δ 10.16 (bs, 1H), 9.19 (bs, 1H), 8.11 (s, 1H), 8.05 (s, 1H), 7.55 (d, *J* = 7.8 Hz, 2H), 7.16 (t, *J* = 7.8 Hz, 2H), 6.93 (t, *J* = 7.8 Hz, 1H), 3.82 (s, 3H), 3.58-3.56 (m, 4H), 3.34-3.30 (m, 2H), 2.65-2.60 (m, 2H), 2.43-2.40 (m, 4H). ¹³C NMR (100 MHz, CDCl₃) δ 168.13, 161.78, 160.07, 154.07, 150.16, 140.46, 138.53, 132.39, 128.61, 123.84, 122.83, 120.39, 99.19, 66.75, 57.75, 53.45, 33.65, 27.83. MS: 495.0 m/z [M-1]⁻.

N-(3-Chlorophenyl)-2-((1-methyl-6-((2-morpholinoethyl)thio)-1H-pyrazolo[3,4-d]pyrimidin-4-yl)amino)thiazole-5-carboxamide (41b)

Yield: 45%. ¹H NMR (400 MHz, DMSO-d₆) δ 10.88 (bs, 1H), 10.32 (bs, 1H), 8.36-8.32 (m, 2H), 7.89 (s, 1H), 7.63 (d, *J* = 8.0 Hz, 1H), 7.38 (t, *J* = 8.0 Hz, 1H), 7.14 (d, *J* = 8.0 Hz, 1H),

3.92 (s, 3H), 3.59-3.57 (m, 4H), 3.42-3.40 (m, 2H), 2.72-2.70 (m, 2H), 2.52-2.49 (m, 4H). ¹³C NMR (100 MHz, DMSO-d₆) δ 167.8, 161.9, 160.3, 154, 150.2, 141.2, 140.8, 133.5, 132.5, 130.9, 128.6, 123.7, 119.9, 118.7, 99.2, 66.7, 57.8, 53.5, 34.0, 27.8. MS: 530.2 m/z [M-1]⁻.

N-(3-Hydroxyphenyl)-2-((1-methyl-6-((2-morpholinoethyl)thio)-1H-pyrazolo[3,4-d]pyrimidin-4-yl)amino)thiazole-5-carboxamide (**41c**)

Yield: 59% ¹H NMR (400 MHz, DMSO-d₆) δ 12.91 (bs, 1H), 10.11 (bs, 1H), 9.48 (bs, 1H), 8.47-8.45 (m, 2H), 7.33 (s, 1H), 7.21-7.16 (m, 2H), 6.57-6.55 (m, 1H), 3.99 (s, 3H), 3.65-3.62 (m, 4H), 3.49-3.47 (m, 2H), 2.81-2.76 (m, 2H), 2.59-2.56 (m, 4H). ¹³C NMR (100 MHz, DMSO-d₆) δ 167.8, 161.5, 159.9, 158.1, 154.1, 150.3, 140.3, 132.5, 129.8, 129.3, 111.3, 107.7, 99.1, 66.6, 57.7, 53.5, 34.1, 27.7. MS: 511.0 m/z [M-1]⁻.

N-(2-Bromo-5-hydroxyphenyl)-2-((1-methyl-6-((2-morpholinoethyl)thio)-1H-pyrazolo[3,4-d]pyrimidin-4-yl)amino)thiazole-5-carboxamide (**41d**)

Yield: 51% ¹H NMR (400 MHz, DMSO-d₆) δ 12.88 (bs, 1H), 10.34 (s, 1H), 10.18 (s, 1H), 8.37 (s, 1H), 8.34 (s, 1H), 7.52 (d, *J* = 2.4 Hz, 1H), 7.40 (d, *J* = 8.7 Hz, 1H), 7.08 (dd, *J* = 8.7, 2.4 Hz, 1H), 3.91 (s, 3H), 3.61 – 3.52 (m, 4H), 3.45 – 3.36 (m, 2H), 2.70 – 2.66 (m, 2H), 2.52 – 2.42 (m, 4H). ¹³C NMR (100 MHz, DMSO-d₆) δ 167.73, 161.80, 160.02, 154.45, 153.98, 150.33, 140.95, 139.64, 132.96, 132.50, 128.83, 112.72, 108.25, 103.69, 99.08, 66.62, 57.79, 53.52, 34.00, 27.69. MS: 590.3 m/z [M-1]⁻.

N-(5-Hydroxy-2-methylphenyl)-2-((1-methyl-6-((2-morpholinoethyl)thio)-1H-pyrazolo[3,4-d]pyrimidin-4-yl)amino)thiazole-5-carboxamide (**41e**)

Yield: 70% ¹H NMR (400 MHz, DMSO-d₆) δ 12.82 (bs, 1H), 9.70 (s, 1H), 9.29 (s, 1H), 8.34 (s, 1H), 8.30 (s, 1H), 7.02 (d, *J* = 8.3 Hz, 1H), 6.80 (d, *J* = 2.5 Hz, 1H), 6.57 (dd, *J* = 8.3, 2.5 Hz, 1H), 3.91 (s, 3H), 3.64 – 3.48 (m, 4H), 3.45 – 3.23 (m, 2H), 2.75 – 2.58 (m, 2H), 2.54 – 2.35 (m, 4H), 2.11 (s, 3H). ¹³C NMR (100 MHz, DMSO-d₆) δ 167.73, 163.43, 161.34, 159.90, 155.83, 153.92, 150.19, 140.45, 136.69, 132.64, 131.25, 128.88, 123.67, 113.63, 99.05, 66.60, 57.77, 53.50, 33.98, 27.55, 17.38. MS: 525.1 m/z [M-1]⁻.

4-Chloro-*N*-(3-hydroxyphenyl)-3-((1-methyl-6-((2-morpholinoethyl)thio)-1H-pyrazolo[3,4-d]pyrimidin-4-yl)amino)benzamide (**43**)

Yield: 65% ¹H NMR (400 MHz, CDCl₃) δ 8.74 (bs, 1H), 8.03 (s, 1H), 7.96 (d, *J* = 8.1 Hz, 1H), 7.59 (d, *J* = 8.1 Hz, 1H), 7.27 – 7.24 (m, 2H), 7.07 (t, *J* = 8.1 Hz, 1H), 6.95 (d, *J* = 7.5 Hz, 1H), 6.88 (s, 2H), 6.54 (d, *J* = 7.5 Hz, 1H), 3.94 (s, 3H), 3.68-3.66 (m, 4H), 3.12-3.10 (m, 2H), 2.66-2.63 (m, 2H), 2.47-2.45 (m, 4H). ¹³C NMR (100 MHz, CDCl₃) δ 180.47, 170.79, 168.02,

156.60, 155.16, 153.44, 139.31, 135.13, 132.72, 132.01, 130.95, 129.95, 129.25, 125.41, 122.32, 111.61, 107.41, 102.60, 66.22, 57.59, 53.12, 34.02, 27.45. MS: 539.2 m/z [M-1]⁻.

1-(2-Chloro-2-phenylethyl)-6-(methylthio)-1H-pyrazolo[3,4-d]pyrimidin-4-amine (44)

Into a pressure vessel tube, compound **31a** (120 mg, 0.355 mmol) was suspended in absolute ethanol (3 mL) and NH₄OH (37 mg, 1.07 mmol) was added dropwise. The reaction mixture stirred for 12 hours at reflux, then it was cooled at room temperature. Solvent was removed under reduced pressure and the residue was purified by flash chromatography using DCM/MeOH (97:3) as eluent to obtain a white solid **44**. Yield: 56%. ¹H NMR (400 MHz, DMSO) δ 7.96 (s, 1H), 7.68 (bs, 2H), 7.46 (d, *J* = 7.5 Hz, 2H), 7.38 – 7.27 (m, 3H), 5.64-5.61 (m, 1H), 4.82 (dd, *J* = 14.2, 8.4 Hz, 1H), 4.72 (dd, *J* = 14.2, 8.4 Hz, 1H), 2.47 (s, 3H). MS: 320.3 m/z [M+1]⁺.

tert-Butyl (1-(2-Chloro-2-phenylethyl)-6-(methylthio)-1H-pyrazolo[3,4-d]pyrimidin-4-yl) carbamate (45)

1-(2-chloro-2-phenylethyl)-6-(methylthio)-1H-pyrazolo[3,4-*d*]pyrimidin-4-amine **44** (90 mg, 0.281 mmol) were dissolved with DMAP (4 mg, 0.028 mmol) into a precooled solution of dry THF (4 mL) at 0° C and di-*tert*-butyl dicarbonate (98 mg, 0.451 mmol) was added. The mixture was stirred at room temperature for 7 hours, then it was concentrated under reduced pressure. The crude product was resolubilized in DCM (70 mL) and washed with saturated solution of NaHCO₃ (60 mL), brine and dried on Na₂SO₄. Purification by flash chromatography using P.E./EtOAc (9:1) as eluent allow to obtain a white solid **45**. Yield: 91%. ¹H NMR (400 MHz, CDCl₃) δ 10.19 (bs, 1H), 8.02 (s, 1H), 7.41 – 7.31 (m, 2H), 7.29-7.23 (m, 3H), 5.50-5.47 (m, 1H), 4.91 (dd, *J* = 14.1, 8.1 Hz, 1H), 4.79 (dd, *J* = 14.1, 8.1 Hz, 1H), 2.55 (s, 3H), 1.22 (s, 9H). MS: 418.1 m/z [M-1]⁻.

General procedure for preparation of 46a-b

To a solution of compound **45** (85 mg, 0.202 mmol) and DMAP (27 mg, 0.222 mmol) in dry DMF (10 mL), the appropriate benzyl amine (0.242 mmol) was added dropwise. Molecular sieves (5 Å) were added and the reaction mixture stirred for 24 hours at reflux. After cooling to room temperature, the crude product was extracted with EtOAc (50 mL x 3). The organic layer was washed with a solution of LiCl 5% (60 mL x 5), brine, then dried on Na₂SO₄ and concentrated under vacuum. Purification by flash chromatography using a proper mix of DCM/MeOH (98:2 for **46a** and 99:1 for **46b**) as eluent and subsequent trituration with MeOH allowed to obtain a white solid.

1-Benzyl-3-(1-(2-chloro-2-phenylethyl)-6-(methylthio)-1H-pyrazolo[3,4-d]pyrimidin-4-yl)urea (46a)

Yield: 56%. ¹H NMR (400 MHz, DMSO-d₆) δ 10.17 (bs, 1H), 9.01 (s, 1H), 8.40 (s, 1H), 7.46 (d, *J* = 7.4 Hz, 3H), 7.38 – 7.18 (m, 7H), 5.62 (t, *J* = 7.1 Hz, 1H), 4.90 (dd, *J* = 14.2, 8.4 Hz, 1H), 4.79 (dd, *J* = 14.3, 6.2 Hz, 1H), 4.45 (d, *J* = 5.5 Hz, 2H), 2.44 (s, 3H). ¹³C NMR (100 MHz, DMSO-d₆) δ 168.18, 154.80, 153.90, 152.85, 139.37, 138.32, 129.45, 129.11, 129.01, 128.02, 127.68, 127.57, 127.54, 99.11, 60.69, 53.14, 43.39, 13.78. MS: 452.2 m/z [M-1]⁻.

1-(1-(2-Chloro-2-phenylethyl)-6-(methylthio)-1H-pyrazolo[3,4-d]pyrimidin-4-yl)-3-(4-methoxybenzyl)urea (46b)

Yield: 56%. ¹H NMR (400 MHz, DMSO-d₆) δ 8.99 (bs, 1H), 8.39 (s, 1H), 8.19 (s, 1H), 7.41 (d, *J* = 7.8 Hz, 2H), 7.28 (t, *J* = 6.7 Hz, 3H), 7.23 (d, *J* = 8.3 Hz, 2H), 6.91 – 6.78 (m, 2H), 5.56 (t, *J* = 7.3 Hz, 1H), 4.86 (dd, *J* = 14.0, 8.4 Hz, 1H), 4.75 (dd, *J* = 14.3, 6.2 Hz, 1H), 4.36 (s, 2H), 3.71 (s, 3H), 2.40 (s, 3H). ¹³C NMR (100 MHz, DMSO-d₆) δ 168.17, 158.83, 154.76, 153.77, 152.61, 138.14, 134.79, 131.08, 129.29, 129.00, 128.96, 127.85, 114.32, 99.06, 60.50, 55.33, 53.21, 42.94, 13.84. MS: 481.0 m/z [M-1]⁻.

1-Methyl-6-(methylthio)-1H-pyrazolo[3,4-d]pyrimidin-4-ol (47)

To a solution of 6-Mercapto-1-methyl-1H-pyrazolo[3,4-*d*]pyrimidin-4-ol **38** (2.03 g, 0.011 mol) in THF (30 mL) iodomethane (7.90 g, 0.056 mol) was added dropwise. The reaction mixture stirred for 12 hours at reflux, then, after cooling at room temperature, the white precipitate was collected by filtration on Gooch. Trituration using toluene allowed to give compound **47** as white solid. Yield: 87%. ¹H NMR (400 MHz, DMSO-d₆) δ 10.18 (bs, 1H), 7.93 (s, 1H), 3.90 (s, 3H), 2.55 (m, 3H). MS: 195.1 m/z [M-1]⁻.

4-Chloro-1-methyl-6-(methylthio)-1H-pyrazolo[3,4-d]pyrimidine (48)

The Vilsmeier complex, previously prepared from fresh distilled POCl₃ (5.86 g, 0.038 mol) and dry DMF (2.79 g, 0.038 mol) at 0°C, was added into a solution of compound **39** (0.750 g, 0.004 mol) in dry CHCl₃ (20 mL) and the reaction mixture stirred for 4 hours at reflux. After cooling at room temperature, water was added and the crude product was extracted in CHCl₃ (40 mL x 3). The organic layer was washed with LiCl 5% solution (50 mL x 3), brine, then dried with Na₂SO₄ and concentrated under reduced pressure. Purification using E.P./EtOAc (8:2) as eluent allowed to obtain halogenated compound **40** as a white solid. Yield: 91%. ¹H NMR (400 MHz, CDCl₃) δ 7.85 (s, 1H), 3.88 (s, 3H), 2.51 (m, 3H). MS: 215.6 m/z [M+1]⁺.

N-(3-Hydroxyphenyl)-2-((1-methyl-6-(methylthio)-1*H*-pyrazolo[3,4-*d*]pyrimidin-4-yl)amino)thiazole-5-carboxamide (**49**)

Compound **49** was synthesized according to general procedure reported for derivatives **30a-d**, **32** and **33a-c**. Yield: 82% ¹H NMR (400 MHz, DMSO-*d*₆) δ 12.85 (bs, 1H), 10.08 (bs, 1H), 9.47 (bs, 1H), 8.48-8.40 (m, 2H), 7.35 (s, 1H), 7.22-7.18 (m, 2H), 6.51-6.48 (m, 1H), 3.95 (s, 3H), 2.53 (s, 3H). MS: 412.2 m/z [M-1]⁻.

2-((6-((2-Hydroxyethyl)amino)-1-methyl-1*H*-pyrazolo[3,4-*d*]pyrimidin-4-yl)amino)-*N*-(3-hydroxyphenyl)thiazole-5-carboxamide (**50**)

Compound **50** was synthesized according to general procedure reported for derivatives **34a,b**. Yield: 43%. ¹H NMR (400 MHz, DMSO-*d*₆) δ 12.40 (bs, 1H), 9.98 (s, 1H), 9.42 (s, 1H), 8.32 (s, 1H), 8.15 (s, 1H), 7.26 (s, 1H), 7.12-7.08 (m, 2H), 6.52 – 6.38 (m, 1H), 4.73 (bs, 1H), 3.76-3.74 (m, 2H), 3.60-3.55 (m, 2H), 3.48 (s, 3H). ¹³C NMR (100 MHz, DMSO-*d*₆) δ 183.64, 173.30, 165.05, 161.86, 160.10, 157.96, 156.23, 140.90, 140.32, 132.32, 129.81, 128.57, 111.19, 107.53, 95.93, 44.21, 38.16, 33.46. MS: 425.3 m/z [M-1]⁻.

2-((1-(2-Chloro-2-phenylethyl)-1*H*-pyrazolo[3,4-*d*]pyrimidin-4-yl)amino)-*N*-phenylthiazole-5-carboxamide (**51a**)

Yield: 57%. ¹H NMR (400 MHz, Acetone-*d*₆) δ 10.5 (bs, 1H), 9.62 (bs, 1H), 8.69 (s, 1H), 8.54 (s, 1H), 8.34 (s, 1H), 7.80 (d, *J* = 8.0 Hz, 2H), 7.53 (d, *J* = 8.0 Hz, 2H), 7.33 – 7.29 (m, 5H), 7.07 (t, *J* = 8.0 Hz, 1H), 5.70-5.67 (m, 1H), 5.07 (dd, *J* = 12.7, 6.3 Hz, 1H), 4.91 (dd, *J* = 12.7, 6.3 Hz, 1H). ¹³C NMR (100 MHz, Acetone-*d*₆) δ 161.60, 159.77, 154.18, 150.75, 139.88, 139.12, 138.30, 132.11, 129.02, 128.77, 128.74, 127.60, 126.41, 123.73, 120.06, 119.97, 101.30, 60.43, 53.43. MS: 473.0 m/z [M-1]⁻.

2-((1-(2-Chloro-2-phenylethyl)-1*H*-pyrazolo[3,4-*d*]pyrimidin-4-yl)amino)-*N*-(3-hydroxyphenyl)thiazole-5-carboxamide (**51b**)

Yield: 48%. ¹H NMR (400 MHz, DMSO-*d*₆) δ 12.91 (bs, 1H), 10.05 (bs, 1H), 9.44 (s, 1H), 8.72 (s, 1H), 8.52 (s, 1H), 8.35 (s, 1H), 7.55-7.51 (m, 1H), 7.42 – 7.22 (m, 5H), 7.12-7.09 (m, 2H), 6.62 – 6.20 (m, 1H), 5.79 – 5.60 (m, 1H), 5.05 (dd, *J* = 14.3, 8.9 Hz, 1H), 4.87 (dd, *J* = 14.3, 8.9 Hz, 1H). ¹³C NMR (100 MHz, DMSO-*d*₆) δ 191.33, 161.54, 159.95, 157.99, 154.72, 153.98, 150.88, 140.12, 138.26, 135.28, 133.11, 129.77, 129.16, 127.91, 126.76, 126.26, 111.25, 107.66, 101.04, 61.02, 53.16. MS: 490.1 m/z [M-1]⁻.

7. References

- [1] Singal, A.G.; Lampertico, P.; Nahon, P. Epidemiology and surveillance for hepatocellular carcinoma: New trends. *J. Hepatol.* **2020**, *72* (2), 250-261.
- [2] Llovet, J.M.; Zucman-Rossi, J.; Pikarsky, E.; Sangro, B.; Schwartz, M.; Sherman, M.; Gores, G. Hepatocellular carcinoma. *Nat. Rev. Dis. Primers.* **2016**, *2*, 16018.
- [3] Brunt, E.M. Histopathologic Features of Hepatocellular Carcinoma. *Clin. Liver. Dis.* **2012**, *1* (6), 194–199.
- [4] Jindal, A.; Thadi, A.; Shailubhai, K. Hepatocellular Carcinoma: Etiology and Current and Future Drugs. *J. Clin. Exp. Hepatol.* **2019**, *9* (2), 221–232.
- [5] Marelli, L.; Stigliano, R.; Triantos, C.; Senzolo, M; Cholongitas, E.; Davies, N.; Yu, D.; Meyer, T.; Patch, D.W.; Burroughs, A.K. Treatment outcomes for hepatocellular carcinoma using chemoembolization in combination with other therapies. *Cancer Treat. Rev.* **2006**, *32*, 594-606.
- [6] Llovet, J.M.; Bruix, J. Systematic review of randomized trials for unresectable hepatocellular carcinoma: Chemoembolization improves survival. *Hepatology* **2003**, *37* (2), 429-442.
- [7] Thomas, M.B.; Zhu, A.X. Hepatocellular carcinoma: the need for progress. *J. Clin. Oncol.* **2005**, *23* (13), 2892-2899.
- [8] Abou-Alfa, G.K.; Schwartz, L.; Ricci, S.; Amadori, D.; Santoro, A.; Figer, A.; De Greve, J.; Douillard, J.Y.; Lathia, C.; Schwartz, B.; Taylor, I.; Moscovici, M.; Saltz, L.B. et al. Phase II study of sorafenib in patients with advanced hepatocellular carcinoma. *J. Clin. Oncol.* **2006**, *24* (26), 4293-4300.
- [9] Bruix, J.; Qin, S.; Merle, P.; Granito, A.; Huang, Y.H.; Bodoky, G.; Pracht, M.; Yokosuka, O.; Rosmorduc, O.; Breder, V; Gerolami, R.; Masi, G.; Ross, P.J.; Song, T.; Bronowicki, J.P.; Ollivier-Hourmand, I.; Kudo, M.; Cheng, A.L.; Llovet, J.M.; Finn, R.S.; LeBerre, M.A.; Baumhauer, A.; Meinhardt, G.; Han, G. RESORCE Investigators. Regorafenib for patients with hepatocellular carcinoma who progressed on sorafenib treatment (RESORCE): a randomised, double-blind, placebo-controlled, phase 3 trial. *Lancet* **2017**, *389* (10064), 56-66.

- [10] Ikeda, M.; Morizane, C.; Ueno, M.; Okusaka, T.; Ishii, H.; Furuse, J. Chemotherapy for hepatocellular carcinoma: current status and future perspectives. *JJCO* **2018**, *48* (2), 103–114.
- [11] Villanueva, A.; Chiang, D.Y.; Newell, P.; Peix, J.; Thung, S.; Alsinet, C.; Tovar, V.; Roayaie, S.; Minguez, B.; Sole, M.; Battiston, C.; van Laarhoven, S.; Fiel, M.I.; Di Feo, A.; Hoshida, Y.; Yea, S.; Toffanin, S.; Ramos, A.; Martignetti, J.A.; Mazzaferro, V.; Bruix, J.; Waxman, S.; Schwartz, M.; Meyerson, M.; Friedman, S.L.; Llovet, J.M. Pivotal Role of mTOR Signaling in Hepatocellular Carcinoma. *Gastroenterology* **2008**, *135* (6), 1972–1983.
- [12] Walker, S.; Wankell, M.; Ho, V.; White, R.; Deo, N.; Devine, C.; Dewdney, B.; Bhathal, P.; Govaere, O.; Roskams, T.; Qiao, L.; George, J.; Hebbard, L. Targeting mTOR and Src restricts hepatocellular carcinoma growth in a novel murine liver cancer model. *PLoS One*. **2019**, *14* (2), e0212860.
- [13] Yori, J.L.; Lozada, K.L.; Seachrist, D.D.; Mosley, J.D.; Abdul-Karim, F.W.; Booth, C.N.; Flask, C.A.; Keri, R.A. Combined SFK/mTOR Inhibition Prevents Rapamycin-Induced Feedback Activation of AKT and Elicits Efficient Tumor Regression. *Cancer Res.* **2014**, *74* (17), 4762–4771.
- [14] Ito, Y.; Kawakatsu, H.; Takeda, T.; Sakon, M.; Nagano, H.; Sakai, T.; Miyoshi, E.; Noda, K.; Tsujimoto, M.; Wakasa, K.; Monden, M.; Matsuura, N. Activation of c-Src gene product in hepatocellular carcinoma is highly correlated with the indices of early stage phenotype. *J. Hepatol.* **2001**, *35* (1), 68-73.
- [15] Lau, G.M.; Lau, G.M.; Yu, G.L.; Gelman, I.H.; Gutowski, A.; Hangauer, D.; Fang, J.W. Expression of Src and FAK in hepatocellular carcinoma and the effect of Src inhibitors on hepatocellular carcinoma in vitro. *Dig. Dis. Sci.* **2009**, *54* (7), 1465-1474.
- [16] Suh, Y.; Yoon, C.H.; Kim, R.K.; Lim, E.J.; Oh, Y.S.; Hwang, S.G.; An, S.; Yoon, G.; Gye, M.C.; Yi, J.M.; Kim, M.J.; Lee, S.J. Claudin-1 induces epithelial-mesenchymal transition through activation of the c-Abl-ERK signaling pathway in human liver cells. *Oncogene* **2013**, *32* (41), 4873-4882.
- [17] Chang, A.Y.; Wang, M. Molecular mechanisms of action and potential biomarkers of growth inhibition of dasatinib (BMS-354825) on hepatocellular carcinoma cells. *BMC Cancer* **2013**, *13* (1), 267.
- [18] Zhou, Q.; Guo, X.; Choksi, R. Activation of Focal Adhesion Kinase and Src Mediates Acquired Sorafenib Resistance in A549 Human Lung Adenocarcinoma Xenografts. *J. Pharmacol. Exp. Ther.* **2017**, *363* (3), 428-443.

- [19] Vlahovic, G.; Crawford, J. Activation of tyrosine kinases in cancer. *Oncologist* **2003**, *8* (6), 531-538.
- [20] Wu, S.; Fu, L. Tyrosine kinase inhibitors enhanced the efficacy of conventional chemotherapeutic agent in multidrug resistant cancer cells. *Mol. Cancer*. **2018**, *17* (1), 25.
- [21] Kurosu, T.; Ohki, M.; Wu, N.; Kagechika, H.; Miura, O. Sorafenib Induces Apoptosis Specifically in Cells Expressing BCR/ABL by Inhibiting Its Kinase Activity to Activate the Intrinsic Mitochondrial Pathway. *Cancer Res.* **2009**, *69* (9), 3927-3936.
- [22] Getlik, M.; Grütter, C.; Simard, J.R.; Klüter, S.; Rabiller, M.; Rode, H.B.; Robubi, A.; Rauh, D. Hybrid Compound Design To Overcome the Gatekeeper T338M Mutation in cSrc. *J. Med. Chem.* **2009**, *52* (13), 3915-3926.
- [23] Schenone, S.; Radi, M.; Musumeci, F.; Brullo, C.; Botta, M. Biologically driven synthesis of pyrazolo[3,4-*d*]pyrimidines as protein kinase inhibitors: an old scaffold as a new tool for medicinal chemistry and chemical biology studies. *Chem. Rev.* **2014**, *114* (14), 7189–7238.
- [24] Fallacara, A.L.; Zamperini, C.; Podolski-Renić, A.; Dinić, J.; Stanković, T.; Stepanović, M.; Mancini, A.; Rango, E.; Iovenitti, G.; Molinari, A.; Bugli, F.; Sanguinetti, M.; Torelli, R.; Martini, M.; Maccari, L.; Valoti, M.; Dreassi, E.; Botta, M.; Pešić, M.; Schenone, S. A New Strategy for Glioblastoma Treatment: In Vitro and In Vivo Preclinical Characterization of Si306, a Pyrazolo[3,4-*d*]Pyrimidine Dual Src/P-Glycoprotein Inhibitor. *Cancers* **2019**, *11* (6), 848.
- [25] Radi, M.; Brullo, C.; Crespan, E.; Tintori, C.; Musumeci, F.; Biava, M.; Schenone, S.; Dreassi, E.; Zamperini, C.; Maga, G.; Pagano, D.; Angelucci, A.; Bologna, M.; Botta, M. Identification of potent c-Src inhibitors strongly affecting the proliferation of human neuroblastoma cells. *Bioorg. Med. Chem. Lett.* **2011**, *21* (19), 5928–5933.
- [26] Angelucci, A.; Schenone, S.; Gravina, G.L.; Muzi, P.; Festuccia, C.; Vicentini, C.; Botta, B.; Bologna, M. Pyrazolo[3,4-*d*]pyrimidines c-Src inhibitors reduce epidermal growth factor-induced migration in prostate cancer cells, *EJC* **2006**, *42* (16), 2838-2845.
- [27] Fallacara, A.L.; Passannanti, R.; Mori, M.; Iovenitti, G.; Musumeci, F.; Greco, C.; Crespan, E.; Kissova, M.; Maga, G.; Tarantelli, C.; Spriano, F.; Gaudio, E.; Bertoni, F.; Botta, M.; Schenone, S. Identification of a new family of pyrazolo[3,4-*d*]pyrimidine derivatives as multitarget Fyn-Blk-Lyn inhibitors active on B- and T-lymphoma cell lines. *Eur. J. Med. Chem.* **2019**, *181*, 111545.

- [28] Tintori, C.; Fallacara, A.L.; Radi, M.; Zamperini, C.; Dreassi, E.; Crespan, E.; Maga, G.; Schenone, S.; Musumeci, F.; Brullo, C.; Richters, A.; Gasparrini, F.; Angelucci, A.; Festuccia, C.; Delle Monache, S.; Rauh, D.; Botta, M. Combining X-ray Crystallography and Molecular Modeling toward the Optimization of Pyrazolo[3,4-*d*]pyrimidines as Potent c-Src Inhibitors Active in Vivo against Neuroblastoma. *J. Med. Chem.* **2015**, *58* (1), 347–361.
- [29] Molinari, A.; Fallacara, A.L.; Di Maria, S.; Zamperini, C.; Poggialini, F.; Musumeci, F.; Schenone, S.; Angelucci, A.; Colapietro, A.; Crespan, E.; Kissova, M.; Maga, G.; Botta, M. 2018. Efficient optimization of pyrazolo[3,4-*d*]pyrimidines derivatives as c-Src kinase inhibitors in neuroblastoma treatment. *Bioorg. Med. Chem. Lett.* **2018**, *28* (21), 3454–3457.
- [30] Sampath Kumar, H.M.; Herrmann, L.; Tsogoeva, S.B. Structural hybridization as a facile approach to new drug candidates. *Bioorg. Med. Chem. Lett.* **2020**, *30* (23), 127514.
- [31] Seeliger, M. A.; Nagar, B.; Frank, F.; Cao, X.; Henderson, M. N.; Kuriyan, J. c-Src Binds to the Cancer Drug Imatinib with an Inactive Abl/c-Kit Conformation and a Distributed Thermodynamic Penalty. *Structure* **2007**, *15* (3), 299–311.
- [32] Weisberg, E.; Manley, P.; Mestan, J.; Cowan-Jacob, S.; Ray, A.; Griffin, J.D. AMN107 (nilotinib): a novel and selective inhibitor of BCR-ABL. *Br. J. Cancer* **2006**, *94* (12), 1765–1769.
- [33] Reddy, E.P.; Aggarwal, A.K. The Ins and Outs of Bcr-Abl Inhibition. *Gen. Cancer* **2012**, *3* (5-6), 447–454.
- [34] Okram, B.; Nagle, A.; Adrian, F.J.; Lee, C.; Ren, P.; Wang, X.; Sim, T.; Xie, Y.; Wang, X.; Xia, G.; Spraggon, G.; Warmuth, M.; Liu, Y.; Gray, N.S. A General Strategy for Creating “Inactive-Conformation” Abl Inhibitors. *Chem. Biol.* **2006**, *13* (7), 779–786,
- [35] Francini, C.M.; Musumeci, F.; Fallacara, A.L.; Botta, L.; Molinari, A.; Artusi, R.; Mennuni, L.; Angelucci, A.; Schenone, S. Optimization of Aminoimidazole Derivatives as Src Family Kinase Inhibitors. *Molecules* **2018**, *23* (9), 2369.

Chapter IV

Optimization of Si306 and Si409: design, synthesis and biological evaluation of novel pyrazolo[3,4-d]pyrimidines active against Glioblastoma Multiforme (GBM)

1. Introduction

1.1 Glioblastoma Multiforme (GBM)

Glioblastoma Multiforme (GBM) is the most frequent malignant intracranial tumor in adults characterized by high invasiveness rate of brain and mortality. Prognosis remains poor in fact, about 25% of patients survive for 2 years and fewer than 10% survive for 5 years [1]. However, as the disease progress, patients show various symptoms, such as headache, which are thought to be caused by increasing intracranial pressure due to tumor growth. The 2016-WHO classification of central nervous system tumors places GBM among diffuse astrocytic and oligodentrogial neoplasms, currently defining it as grade IV glioma [2]. GBM demonstrates very aggressive histology features such as atypical nuclei, increased microvasculature (angiogenesis), hypercellularity, and necrosis [1,3]. Several genetic or chromosomal alterations and the signaling pathways deregulation can contribute to GBM formation and progression. Genetic abnormalities include MDM2 protein gene amplification and overexpression [4], LOH 10q and p16Ink4a/p14ARF loss, PTEN and Rb mutations, inactivation of the p53 pathway, PI3K mutation or amplification, and upregulation of HEY1 [5], whereas the abnormalities in growth factor signaling are caused by EGFR, PDGFR, and VEGF overexpression. However, all these varieties of GBM abnormalities contribute to therapeutic resistance. Expression of a wide range of mutations and abnormalities—generates heterogeneous cells populations that may not respond similarly to any individual therapy.

1.2 Treatment options

The standard of care for GBM is surgical resection, followed by concomitant radiotherapy and temozolomide (TMZ)-based chemotherapy for 6 weeks and, then, by an adjuvant cycle of chemotherapy with TMZ for 6-12 months. Clinical trials demonstrated that the combination of radiotherapy-TMZ followed by adjuvant TMZ is more effective than radiotherapy alone, leading to a prolongation of the median survival of patients [6]. Other chemotherapeutic options in GBM used are nitrosoureas and the humanized monoclonal antibody bevacizumab targeting the vascular endothelial growth factor (VEGF), the latter approved for the treatment of recurrent GBM by the U.S. Food and Drug Administration (FDA) in May 2009. Bevacizumab is well tolerated and administered concomitantly with irinotecan [7]. However, to date chemotherapy of GBM remains a palliative treatment and for this reason is necessary to encourage the search for new pharmacological agents that are effective and safe in the treatment of the disease. After examining the targets implicated in GBM signaling pathways, several orphan drugs have been designated and approved for therapy by FDA. Regorafenib **1** (Figure 4.1), an inhibitor of several kinases involved in the mechanisms that regulate neoangiogenesis processes, such as the vascular endothelial growth factor receptors (VEGFR), was investigated for its pharmacologic properties against GBM.

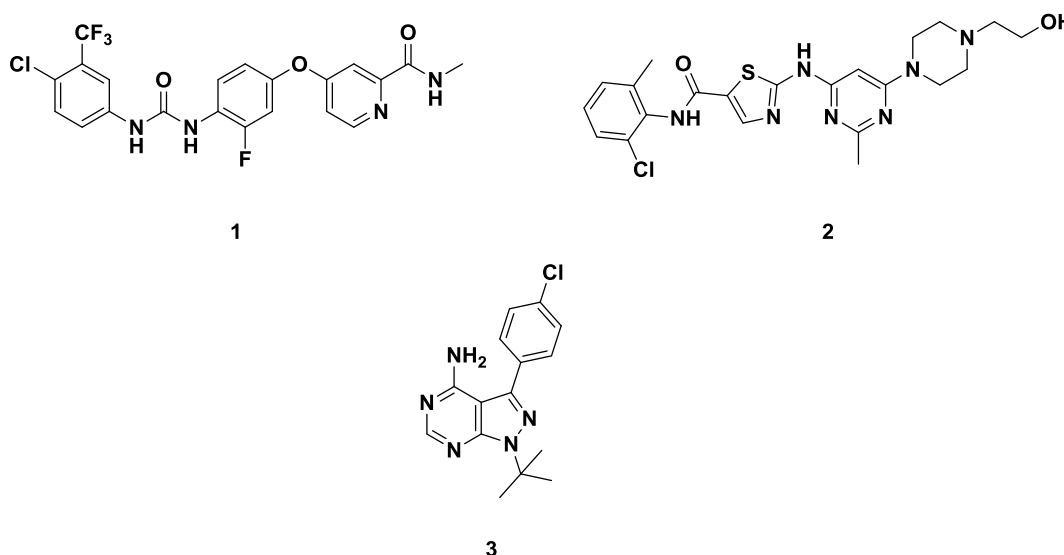


Figure 4.1 Structure of TKIs Regorafenib **1**, Dasatinib **2**, and PP2 **3**.

Recently, REGOMA study showed the superiority of regorafenib over lomustine in patients with first relapse of glioblastoma. Moreover, treatment with Regorafenib **1** was beneficial in terms of overall survival benefit in patients with GBM, associated with acceptable toxicity. [8] Identification of upregulated and hyperactivated proteins in the disease may represent a valid

Specifically, c-Src inhibitor **4a** exhibited antiproliferative activity on U87 and LN229 cell lines (Table 1), typical of GBM, at low micromolar concentrations and showed appreciable *in vivo* PK properties, such as high distribution in the brain tissue [15-17].

Table 1. Biological and PK data of Si306 (**4a**)

Compd	Ki on c-Src (μM)	IC₅₀ on U87 (μM)	IC₅₀ on LN229 (μM)	Water solubility $\mu\text{g/mL}$	Papp. 10⁻⁶ cm/sec	Metabolic stability %
4a	0.13	1.91	8.0	3.70	5.27	97.2

However, the inhibitory activity of **4a** on c-Src proved unexciting when compared with other pyrazolo[3,4-*d*]pyrimidines developed over the years [18] and showed low water solubility. To this end, drug delivery systems, such as liposomes or nanoparticles, have been developed to target **4a** to the appropriate tumor site. Also, a second mechanism for **4a** has recently been demonstrated, which inhibits the P-Glycoprotein involved in tumor resistances [16]. In view of these properties, the Si306 compound has acquired some relevance for our research, becoming one of the most representative members of all the pyrazolo[3,4-*d*]pyrimidines developed in recent years. On the other hand, in a recent internal test it was observed that **5a** (compound **8j** in chapter II) exerts a significant activity against the GBM (unpublished results). Si409 **5a**, which has been extensively studied as c-Src/Abl inhibitor, exhibited a favorable antiproliferative activity on LN229 cell line, resulting two-fold more potent than **4a** (Table 2).

Table 2. Biological data of Si409 (**5a**)

Compd	Ki on c-Src (μM)	IC₅₀ on U87 (μM)	IC₅₀ on LN229 (μM)	Water solubility $\mu\text{g/mL}$	Papp. 10⁻⁶ cm/sec	Metabolic stability %
5a	0.3	1.91	4.0	134.2	0.2	99.4

Nevertheless, this compound shows little inhibitory potency towards c-Src and low permeability of biological membranes (Table 2). In addition, a high tendency of **5a** to undergo O-glucuronidation *in vivo* was recently observed in PK experiments (unpublished results). However, these negative properties were balanced by its high water solubility (134.2 $\mu\text{g/mL}$), which favors its dissolution in aqueous buffers used in biological tests, avoiding the precipitation in culture media, unlike was experimentally observed for other similar compounds.

3. Aim of the project

In this project I dealt with the synthesis of Si306 and Si409 derivatives (**4a-d** and **5a-e**) in order to obtain a set of novel pyrazolo[3,4-*d*]pyrimidines characterized by improved pharmacological properties. Specifically, Si306 derivatives have been designed with the aim of increasing c-Src inhibitory activity, which is not so relevant in Si306 when compared with other c-Src inhibitors on the market. On the other hand, the design of Si409 derivatives was realized to improve some PK properties, such as membrane permeability, or to overcome the metabolic O-glucuronidation. Subsequently, through the inhibitory screening on c-Src, the most promising compounds were selected and analyzed on the U87 and U386 cell lines, typical of GBM, with the objective of discovering new pharmacological agents more effective than the starting precursors.

4. Results

4.1 Development of Si306 derivatives: design, synthesis and enzymatic assay

The design of Si306 derivatives was realized by replacing the bromine atom on aniline ring, located in C4 position of the pyrazolo[3,4-*d*]pyrimidine core, with other substituents (Figure 4.2). X-ray crystallographic studies of the c-Src complex with the Si192 ligand [19] have shown that this aniline portion of the ligand is of major importance for the interaction with the protein pocket in order to block the kinase activity; we therefore thought of modifying it to possibly increase the inhibitory power of the compounds.

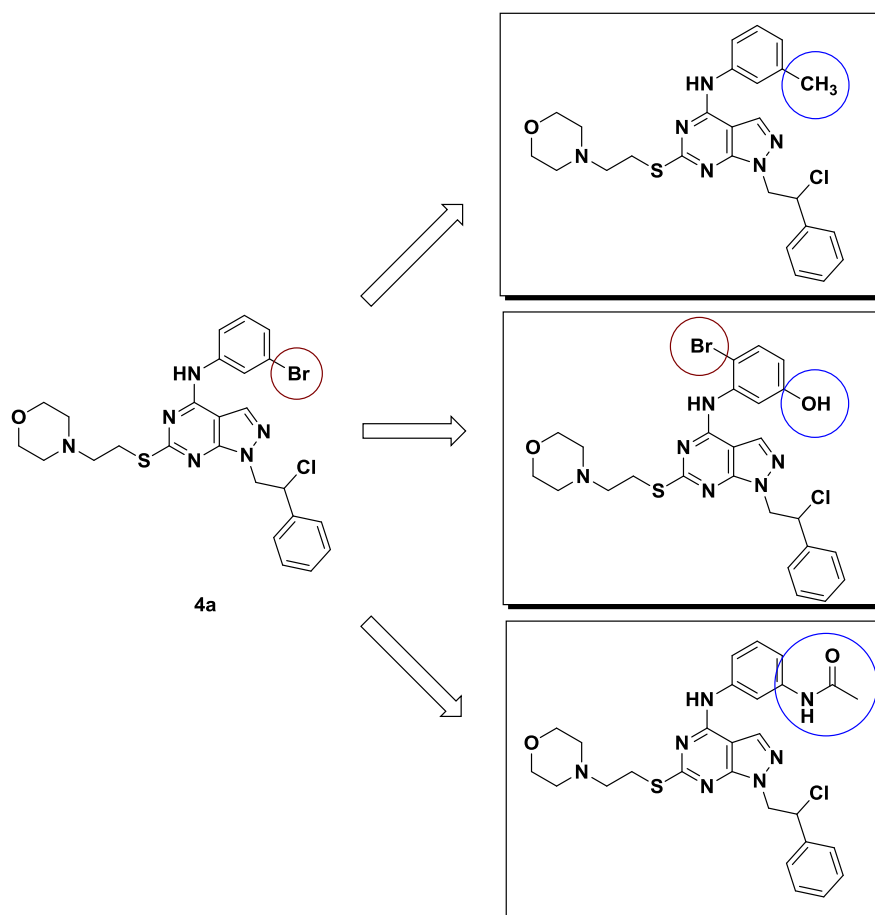
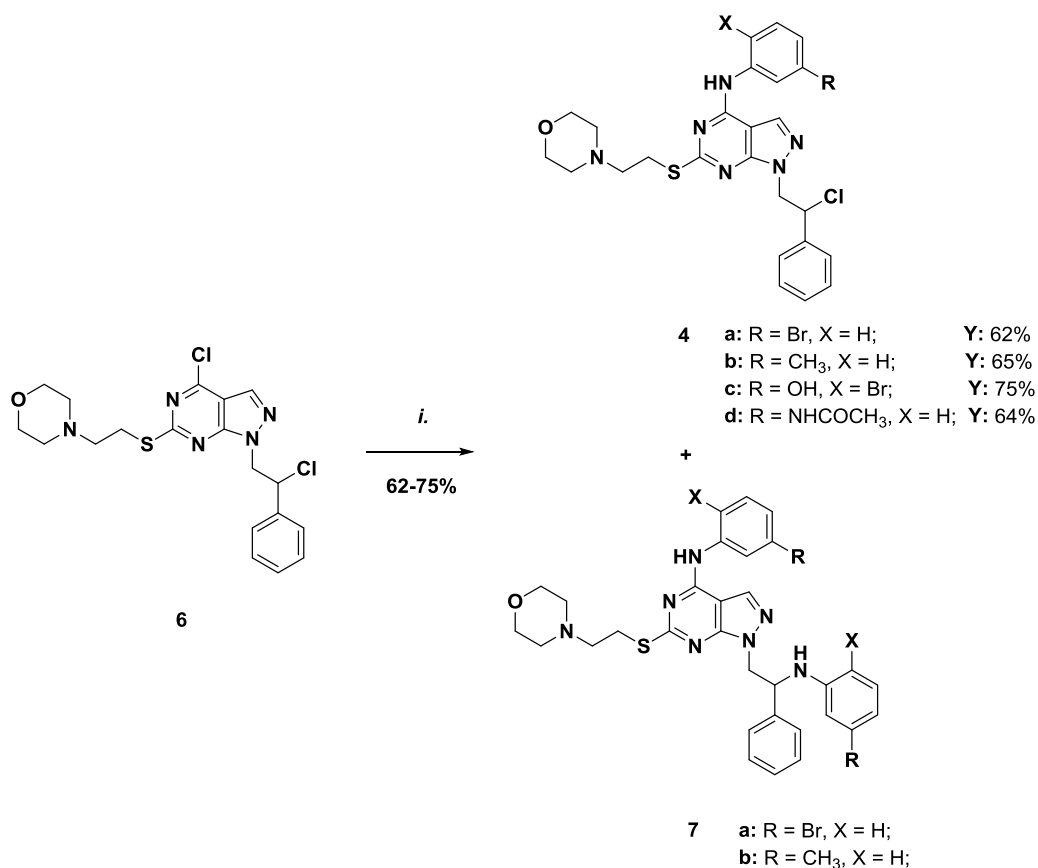


Figure 4.3 Optimization of **4a**.

The first **4a** modification concerned the replacement of *meta* bromine atom with a methyl group on aniline ring in order to evaluate how the inductive electronic effect of this substituent can modulate the inhibitory activity on c-Src, with respect to the precursor. Further modification entailed the decoration of aniline ring with a meta hydroxy group and ortho bromine atom, according to suggestions from the MC/FEP analysis elaborated by *Tintori et al* [19] Finally, as a last modification, the meta bromine atom was replaced with the acetamido group as hydroxy bioisostere (Figure 4.3).

4a and derivatives **4b-d** were synthesized by the usual procedure described in chapter II in a rapid and smooth way (Scheme I).

Scheme I. Synthesis of **4a** and derivatives **4b-d**



Reagents and conditions: *i.*) appropriate aniline, abs. EtOH, reflux, 3-8 hours.

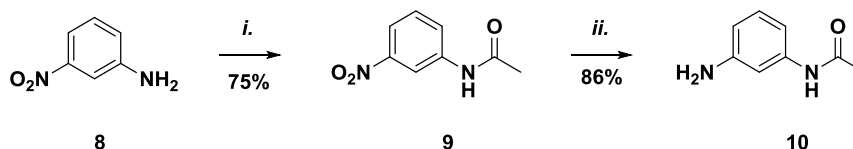
The intermediate **6** underwent aromatic nucleophilic substitution reaction with differently substituted anilines in ethanol at reflux. However, compounds **4a,b**, bearing a bromine atom or a methyl group, respectively, in the *meta* position, gave rise to side reactions leading to by-products, unlike for derivatives **4c,d**. MS and ¹H-NMR experiments allowed to identify the by-products **7a,b** deriving from double substitution on **6** during the preparation of **4a,b**. However, changing some parameters of the experimental conditions, such as temperature, reaction time, equivalents of nucleophile (Table 3), **4a** was obtained in better yield with concomitant reduction of the formation of **7a**.

Table 3. Conditions for the synthesis of **4a**

Test	Solvent	Time (hours)	Temperature (°C)	Equivalent of aniline	Yield % (4a)	Yield % (7a)
1	absolute ethanol	6	110	4	40	40
2	absolute ethanol	9	80	4	45	34
3	absolute ethanol	3.5	90	2.5	75	10
4	absolute ethanol	3	100	2	65	15

The preparation of the 3-acetamido derivative **10**, used for the synthesis of **4d**, started with the acetylation of 3-nitroaniline **8** to **9** using acetic anhydride and TEA, followed by reduction of the nitro group.

Scheme II. Synthesis of 3-aminoacetanilide 10



Reagents and condition: i.) Ac₂O, DIPEA, dry DMF, rt, 12 hours. ii.) Fe, NH₄Cl, EtOH/H₂O 3:1, reflux, 2.5 hours.

Si306 analogues **4b-d** were analyzed through the inhibitory enzymatic assay on c-Src and the results are reported in Table 4.

Table 4. c-Src screening of novel Si306 derivatives **4b-c**

Compd			K _i on c-Src ^a (μM)
	R	R ₁	
4a	Br	H	0.13
4b	CH ₃	H	>10
4c	OH	Br	0.16
4d		H	>10

^a Values are the means of two experiments

Looking at the data reported in Table 4, it is easy to see that compounds **4b** and **4d** do not represent a step forward compared to **4a**. However, a favorable inhibitory effect was observed in compound **4c**, which is characterized by *meta* phenol and *ortho* bromine substitution on the

aniline ring. Compound **4c** inhibits c-Src with a potency (IC_{50} value = 0.16 μ M) quite comparable to that of compound **4a** (IC_{50} value = 0.13 μ M). Ultimately, **4c** represents a further compound of the series for which it would be interesting to investigate other pharmacological properties.

4.2 Development of Si409 derivatives: design, synthesis and enzymatic assay

The design of Si409-derivatives was realized with the aim of overcoming some pharmacokinetic drawbacks, by modifying the chemical structure of precursor **5a**.

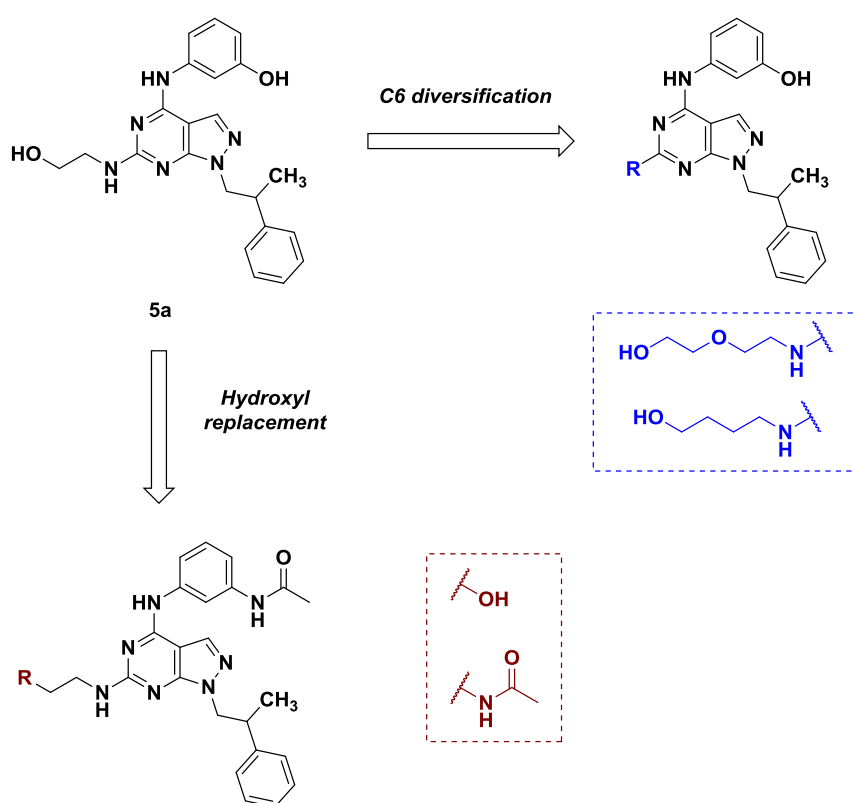


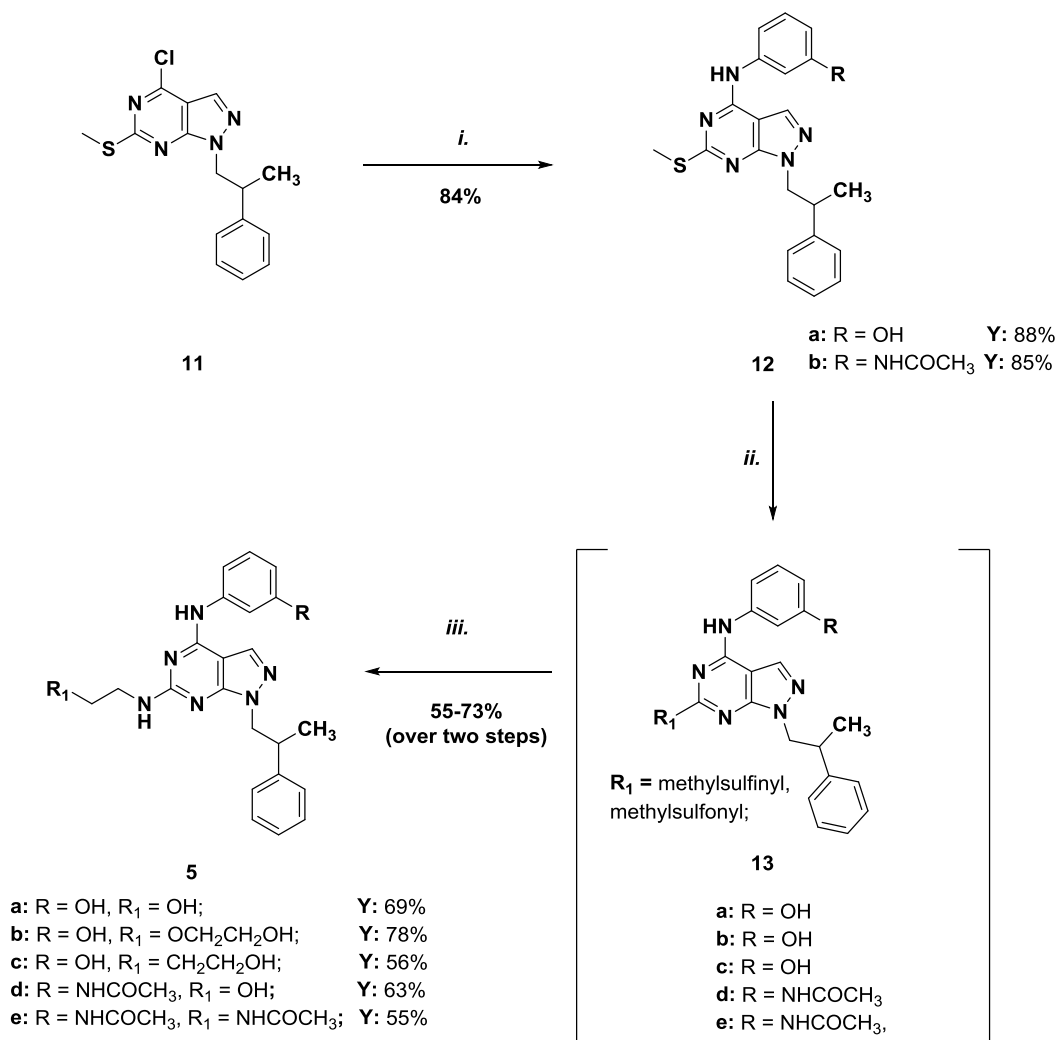
Figure 4.4 Design of Si409 derivatives.

C6 diversification with different aliphatic chains was realized in order to evaluate an improvement of membrane permeability. In fact, by replacing ethanolamine with longer chains, such as 2-(2-aminoethoxy)ethanol and 4-aminobutanol, an increase in lipophilicity in the new derivatives is conceivable (Figure 4.4). Furthermore, structural modifications at this point of

the scaffold were decided because, from the study of the c-Src crystal complexed with the Si192 inhibitor [19], it was found that the C6 chain is localized in the region exposed to the solvent and does not generate interactions within the active site of the kinase.

On the other hand, it was decided to replace the hydroxyl of precursor **5a** with the bioisosteric acetamido group, thus reducing the O-glucuronidation liability of the new compounds, while preserving their ability to act as hydrogen bond donor into the c-Src pocket. The preparation of the **5a** analogs followed a different synthetic approach (Scheme III) with respect to **4a** derivatives.

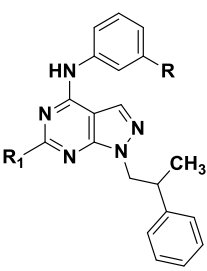
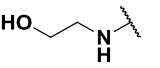
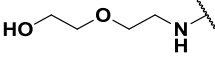
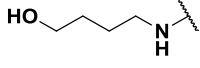
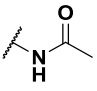
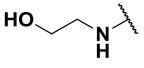
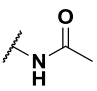
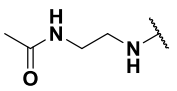
Scheme III. Synthesis of **5a and derivatives **5b-e****



Reagents and conditions: *i.*) appropriate aniline, abs. EtOH, reflux, 3-5 hours. *ii.*) *m*-CPBA, dry DCM, rt, 2.5 hours. *iii.*) appropriate amine, 1-butanol/DMSO (2:1), reflux, 10 hours.

Scheme III starts with the usual aromatic nucleophilic substitution reaction between intermediate **11**, prepared as described in chapter II, and the appropriate aniline to give compounds **12a,b**. C6 diversification was realized in the last step by oxidation of the thiomethyl group on **12a,b** allowed to obtain a mixture of the corresponding sulfone and sulfoxide which was reacted directly in the next step without purification. Subsequent displacement of these groups with ethanolamine led to compounds **5a-e**.

Table 5. c-Src screening of Si409 derivatives **5b-e**.

Compd			<i>K_i</i> on c-Src ^a (μ M)
	R	R ₁	
5a	OH		0.30
5b	OH		2.42
5c	OH		1.75
5d			>10
5e			>10

^a Values are the means of two experiments

The screening of Si409 derivatives **5b-e** on the c-Src has shown that generally all compounds are poor inhibitors of this target. Although the *K_i* value for derivatives **5b** and **5d** could be calculated (Table 5), these showed less inhibitory potency than the precursor **5a** (*K_i* value = 0.30 μ M). Besides, the replacement of the hydroxyl group with the bioisosteric amide in both derivatives **5d,e** gave completely disappointing results, as these compounds exhibited concentration value > 10 μ M.

4.3 Cells viability assay

Based on c-Src inhibition data, it was decided to subject compounds **4c** and **5b** to the antiproliferative assay on typical GBM cell cultures. The Si306-derivative **4c** was selected due to its similar potency on c-Src compared to the precursor **4a**, while the derivative **5b** was chosen based on other considerations. The C6 chain of compound **5b** was predicted as a possible metabolic hot spot, assuming that **5b** could be converted back into compound **5a** (Figure 4.5) by oxidation.

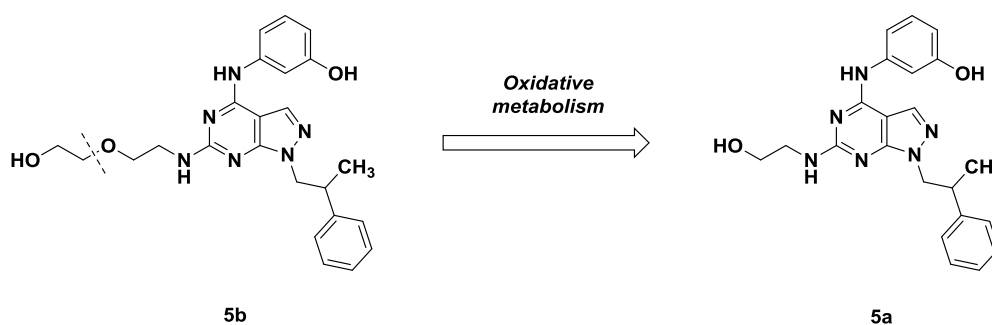


Figure 4.5 Possible transformation of **5b** into **5a**.

Accordingly, compounds **4c** and **5b** were evaluated in the enzymatic assay on U87 and U138 cell lines.

Table 6. Antiproliferative assay on U87 and U138 cell lines

Compd	IC ₅₀ (μM) on U87 cell line	IC ₅₀ (μM) on U138 cell line
2	5.1	24.9
4a	1.9	3.5
4c	6.9	6.8
5a	5.2	6.7
5b	4.7	8.9

^a Values are the means of three experiments

Data reported in Table 6 show a lower antiproliferative activity for derivatives **4c** and **5b** compared to the precursors **4a** and **5a**, respectively; in particular, compound **5b** displayed cell viability inhibition on U87 line similar to that of compound **5a**. However, the greatest cell viability inhibition was once again demonstrated by precursor **4a**, showing that the global optimization process was rather unsuccessful. Finally, the analyses of the ADME properties of

the compounds, such as permeability in membranes and water solubility, are still ongoing. Through a careful evaluation of these parameters, it will be possible to explain the behavior of the compounds and why they are hampered from achieving the intracellular target.

5. Conclusion

Unlike the research projects reported in Chapters II and III, the optimization process of Si306 and Si409 did not lead to the discovery of better molecules, but with similar or even worse pharmacological properties. Poor results were obtained in the enzymatic inhibition assay, in which the compounds revealed lower inhibitory potency than their corresponding precursors. However, the analog of Si306 showed an acceptable antiproliferative activity on the cell lines examined, so it could be used together with Si409 as a backup compound should Si306 not progress in the preclinical evaluation. However, the synthetic approach used has shown high versatility in the preparation of all derivatives, allowing the molecules to be obtained with a favorable reaction yield.

6. Materials and methods

All commercially available chemicals were used as purchased. DCM was dried over calcium hydride. Anhydrous reactions were run under a positive pressure of dry N₂ or argon. TLC was carried out using Merck TLC plates silica gel 60 F254. Chromatographic purifications were performed on columns packed with Merk 60 silica gel, 23-400 mesh, for flash technique. ¹H NMR and ¹³C NMR spectra were recorded on a Bruker Avance DPX400 (at 400 MHz for ¹H and 101 MHz for ¹³C). Chemical shifts are reported relative to tetramethylsilane at 0.00 ppm. Mass spectra (MS) data were obtained using an Agilent 1100 LC/MSD VL system (G1946C) with a 0.4 mL min⁻¹ flow rate using a binary solvent system of 95:5 = CH₃OH:H₂O. UV detection was monitored at 254 nm. MS were acquired in positive and negative mode scanning over the mass range m/z 50-1500. The following ion source parameters were used: drying gas flow, 9 mL min⁻¹; nebulizer pressure, 40 psi; drying gas temperature, 350 °C. The accurate masses were measured by the LTQ-Orbitrap XL (Thermo Scientific, Bremen, Germany) mass spectrometer interfaced with an electrospray ionization (ESI)

source characterized by spray voltage 4.5 kV, nitrogen as sheat gas (10 a.u). The resolution of accurate masses is 30000. MS/MS spectra were recorded with an isolation windows of 2 mass units, collision energy of 15, 16 or 17 V and Helium as collision gas.

Procedures

General procedure for the synthesis of compounds 4a-d and 12a,b.

The suitable aniline (0.57 mmol) was added to a suspension of the intermediate **6** or **11** (0.23 mmol) in absolute ethanol (4 mL), and the reaction mixture was stirred at reflux for 3-8 hours. After cooling, ethanol was removed under reduced pressure and the crudes were purified by flash chromatography using a mixture of P.E./Acetone (9:1 to 7:3) as eluent to afford the desired compounds **4a-d** and **12a,b** as white solids.

N-(3-Bromophenyl)-1-(2-chloro-2-phenylethyl)-6-((2-morpholinoethyl)thio)-1H-pyrazolo[3,4-d]pyrimidin-4-amine (4a)

Yield: 62%. ¹H NMR (400 MHz, CDCl₃) δ 7.56 (s, 1H), 7.54 (s, 1H), 7.48-7.42 (m, 2H), 7.40-7.31 (m, 4H), 7.20-7.18 (m, 2H), 5.54-5.47 (m, 1H), 4.89 (dd, *J* = 14.1, 8.9 Hz, 1H), 4.66 (dd, *J* = 14.1, 8.9 Hz, 1H), 3.85 – 3.63 (m, 4H), 3.48 – 3.42 (m, 2H), 2.95-2.69 (m, 2H), 2.73-2.58 (m, 4H). ¹³C NMR (100 MHz, CDCl₃) δ 168.20, 152.47, 149.40, 138.21, 135.67, 132.05, 129.68, 124.09, 123.80, 123.52, 122.34, 122.09, 116.96, 92.86, 61.71, 56.08, 53.14, 48.49, 48.30, 28.35. MS: 274.2 m/z [M+1]⁺.

1-(2-Chloro-2-phenylethyl)-6-((2-morpholinoethyl)thio)-N-(m-tolyl)-1H-pyrazolo[3,4-d]pyrimidin-4-amine (4b)

Yield: 65%. ¹H NMR (400 MHz, CDCl₃) δ 7.69 (s, 1H), 7.47 – 7.37 (m, 2H), 7.36 – 7.18 (m, 6H), 7.16-7.11 (m, 2H), 5.53-5.47 (m, 1H), 4.88 (dd, *J* = 14.1, 8.9 Hz, 1H), 4.65 (dd, *J* = 14.1, 8.9 Hz, 1H), 3.84 – 3.63 (m, 4H), 3.51 – 3.14 (m, 2H), 2.80-2.69 (m, 2H), 2.58-2.41(m, 4H), 2.36 (s, 3H). ¹³C NMR (100 MHz, CDCl₃) δ 163.20, 150.37, 149.94, 134.23, 132.67, 132.05, 127.69, 124.09, 123.80, 123.52, 122.34, 122.09, 116.96, 92.86, 61.71, 55.08, 53.14, 48.48, 48.31, 22.35, 16.21. MS: 509.4 m/z [M+1]⁺.

4-Bromo-3-((1-(2-chloro-2-phenylethyl)-6-((2-morpholinoethyl)thio)-1H-pyrazolo[3,4-d]pyrimidin-4-yl)amino)phenol (4c)

Yield: 75%. ¹H NMR (400 MHz, DMSO-d₆) δ 10.46 (bs, 1H), 10.07 (s, 1H), 8.19 (s, 1H), 7.59 – 7.27 (m, 7H), 7.13 (d, 1H), 5.68-5.65 (m, 1H), 4.91 (dd, *J* = 14.3, 9.0 Hz, 1H), 4.75 (dd, *J* = 14.3, 9.0 Hz, 1H), 3.65 – 3.48 (m, 4H), 3.38 – 3.09 (m, 2H), 2.70 – 2.56 (m, 2H), 2.45 – 2.40 (m, 4H). ¹³C NMR (100 MHz, DMSO-d₆) δ 168.42, 154.68, 154.53, 153.50, 139.49, 138.45, 133.12, 132.99, 129.49, 129.18, 127.93, 113.99, 109.75, 104.00, 99.20, 66.51, 61.02, 58.41, 53.57, 53.16, 27.57. MS: 588.4 m/z [M+1]⁺.

N-(3-((1-(2-Chloro-2-phenylethyl)-6-((2-morpholinoethyl)thio)-1H-pyrazolo[3,4-d]pyrimidin-4-yl)amino)phenyl)acetamide (4d)

Yield: 64%. ¹H NMR (400 MHz, DMSO-d₆) δ 10.14 (s, 1H), 10.00 (s, 1H), 8.18 (s, 1H), 8.03 (s, 1H), 7.63 – 7.43 (m, 3H), 7.43 – 7.31 (m, 3H), 7.27 (t, *J* = 8.0 Hz, 1H), 7.19 (d, *J* = 8.0 Hz, 1H), 5.70-5.63 (m, 1H), 4.90 (dd, *J* = 14.3, 9.0 Hz, 1H), 4.73 (dd, *J* = 14.3, 9.0 Hz, 1H), 3.58-3.52 (m, 4H), 3.37 – 3.07 (m, 2H), 2.67-2.61 (m, 2H), 2.45-2.35 (m, 4H), 2.10 (s, 3H). ¹³C NMR (100 MHz, DMSO-d₆) δ 207.83, 173.54, 173.20, 159.38, 158.53, 144.79, 144.11, 143.06, 137.99, 134.21, 133.99, 133.90, 132.69, 121.52, 119.71, 117.15, 103.85, 71.43, 65.80, 63.00, 58.18, 57.84, 29.23. MS: 552.3 m/z [M+1]⁺.

N-(3-Bromophenyl)-1-(2-((3-bromophenyl)amino)-2-phenylethyl)-6-((2-morpholinoethyl)thio)-1H-pyrazolo[3,4-d]pyrimidin-4-amine (7)

Yield: 48%. ¹H NMR (400 MHz, CDCl₃) δ 10.11 (bs, 1H), 7.73 (s, 1H), 7.49 – 7.15 (m, 10H), 6.82 (t, *J* = 8.0 Hz, 1H), 6.67 (d, *J* = 7.0 Hz, 1H), 6.56 (s, 1H), 6.27 (d, *J* = 8.0 Hz, 1H), 5.50-5.45 (m, 1H), 4.92 (dd, *J* = 14.1, 8.9 Hz, 1H), 4.67 (dd, *J* = 14.1, 8.9 Hz, 1H), 3.87-3.81 (s, 4H), 3.48-3.42 (s, 2H), 2.95-2.90 (s, 2H), 2.73-2.60 (s, 4H). MS: 709.9 m/z [M+1]⁺.

N-(3-Nitrophenyl)acetamide (9)

Yield: 75%. ¹H NMR (400 MHz, DMSO-d₆) δ 10.39 (s, 1H), 8.60 (s, 1H), 7.93-7.88 (m, 2H), 7.60-7.58 (m, 1H), 2.12 (3H). MS: 179.22 m/z [M-1]⁻.

N-(3-Aminophenyl)acetamide (10)

Yield: 86%. ¹H NMR (400 MHz, DMSO-d₆) δ 10.01 (s, 1H), 7.32 (s, 1H), 7.07-6.92 (m, 2H), 6.52-6.49 (m, 1H), 2.06 (3H). MS: 151.12 m/z [M+1]⁺.

3-((6-(Methylthio)-1-(2-phenylpropyl)-1H-pyrazolo[3,4-d]pyrimidin-4-yl)amino)phenol (12a)

Yield: 88%. ¹H NMR (400 MHz, CD₃OD) δ 7.85 (s, 1H), 7.28-7.14 (m, 8H), 6.59-6.56 (m, 1H), 4.40-4.35 (m, 2H), 3.45-3.41 (m, 1H), 2.50 (s, 3H), 1.20 (d, J = 7.0 Hz, 3H). MS: 390.4 m/z [M-1]⁻.

N-(3-((6-(Methylthio)-1-(2-phenylpropyl)-1H-pyrazolo[3,4-d]pyrimidin-4-yl)amino)phenyl)acetamide (12b)

Yield: 85%. ¹H NMR (400 MHz, CD₃OD) δ 7.83 (s, 1H), 7.24-7.10 (m, 8H), 6.55-6.51 (m, 1H), 4.39-4.34 (m, 2H), 3.43-3.38 (m, 1H), 2.51 (s, 3H), 2.20 (s, 3H), 1.22 (d, J = 7.1 Hz, 3H). MS: 431.1 m/z [M-1]⁻.

General procedure for the synthesis of compounds 5a-e

3-Chloroperbenzoic acid (*m*-CPBA) (2.25 mmol, 388 mg) was added to a solution of suitable compound **12a,b** (1.07 mmol) in anhydrous DCM (20 mL) at 0 °C and the reaction mixture was stirred at room temperature for 2.5 hours. After removing solvent under vacuum, the residue was resolubilized in EtOAc (180 mL) and saturated solution of NaHCO₃ was added dropwise until pH 7. Organic phase was washed with brine, then dried (Na₂SO₄), filtered and concentrated under reduced pressure, affording a mixture of sulfone and sulfoxide derivatives, which was employed in the next step without additional purification. The crude was dissolved in DMSO/butan-1-ol (1:2) (6 mL), then appropriate amine (5.35 mmol) was added and the reaction mixture was stirred at 120 °C for 10 h. Water was added and the product was extracted with EtOAc (60 mL x 5), washed with brine (40 mL), then dried (Na₂SO₄), and concentrated under reduced pressure. The residual solvents, 1-butanol and DMSO, were removed under nitrogen flow affording a brown solid. The crudes were purified by flash chromatography, using PE/EtOAc (8:2 to 6:4) as the eluent, followed by crystallization in DCM, thus obtain the final compounds **5a-e** as white solid.

3-((6-((2-Hydroxyethyl)amino)-1-(2-phenylpropyl)-1H-pyrazolo[3,4-d]pyrimidin-4-yl)amino)phenol (5a)

Yield: 69%. ¹H NMR (400 MHz, DMSO-d₆) δ 9.35 (s, 1H), 9.29 (bs, 1H), 7.94 (s, 1H), 7.34-7.31 (m, 2H), 7.29 – 7.22 (m, 4H), 7.20 – 7.13 (m, 1H), 7.08 (t, J = 8.0 Hz, 1H), 6.62 (s, 1H), 6.44 (d, J = 8.0, 1H), 4.71 (bs, 1H), 4.28 (dd, J = 13.2, 8.4 Hz, 1H), 4.20 (dd, J = 13.2, 8.4 Hz, 1H), 3.59-3.57 (m, 2H), 3.50 – 3.36 (m, 3H), 1.13 (d, J = 7.0 Hz, 3H). ¹³C NMR (100 MHz, DMSO-d₆) δ 161.8, 157.4, 155.8, 155.4, 143.5, 140.4, 131.7, 129.1, 128.1, 126.9, 126.3, 112.7, 110.4, 108.7, 96.1, 61.3, 52.7, 43.7, 39.8, 17.7. MS: 404.4 m/z [M-1]⁻.

3-((6-((2-(2-Hydroxyethoxy)ethyl)amino)-1-(2-phenylpropyl)-1H-pyrazolo[3,4-d]pyrimidin-4-yl)amino)phenol (5b)

Yield: 78%. ¹H NMR (400 MHz, DMSO-d₆) δ 9.32 (s, 1H), 9.21 (bs, 1H), 7.85 (s, 1H), 7.32-7.29 (m, 2H), 7.27 – 7.21 (m, 4H), 7.20 – 7.13 (m, 1H), 7.10 (t, *J* = 8.1 Hz, 1H), 6.60 (s, 1H), 6.40 (d, *J* = 8.0, 1H), 4.71 (bs, 1H), 4.24 (dd, *J* = 13.2, 1H), 4.18 (dd, *J* = 13.2, 1H), 3.64-3.55 (m, 4H), 3.51 – 3.31 (m, 5H), 1.12 (d, 3H). ¹³C NMR (100 MHz, DMSO-d₆) δ 161.40, 157.97, 156.32, 154.76, 144.29, 141.33, 132.15, 129.61, 128.81, 127.55, 126.88, 111.96, 110.29, 108.14, 96.31, 72.64, 71.48, 69.59, 67.23, 60.74, 52.64, 19.51. MS: 447.2 m/z [M-1]⁻.

3-((6-((4-Hydroxybutyl)amino)-1-(2-phenylpropyl)-1H-pyrazolo[3,4-d]pyrimidin-4-yl)amino)phenol (5c)

Yield: 56%. ¹H NMR (400 MHz, DMSO-d₆) δ 9.40 (bs, 1H), 9.30 (bs, 1H), 7.32 (bs, 1H), 7.32-7.30 (m, 2H), 7.28 – 7.19 (m, 4H), 7.18 – 7.10 (m, 1H), 7.00-6.88 (m, 1H), 6.57 (s, 1H), 6.49 (d, *J* = 8.0, 1H), 4.31 (bs, 1H), 4.27-4.20 (m, 2H), 3.67-3.58 (m, 4H), 3.55 – 3.35 (m, 3H), 1.12 (d, 3H). ¹³C NMR (100 MHz, DMSO-d₆) δ 161.9, 159.3, 157.8, 155.6, 143.4, 140.1, 133.5, 128.2, 128.0, 126.4, 126.1, 111.1, 110.1, 106.7, 94.2, 62.6, 61.3, 55.5, 52.9, 42.7, 40.8, 19.1. MS: 431.4 m/z [M-1]⁻.

N-(3-((6-((2-Hydroxyethyl)amino)-1-(2-phenylpropyl)-1H-pyrazolo[3,4-d]pyrimidin-4-yl)amino)phenyl)acetamide (5d)

Yield: 63%. ¹H NMR (400 MHz, acetone-d₆) δ 9.21 (bs, 1H), 8.95 (bs, 1H), 8.31 (bs, 1H), 7.86 (s, 1H), 7.35 – 7.22 (m, 5H), 7.22 – 7.13 (m, 3H), 6.27-6.21 (m, 1H), 4.47 (bs, 1H), 4.38 – 4.21 (m, 2H), 3.85-3.76 (m, 2H), 3.68-3.61 (m, 2H), 3.52 (q, 7.0 Hz, 1H), 2.09 (s, 3H), 1.19 (d, *J* = 7.0 Hz, 3H). ¹³C NMR (100 MHz, acetone-d₆) δ 203.02, 173.21, 167.04, 160.01, 149.15, 145.51, 144.98, 136.11, 133.84, 133.43, 132.21, 131.52, 118.62, 116.47, 101.41, 57.79, 49.31, 44.80, 28.55, 24.56, 23.66. MS: 444.1 m/z [M-1]⁻.

N-(3-((6-((2-Acetamidoethyl)amino)-1-(2-phenylpropyl)-1H-pyrazolo[3,4-d]pyrimidin-4-yl)amino)phenyl)acetamide (5e)

Yield: 55%. ¹H NMR (400 MHz, DMSO-d₆) δ 9.65 (bs, 1H), 9.29 (bs, 1H), 8.97 (s, 1H), 8.28 (s, 1H), 7.88 (s, 1H), 7.65-7.47 (m, 2H), 7.38 – 7.05 (m, 6H), 6.43 – 6.07 (m, 1H), 4.46 – 4.16 (m, 2H), 3.64 (bs, 1H), 3.61 – 3.36 (m, 3H), 3.08-3.02 (m, 1H), 2.11 (s, 3H), 1.89 (s, 3H), 1.19 (d, *J* = 7.0 Hz, 1H). ¹³C NMR (100 MHz, DMSO-d₆) δ 191.03, 168.31, 156.28, 154.71, 144.01, 140.28, 139.91, 131.09, 128.65, 128.21, 126.98, 126.38, 115.16, 113.43, 111.36, 96.15, 87.48, 52.54, 41.27, 39.71, 23.53, 22.09, 18.43, 16.88. MS: 485.3 m/z [M-1]⁻.

7. References

- [1] Wen, P.Y.; Kesari, S. Malignant gliomas in adults. *N. Engl. J. Med.* **2008**, *359* (5), 492-507.
- [2] Louis, D.N.; Perry, A.; Reifenberger, G.; von Deimling, A.; Figarella-Branger, D.; Cavenee, W.K.; Ohgaki, H.; Wiestler, O.D.; Kleihues, P.; Ellison, D.W. The 2016 World Health Organization Classification of Tumors of the Central Nervous System: a summary. *Acta Neuropathol.* **2016**, *131* (6), 803-820.
- [3] Burger, P.C.; Green, S.B. Patient Age, Histologic Features, and Length of Survival in Patients With Glioblastoma Multiforme. *Cancer* **1987**, *59* (9), 1617-1625.
- [4] Biernat, W.; Kleihues, P.; Yonekawa, Y.; Ohgaki, H. Amplification and Overexpression of MDM2 in Primary (de novo) Glioblastomas. *J. Neur. Exp. Neur.* **1997**, *56* (2), 180–185.
- [5] Furnari, F.B.; Fenton, T.; Bachoo, R.M.; Mukasa, A.; Stommel, J.M.; Stegh, A.; Hahn, W.C.; Ligon, K.L.; Louis, D.N.; Brennan, C.; Chin, L.; DePinho, R.A.; Cavenee, W.K. Malignant astrocytic glioma: genetics, biology, and paths to treatment. *Genes Dev.* **2007**, *21* (21), 2683-2710.
- [6] Stupp, R.; Mason, W.P.; van den Bent, M.J.; Weller, M.; Fisher, B.; Taphoorn, M.J.; Belanger, K.; Brandes, A.A.; Marosi, C.; Bogdahn, U.; Curschmann, J.; Janzer, R.C.; Ludwin, S.K.; Gorlia, T.; Allgeier, A.; Lacombe, D.; Cairncross, J.G.; Eisenhauer, E.; Mirimanoff, R.O.; European Organisation for Research and Treatment of Cancer Brain Tumor and Radiotherapy Groups; National Cancer Institute of Canada Clinical Trials Group. Radiotherapy plus concomitant and adjuvant temozolomide for glioblastoma. *N. Engl. J. Med.* **2005**, *352* (10), 987-996.
- [7] Friedman, H.S.; Prados, M.D.; Wen, P.Y.; Mikkelsen, T.; Schiff, D.; Abrey, L.E.; Yung, W.K.; Paleologos, N.; Nicholas, M.K.; Jensen, R.; Vredenburgh, J.; Huang, J.; Zheng, M.; Cloughesy, T. Bevacizumab alone and in combination with irinotecan in recurrent glioblastoma. *J. Clin. Oncol.* **2009**, *27* (28), 4733–4740.
- [8] Lombardi, G.; De Salvo, G.L.; Brandes, A.A.; Eoli, M.; Rudà, R.; Faedi, M.; Lolli, I.; Pace, A.; Daniele, B.; Pasqualetti, F.; Rizzato, S.; Bellu, L.; Pambuku, A.; Farina, M.; Magni, G.; Indraccolo, S.; Gardiman, M.P.; Soffietti, R.; Zagonel, V. Regorafenib compared with

lomustine in patients with relapsed glioblastoma (REGOMA): a multicentre, open-label, randomised, controlled, phase 2 trial. *Lancet Oncol.* **2019**, *20* (1), 110-119.

[9] Lewis-Tuffin, L.J.; Feathers, R.; Hari, P.; Durand, N.; Li, Z.; Rodriguez, F.J.; Bakken, K.; Carlson, B.; Schroeder, M.; Sarkaria, J.N.; Anastasiadis, P.Z. Src family kinases differentially influence glioma growth and motility. *Mol. Oncol.* **2005**, *9* (9), 1783–1798.

[10] Ahluwalia, M.S.; de Groot, J.; Liu, W.M.; Gladson, C.L. Targeting SRC in glioblastoma tumors and brain metastases: rationale and preclinical studies. *Cancer Lett.* **2010**, *298* (2), 139-149.

[11] Du, J.; Bernasconi, P.; Clauser, K.R.; Mani, D.R.; Finn, S.P.; Beroukhim, R.; Burns, M.; Julian, B.; Peng, X.P.; Hieronymus, H.; Maglathlin, R.L.; Lewis, T.A.; Liao, L.M.; Nghiemphu, P.; Mellinghoff, I.K.; Louis, D.N.; Loda, M.; Carr, S.A.; Kung, A.L.; Golub, T.R.; Bead-based profiling of tyrosine kinase phosphorylation identifies SRC as a potential target for glioblastoma therapy. *Nat. Biotech.* **2009**, *27* (1), 77–83.

[12] Milano, V.; Piao, Y.; LaFortune, T.; de Groot, J. Dasatinib-induced autophagy is enhanced in combination with temozolomide in glioma. *Mol. Cancer Ther.* **2009**, *8* (2), 394–406.

[13] Nomura, N.; Nomura, M.; Sugiyama, K.; Hamada, J. Src regulates phorbol 12-myristate 13-acetate-activated PKC-induced migration via Cas/Crk/Rac1 signaling pathway in glioblastoma cells. *Int. J. Mol. Med.* **2007**, *20* (4), 511-519.

[14] Schenone, S.; Radi, M.; Musumeci, F.; Brullo, C.; Botta, M. Biologically driven synthesis of pyrazolo[3,4-*d*]pyrimidines as protein kinase inhibitors: an old scaffold as a new tool for medicinal chemistry and chemical biology studies. *Chem. Rev.* **2014**, *114* (14), 7189–7238.

[15] Calgani, A.; Vignaroli, G.; Zamperini, C.; Coniglio, F.; Festuccia, C.; Di Cesare, E.; Gravina, G.L.; Mattei, C.; Vitale, F.; Schenone, S.; Botta, M.; Angelucci, A. Suppression of SRC Signaling Is Effective in Reducing Synergy between Glioblastoma and Stromal Cells. *Mol. Cancer Ther.* **2016**, *15* (7), 1535–1544.

[16] Fallacara, A.L.; Zamperini, C.; Podolski-Renić, A.; Dinić, J.; Stanković, T.; Stepanović, M.; Mancini, A.; Rango, E.; Iovenitti, G.; Molinari, A.; Bugli, F.; Sanguinetti, M.; Torelli, R.; Martini, M.; Maccari, L.; Valoti, M.; Dreassi, E.; Botta, M.; Pešić, M.; Schenone, S. A New Strategy for Glioblastoma Treatment: In Vitro and In Vivo Preclinical Characterization of Si306, a Pyrazolo[3,4-*d*]Pyrimidine Dual Src/P-Glycoprotein Inhibitor. *Cancers* **2019**, *11* (6), 848.

- [17] Nešović, M.; Divac Rankov, A.; Podolski-Renić, A.; Nikolić, I.; Tasić, G.; Mancini, A.; Schenone, S.; Pešić, M.; Dinić, J. Src Inhibitors Pyrazolo[3,4-*d*]pyrimidines, Si306 and Pro-Si306, Inhibit Focal Adhesion Kinase and Suppress Human Glioblastoma Invasion In Vitro and In Vivo. *Cancers* **2020**, *12* (6), 1570.
- [18] Molinari, A.; Fallacara, A.L.; Di Maria, S.; Zamperini, C.; Poggialini, F.; Musumeci, F.; Schenone, S.; Angelucci, A.; Colapietro, A.; Crespan, E.; Kissova, M.; Maga, G.; Botta, M. 2018. Efficient optimization of pyrazolo[3,4-*d*]pyrimidines derivatives as c-Src kinase inhibitors in neuroblastoma treatment. *Bioorg. Med. Chem. Lett.* **2018**, *28* (21), 3454–3457.
- [19] Tintori, C.; Fallacara, A.L.; Radi, M.; Zamperini, C.; Dreassi, E.; Crespan, E.; Maga, G.; Schenone, S.; Musumeci, F.; Brullo, C.; Richters, A.; Gasparrini, F.; Angelucci, A.; Festuccia, C.; Delle Monache, S.; Rauh, D.; Botta, M. Combining X-ray Crystallography and Molecular Modeling toward the Optimization of Pyrazolo[3,4-*d*]pyrimidines as Potent c-Src Inhibitors Active in Vivo against Neuroblastoma. *J. Med. Chem.* **2015**, *58* (1), 347–361.

